Aqueous humour protein imbalances in primary open-angle glaucoma and their effects on trabecular meshwork cell function

Esther Lara Ashworth Briggs

BSc (Hons)

September 2018

Submitted in fulfilment of the requirements for the Degree of Doctor of Philosophy

School of Health Sciences, College of Health and Medicine, University of Tasmania.

DECLARATION OF ORIGINALITY

This thesis contains no material which has been accepted for a degree or diploma by the university or any other institution, except by the way of background information and duly acknowledged in the thesis, and to the best of my knowledge and belief no material previously published or written by another person except where due acknowledgement is made in the text of the thesis, nor does the thesis contain any material that infringes copyright.

____________________ 16.09.2018

STATEMENT OF AUTHORITY OF ACCESS

This thesis may be made available for loan and limited copying and communication in accordance with the *Copyright Act 1968*.

____________________ 16.09.2018

STATEMENT REGARDING PUBLISHED WORK

The publishers of the papers comprising Chapters 2 and 3 hold the copyright for that content and access to the material should be sought from the respective journals. The remaining non-published content of the thesis may be made available for loan and limited copying and communication in accordance with the *Copyright Act 1968*.

Due to the inclusion of published material there is unavoidable repetition of material between chapters in this thesis.

____________________________ 16.09.2018

STATEMENT OF ETHICAL CONDUCT

The research associated with this thesis abides by the international and Australian codes on human and animal experimentation, the guidelines by the Australian Government's Office of the Gene Technology Regulator and the rulings of the Safety, Ethics and Institutional Biosafety Committees of the University. This study was approved by the Human Research Ethics Committee Network, Tasmania (Approval no. H0013502 and H0013264).

____________________________ 16.09.2018

STATEMENT OF CO-AUTHORSHIP

The following people and institutions contributed to the publication of work undertaken as part of this thesis:

Candidate: Esther L Ashworth Briggs (ELAB), *School of Health Sciences, College of Health and Medicine, University of Tasmania*

Author 1: Anthony L Cook (ALC), *School of Health Sciences, College of Health and Medicine, University of Tasmania* and *Wicking Dementia Research and Education Centre, College of Health and Medicine, University of Tasmania*

Author 2: Alex W Hewitt (AWH), *Menzies Institute for Medical Research, College of Health and Medicine, University of Tasmania* and *Centre for Eye Research Australia, University of Melbourne, Victoria*

Author 3: Rajaraman Eri (RE), *School of Health Sciences, College of Health and Medicine, University of Tasmania*

Author 4: Tze'Yo Toh (TYT), *Launceston Eye Institute and Launceston Eye Doctors, Tasmania*

Author 5: Stephen Myers (SM), *School of Health Sciences, College of Health and Medicine, University of Tasmania*

Contribution of work by co-authors for each published manuscript:

MANUSCRIPT 1: Located in Chapter 2

Ashworth Briggs EL, Toh TY, Eri R, Hewitt AW, and Cook AL. TIMP1, TIMP2, and TIMP4 are increased in aqueous humor from primary open angle glaucoma patients. *Mol Vis* 2015;21:1162-1172.

Author contributions:

The candidate performed the laboratory data collection, analysis and interpretation and drafted the manuscript. The study was conceived and designed by author 1 with the assistance of author 2 and author 3. Author 4 recruited all study participants, recorded clinical data, and performed sample collection during surgery. Author 1 and author 2 provided assistance with data analysis and interpretation. Each author assisted in the refinement and presentation of the final manuscript.

Percentage estimate of the contribution made by each author:

Candidate: 65%

Author 1: 15%

Author 2: 5%

Author 3: 5%

Author 4: 10%

MANUSCRIPT 2: Located in Chapter 3

Ashworth Briggs EL, Toh TY, Eri R, Hewitt AW, and Cook AL. Uteroglobin and FLRG concentrations in aqueous humor are associated with age in primary open angle glaucoma patients. *BMC Ophthalmology* 2018;18:57-64.

Authors' contributions

The candidate performed the laboratory data collection, analysis and interpretation and drafted the manuscript. The study was conceived and designed by author 1 with the assistance of author 2 and author 3. Author 4 recruited all study participants, recorded clinical data, and performed sample collection during surgery. Author 1 and author 2 provided assistance with data analysis and interpretation. Each author assisted in the refinement and presentation of the final manuscript.

Percentage estimate of the contribution made by each author:

Candidate: 65%

Author 1: 15%

Author 2: 5%

Author 3: 5%

Author 4: 10%

We, the undersigned agree with the above stated contributions to the listed manuscripts.

Signed: ______________________ Date: 11.09.2018

Anthony Cook

Primary supervisor

School of Health Sciences, College of Health and Medicine, University of Tasmania

Signed: ______________________ Date: 17.09.2018

James Fell

Associate Head of Research

School of Health Sciences, College of Health and Medicine, University of Tasmania

Contribution of work by co-authors for unpublished data chapter:

CHAPTER 4:

Molecular and functional characterisation of primary human trabecular meshwork cells and the effect of uteroglobin on trabecular meshwork contraction *in vitro.*

Author contributions:

The candidate conceived and designed the study, performed all laboratory data collection, analysis and interpretation and wrote the chapter. Author 1, author 2, and author 5 assisted with the conception and design of the study, and gave input with regard to analysis, interpretation and data presentation.

Percentage estimate of the contribution made by each author:

Candidate: 85%

Author 1: 5%

Author 2: 5%

Author 5: 5%

PUBLICATIONS AND CONFERENCE PRESENTATIONS DURING PHD CANDIDATURE

Published manuscripts:

Ashworth Briggs EL, Toh TY, Eri R, Hewitt AW, and Cook AL. TIMP1, TIMP2, and TIMP4 are increased in aqueous humor from primary open angle glaucoma patients. *Mol Vis* 2015;21:1162-1172.

Ashworth Briggs EL, Toh TY, Eri R, Hewitt AW, and Cook AL. Uteroglobin and FLRG concentrations in aqueous humor are associated with age in primary open angle glaucoma patients. *BMC Ophthalmology* 2018;18:57-64.

Conference presentations:

Ashworth Briggs EL, Toh TY, Eri R, Hewitt AW, and Cook AL. Imbalance between MMPs and TIMPs in aqueous humour from primary open angle glaucoma patients due to increased levels of TIMP1, TIMP2 and TIMP4. Oral presentation, abstract no. 83. Proceedings of the Australian Health and Medical Research Congress 2014, 16th – 19th November, Melbourne Convention and Exhibition Centre, Victoria, Australia.

Ashworth Briggs EL, Hewitt AW, SA Myers and Cook AL. Effect of uteroglobin on trabecular meshwork cell contraction. Poster presentation, presentation no. 3519. Proceedings of the Association for Research in Vision and Ophthalmology 2018 annual meeting, 29th April- 3rd May, Hawaii Convention Center, Honolulu, Hawaii.

ACKNOWLEDGEMENTS

I am deeply grateful to all the people who supported me during my PhD. You all contributed to its success in your own wonderful ways. Firstly, I would like to thank my supervisors Dr. Anthony Cook, Dr. Steve Myers, and Prof. Alex Hewitt. Tony, I am deeply grateful that you took me on as your PhD student and made this thesis possible. I am yet to find out about all the hoops you had to jump through to make it happen! Thank you for all the support you have provided throughout my candidature. Steve, thank you for your kindness, enthusiasm, and support, and for always carrying a smile on your face. It is always a joy to see you. Alex, thank you for your support and guidance, especially with regards to the clinical aspects of my research. I would also like to extend my sincere gratitude to Dr. Murray Adams and Prof. Dominic Geraghty, my graduate research coordinators and avid supporters. Your support and encouragement have been invaluable throughout my candidature.

I would like to acknowledge the generous support of the Clifford Craig Medical Research Trust (CCMRT, Launceston, Australia), who funded the research contained in this thesis, and the Schulthess'sche Familienstiftung (Zürich, Switzerland), whose support enabled me to move across the world to obtain my PhD. Without their financial support this thesis would not have been possible. Furthermore, I would like to extend my gratitude to the study participants, Dr. Tze'Yo Toh, and Sally Baxter, without whom the clinical studies in chapters 2 and 3 would not have been possible.

I would like to thank all the beautiful souls who work tirelessly in the prep room and keep the laboratory engines running. Your interest, assistance, and emotional support made the journey smoother and easier. I would also like to thank Dr. Dale Kunde for the technical support provided throughout my PhD, and the teaching staff within the School of Health Sciences for their general support and encouragement.

I wish to acknowledge my peers within the School of Health Sciences, Sarron Randall-Demllo, Waheeda Basheer, Safa Al-maghrabi, Kate Herbert, Liz Witherden, Nicole Ranson, Dana Lis, Sally McLaine, Shada Norouzi, John Adulcikas, Laura Danderian, and Nicola McDonald. Thank you for your support, friendship and all the fun times together! I would like to especially thank Emma Zadow for our impromptu chats whilst my coffee was brewing (and going cold again :D). Our conversations kept me going when I was feeling isolated and alone in my little glaucoma world. Also, a heartfelt thank you to Kate Edwards, thank you for your friendship and support, the many coffees, and the lunch time runs, which helped keep me mostly sane in my final months!

Not only did I learn and grow a lot through this experience, I also made great friends to whom I am very grateful for their support: Chris and Natalie Polis, the Cook family, Phil Marsh and Deb Osterhage, Rob and Miranda Gracie, Andrew Rath and Sharon Fraser, Kate and Fergus Edwards, Zhi Quan Leong, and Alex Conway. Thank you for cheering me along and for all the good times together, which provided a much-needed balance to my studies.

I would like to acknowledge the fellow researchers I had the pleasure of meeting at ARVO 2018, especially Prof. Daniel Stamer, Prof. Rudolf Fuchshofer, Dr. Mary Kelley, Dr. Mitchell deLong, and Dr. Padmanabhan Pattabiraman. Your kindness and your enthusiasm for trabecular meshwork research inspired me and your feedback helped to make this thesis the best it can be. Furthermore, I would like to thank Simon Bakker of Kugler Publications. Our conversations at ARVO 2018 gave me confidence in my ideas for the future and our joint plans provided me with extra motivation to finish my PhD.

I wish to extend a deep and heartfelt thank you to Prof. Dr. med. Christoph W. Spraul and Dr. Christian Lingenfelder. Thank you for your friendship, encouragement, and support in the final months of this epic journey. Your mentorship has been truly invaluable and your enthusiasm and curiosity with regards to my research gave me the motivation and drive required to finish my thesis; to finish it well and with purpose. I will forever be grateful that we met at ARVO 2018. Herzlichen Dank!

Finally, I would like to thank my family for their ongoing support. Thank you, Mum, Dad, and Chris, for your encouragement and for biting your tongue and letting me fly far, far away from home to explore a new life and tackle this challenge. And most importantly, my deepfelt gratitude towards my husband Alex. You never failed to show me your belief in my abilities, supported me at all hours of the day and days of the week (hello cell culture :D) and helped me navigate the stormy waters. Many people thought we were mad to be doing our PhDs simultaneously, I believed all along that it was the best way for us. Thank you all for believing in me and for your patience, I am truly grateful.

Yours sincerely,

Esther Lara Ashworth Briggs

TABLE OF CONTENTS

LIST OF FIGURES

LIST OF TABLES

LIST OF APPENDICES

LIST OF ABBREVIATIONS

The following abbreviations are used in this thesis. Due to the inclusion of published manuscripts, some abbreviations are defined more than once.

ADAM	A disintegrin and metalloprotease
ADAMT	ADAM metallopeptidase with thrombospondin type 1 motif
ANOVA	Analysis of variance
AQP1	Aquaporin 1
αSMA	Alpha-smooth muscle actin
bFGF	Basic fibroblast growth factor
BMP	Bone morphogenic protein
BSA	Bovine serum albumin
CCL27	C-C motif chemokine ligand 27
cDNA	Complementary deoxynucleic acid
CDR	Cup-to-disc ratio
CHI3L1	Chitinase 3 like 1
CLANs	Cross-linked actin networks
C_T	Threshold cycle
CTGF	Connective tissue growth factor
CXCL9	C-X-C motif chemokine ligand 9
DcR3	Decoy receptor 3
DMEM	Dulbecco's modified Eagle's medium
DMSO	Dimethyl sulfoxide
DNA	Deoxyribonucleic acid
ECM	Extracellular matrix
EDTA	Ethylenediaminetetraacetic acid
EGF	Epidermal growth factor
EPO	Erythropoietin
ER	Endoplasmic reticulum
FBS	Foetal bovine serum
FI	Fluorescence intensity
FLRG	Follistatin-related gene
FOXC1	Forkhead Box C1
FPR2	Formyl peptide receptor 2
GON	Glaucomatous optic neuropathy
GWAS	Genome-wide association studies
HBSS	Hank's balanced salt solution
HDFn	Human dermal fibroblasts, neonatal
HepII	Heparin-binding domain II
HGF	Hepatocyte growth factor
HPRT1	Hypoxanthine phosphoribosyltransferase 1
HRP	Horseradish peroxidase
IGFBP	Insulin-like growth factor binding protein
IL	Interleukin

INFα	Interferon alpha
INFγ	Interferon gamma
IOP	Intraocular pressure
iPSCs	Induced pluripotent stem cells
JCT	Juxtacanalicular tissue
kDa	Kilodalton
LIF	Leukemia inhibitory factor
LMBR1L	Limb development membrane protein 1 like
LMX1B	LIM Homeobox Transcription Factor 1 beta
MD	Mean deviation
MFG-E8	Milk fat globule-EGF factor 8
MGP	Matrix gla protein
MIF	Macrophage migration inhibitory factor
MMP	Matrix metalloproteinase
MYOC	Myocilin
OCT	Optical coherence tomography
PAX6	Paired Box 6
PBS	Phosphate-buffered saline
pHTMCs	Primary human trabecular meshwork cells
PITX2	Paired Like Homeodomain Transcription Factor 2
PLA_2	Phospholipase A2
POAG	Primary open-angle glaucoma
POM	Periocular mesenchyme
PSD	Pattern standard deviation
PVDF	Polyvinylidene difluoride
qPCR	Quantitative polymerase chain reaction
RGC	Retinal ganglion cell
RNA	Ribonucleic acid
ROCK	Rho-associated, coiled-coil containing protein kinase
r_s	Spearman's correlation coefficient
SAA	Serum amyloid A
SCGB1A1	Secretoglobin 1A1 (uteroglobin)
SDS-PAGE	Sodium dodecyl sulfate polyacrylamide gel
TBST	Tris-buffered saline Tween20
TGF-β	Transforming growth factor beta
TGM2	Tissue transglutaminase
TIMP	Tissue inhibitor of metalloproteinase
TM	Trabecular meshwork
TNFα	Tumour necrosis factor alpha
VCAM-1	Vascular cell adhesion molecule 1
VEGF	Vascular endothelial growth factor
vWF-A2	Von Willebrand factor A2

ABSTRACT

Purpose

Glaucoma is the leading cause for irreversible blindness worldwide. The term encompasses several ocular disease subtypes with the same end result, namely damage to the optic nerve head, of which primary open-angle glaucoma (POAG) is the most common. Despite extensive research, the aetiology and progression of POAG remain largely elusive. The development of early diagnostic strategies and more effective treatment approaches requires a better understanding of the cellular mechanisms involved in POAG.

Problem

Elevated intraocular pressure (IOP) is a key risk factor for POAG and the focus of all current treatment strategies. IOP homeostasis is regulated by the trabecular meshwork (TM), a specialised tissue within the anterior chamber of the eye that determines the rate of aqueous humour outflow. In POAG, a dysfunctional TM leads to elevated IOP and consequently damage to the optic nerve head. To date, the processes involved in TM dysfunction remain unclear.

Methodology

Two studies investigated imbalances in human aqueous humour protein concentrations using multiplex immunoassays. Proteins measured included matrix metalloproteinases (MMPs) and their endogenous tissue inhibitors (TIMPs), various cytokines, and growth factors. Samples from POAG patients were compared to non-glaucomatous cataract patients and results were correlated to disease descriptors

including age, IOP, cup-disk-ratio (CDR), Humphrey's visual field pattern standard deviation (PSD), and disease duration since diagnosis. Based on the results from the second study, the anti-inflammatory cytokine uteroglobin was selected for *in vitro* investigation using a human TM cell model. TM cells were first characterised using a panel of TM marker genes and two functional assays: Dexamethasone-stimulated myocilin upregulation and collagen gel contraction. For the latter, contractile (human fibroblast) and non-contractile (HeLa) control cell lines were included, and ROCK inhibitor Y-27632 was used to inhibit contraction. Subsequently, the collagen gel contraction assay was used to investigate the effect of 1 and 2 μg/ml uteroglobin on TM cell contraction over a period of 96 hours.

Results

The first study found significantly elevated levels of TIMP1, TIMP2, TIMP4, and MMP2 concentrations in aqueous humour samples from POAG compared to cataract control. Imbalances in MMP/TIMP molar ratios were also determined in POAG, several of which correlated with IOP and PSD, but not with other disease descriptors. In the second study, several cytokines and growth factors, including uteroglobin, HGF, and FLRG, were detected in aqueous humour samples from POAG and cataract control patients. Uteroglobin and FLRG concentrations correlated significantly with age in POAG but not cataract samples. Furthermore, HGF concentrations resulted in a negative correlation with disease duration. Gene expression and immunofluorescence experiments using primary TM cells determined expression of the uteroglobin receptor LMBR1L but not uteroglobin itself. Treatment of primary TM cells with recombinant uteroglobin did not significantly affect cell contraction at the concentrations tested.

Conclusions

The differences identified in MMPs, TIMPs, and various cytokine concentrations in aqueous humour from POAG patients add to our knowledge on aqueous humour imbalances in POAG. The analysis of MMP-to-TIMP ratios showed a shift towards increased TIMP levels, suggesting a potential increase in MMP inhibition, which may affect extracellular matrix composition and thus contribute to elevated aqueous humour outflow resistance. Several of the cytokines reported in the second study have not previously been quantified in aqueous humour. Correlations of age with uteroglobin and FLRG in POAG may indicate an increased need for anti-inflammatory (uteroglobin) or anti-calcification (FLRG) activity in the aging glaucomatous TM. While no effect of uteroglobin on TM cell contraction was found in the final study, further experiments may elucidate the effects this protein has on TM cell function. Specifically, phospholipase A2 activity, tissue transglutaminase activity, and phagocytosis assays are required to determine the potential effect of uteroglobin on TM cells. Determination of the effects of the aqueous humour proteins quantified in this thesis on TM cell behaviour may lead to new insights with regards to TM dysfunction in POAG and possibly provide new targets for pharmaceutical intervention or result in diagnostic biomarkers for POAG.

CHAPTER 1 LITERATURE REVIEW

1.1 GLAUCOMA – A COMPLEX OPTIC NEUROPATHY

Glaucoma is the leading cause of irreversible blindness, affecting an estimated 60.5 million people worldwide in 2010, with a predicted increase to 111.8 million by 2040 (1), due to the rapid rise in the aging population. In Australia, a prevalence of 3% has been reported in people over the age of 49 (2, 3), which equates to approximately 300,000 individuals. Typically, glaucoma affects peripheral vision first and blindness can ensue if left untreated (4). Whilst treatment can slow down or even arrest disease progression (5), existing visual field defects are irreversible, making early detection critical. The slow, insidious progression of chronic glaucoma, occurring over many years, combined with the late appearance of symptomatic visual field defects, means that diagnosis often does not occur until the disease has reached an advanced stage, and for the same reasons, many cases remain undiagnosed (6, 7). By these later stages, central visual acuity and the ability to read are affected, which severely impact on a patient's quality of life (8). Glaucoma therefore presents a considerable burden on health care systems (9), particularly due to the chronic nature of the disease, requiring life-long treatment and regular clinical reviews. Specifically, a study by the Centre for Eye Research Australia (CERA) reported an annual health care cost due to glaucoma of AUD 342 million in 2005 (10). As a consequence, efforts have been made to introduce population screenings for glaucoma to enable early detection and treatment, although the lack of a single, definitive test for glaucoma presents a considerable challenge (11, 12). Current research mainly focusses on more reliable early diagnosis and improved treatment strategies to lessen the social burden and improve patient quality of life.

1.1.1 Definition

The term glaucoma encompasses a heterogeneous group of ocular diseases with the common clinical denominator of progressively degenerating retinal ganglion cell (RGC) axons, which leads to a distinct cupping of the optic nerve head and characteristic visual field damage (13-15). This common clinical characteristic is known as glaucomatous optic neuropathy (GON). Whilst the pathogenesis of GON remains unclear, several potential mechanisms leading to RGC degeneration and resultant visual field damage have been described in the literature and are outlined in section 1.1.3.3. In addition to the uncertain development of glaucomatous damage, the numerous glaucoma subtypes present with varied aetiologies, risk factors, demographics, symptoms, disease durations, and prognoses and require differing treatment strategies (8). For these reasons, correct diagnosis and treatment of glaucoma remains a challenge.

1.1.2 Glaucoma subtypes

The different forms of glaucoma are divided into subcategories, based on the morphology of the anterior chamber angle, the age of onset, and whether the disease results from an identifiable cause or not (4, 15). This subdivision is summarised in Figure 1.1. Whilst intraocular pressure (IOP) is not a defining criterion for glaucoma (13), it does play a role in categorising different forms of glaucoma. The existence of a clear cause for IOP elevation in association with GON, such as an inflammation, eye injury, or steroid treatment, divides the glaucomas into primary and secondary forms. The former lacks an identifiable cause, whereas in the latter, the source of increased IOP is recognizable. A second subdivision is made based on the status of the iridocorneal angle (Figure 1.2). In open-angle glaucoma, the chamber angle is unobstructed (Figure 1.2B), and any increase in IOP cannot be explained by visible changes to the anterior chamber. Contrarily, a closed, physically obstructed angle blocks aqueous humour outflow at a macroscopic level and is labelled closed-angle glaucoma (Figure 1.2C). Although the relevance is disputed (16), a further subdivision exists in primary open-angle glaucoma (POAG), depending on the level of IOP. A subset of POAG patients do not present with elevated IOP, which has been termed normal tension glaucoma (13, 15). Depending on the age of onset, glaucoma subtypes can be further classified as congenital, juvenile, or adult onset glaucoma. Among these different types of glaucoma, all of which are potentially progressive and can lead to blindness (15), POAG is the most common form (14, 17) and will be the focus of this review.

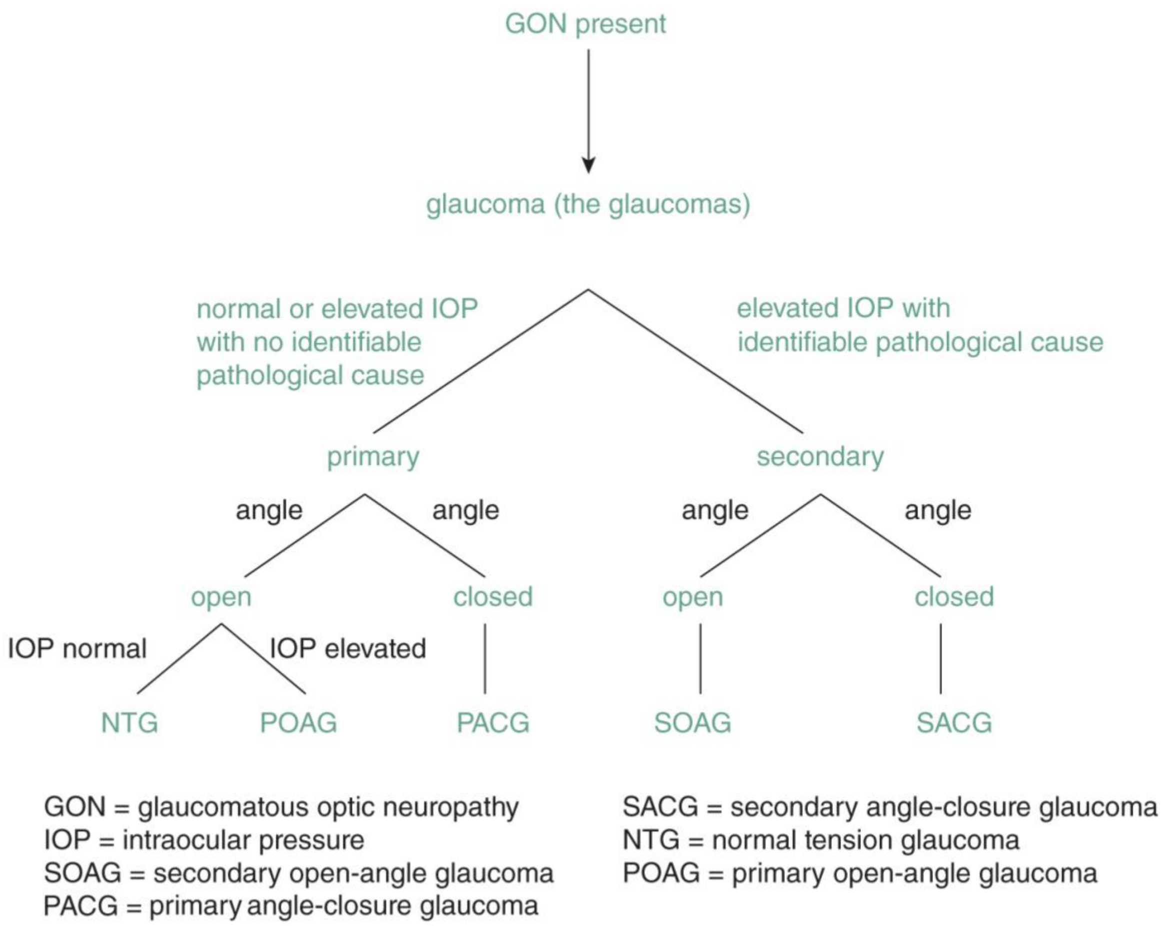

Figure 1.1 Glaucoma subcategories based on cause, anterior chamber angle morphology, and IOP. Figure adapted from (15).

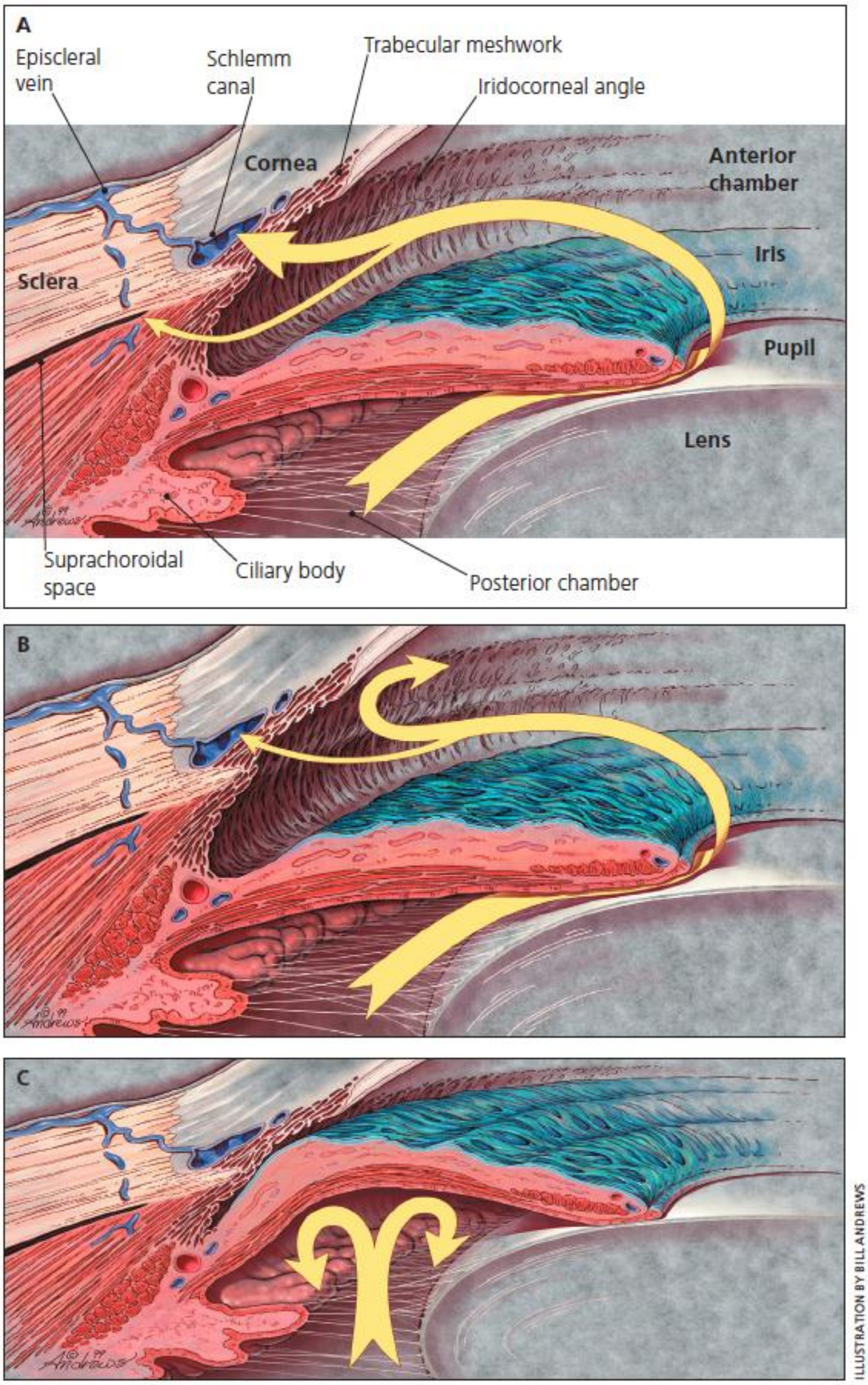

Figure 1.2 Iridocorneal angle morphology and aqueous humour outflow pathways (yellow arrows). A) Aqueous humour flow in a healthy eye. B) Aqueous humour outflow is reduced despite an open iridocorneal angle. C) Angle closure prevents

aqueous humour from passing between the lens and iris into the anterior chamber. Image reproduced from (18).

1.1.3 Primary open-angle glaucoma

1.1.3.1 *Definition and clinical assessment*

POAG is a complex, multifactorial disease with a development that remains largely elusive. The disease is defined as glaucomatous damage to the optic nerve head in the presence of an open iridocorneal angle (Figure 1.2B), with no determinable cause for IOP elevation (15). Early POAG diagnosis is critical but also challenging, as the diagnosis is often not clear-cut. Due to this uncertainty, regular clinical reviews are required to assess whether there is a progression of symptoms necessitating medical treatment.

POAG diagnosis is based on the presence of characteristic optic disc cupping, corresponding visual field defects, and a thinning of the retinal nerve fibre layer (19). Optic disc cupping is assessed by means of the vertical cup-to-disc ratio (CDR). An enlarged optic cup results in an increased CDR value and is due to the loss of RGC axons. RGC axonal degeneration is also responsible for the thinning of the retinal nerve fibre layer, which is measurable by ocular coherence tomography (14). The resulting glaucomatous visual field defects can be detected by means of perimetry, although functional loss is generally not detectable until at least 20-50% of RGCs have been lost (20, 21). A visual field test maps specific locations of damage and provides parameters such as mean deviation (MD) and pattern standard deviation (PSD). The former compares the mean deviation of a patient's results to an age-matched normative database, whereas the latter highlights focal variation within the visual field of one patient (22). Additional methods can be used to assess visual field defects, such as blue-on-yellow perimetry to test loss of colour-contrast sensitivity (23, 24). To determine whether the patient is presenting with open- or closed-angle glaucoma, the anatomy of the iridocorneal angle is assessed by means of gonioscopic examination. As POAG can present without IOP elevation, the diagnosis is made irrespective of the pressure measured.

1.1.3.2 *Risk factors*

POAG aetiology involves a variety of ocular, systemic, environmental, and genetic risk factors. The main risk factors for POAG are advancing age and elevated IOP. A family history of POAG and African ethnicity are also strongly associated with an increased risk for developing the disease (25). Of these, IOP is the only modifiable risk factor and the current focus of all treatment strategies.

It is well known that genetics play an important role in POAG. A first-degree relative with POAG increases the risk of developing the disease by ten-fold in comparison to the general population (26). However, POAG is a genetically complex and heterogeneous disease and the majority of cases are adult onset and not inherited in a Mendelian fashion. The use of family linkage studies has revealed causative mutations for adult-onset POAG in a number of genes, including myocilin, optineurin, and WD repeat domain 36 (reviewed in (27)), yet these only explain up to 10% of all POAG cases (28). More recently, genome-wide association studies (GWAS) have identified numerous loci associated with POAG. The variants detected in GWAS are more common than those described above and present risk alleles for POAG rather than causative mutations (29, 30). The information obtained through GWAS has highlighted several cellular pathways that may be involved in POAG pathogenesis, such as extracellular matrix (ECM) metabolism, TGF-β signalling, and the rhoA/rho-associated kinase pathway (reviewed in (31)).

Whilst several additional factors have been associated with an increased prevalence of POAG, their validity as risk factors is uncertain. Association of gender with the prevalence of POAG has been inconsistent (32), yet some meta-analyses of population studies have found a higher prevalence in men (1, 33, 34). The validity of myopia as a risk factor has been questioned due to the difficulty of detecting GON in myopic eyes (35). Further factors that may be associated with a greater risk for POAG include diabetes mellitus, arterial hypertension, body mass index, central corneal thickness, obstructive sleep apnoea, and atherosclerosis, although these associations are uncertain and require further research (reviewed in (8, 27, 36)).

1.1.3.3 *Aetiology of primary open-angle glaucoma and the relevance of intraocular pressure*

Many mechanisms have been suggested to explain the loss of RGC axons that underlies optic nerve head damage, some of which are directly related to elevated IOP. These mechanisms include impaired axonal transport, which deprives RGCs of neurotrophic factors critical to survival, glial cell activation in response to elevated IOP, and hypoxia caused by reduced blood flow at the optic nerve head (reviewed in (4, 37, 38)).

Elevated IOP has commonly been defined as a pressure that exceeds 21 mm Hg. This value represents a purely statistical concept and corresponds to two standard deviations above the mean value of 16 mm Hg, assuming a Gaussian distribution (16). Elevated IOP was long thought to be a causative factor for POAG but is now considered merely a risk factor (15) for two reasons: First, increased IOP does not necessarily lead to GON (39). Secondly, GON may present itself in the absence of elevated IOP, which is often referred to as normal tension glaucoma (13, 15). Thus, elevated IOP is not a defining feature of POAG and IOP-independent mechanisms are likely involved in the development of GON, such as ischemia, loss of neurotrophic signalling, and neurotoxicity (37, 38).

Although POAG can occur in people with normal IOP, ocular hypertension is a risk factor for the development of GON, and the likelihood of developing POAG is increased at higher IOP levels (40, 41). Several randomized clinical trials have shown that reduction of IOP by means of hypotensive medication, laser therapy, or surgical intervention delays the onset and progression of glaucoma (5, 42-44), and lowering IOP not only benefits patients with elevated pressures, but also improves outcomes for so-called normal tension glaucoma (45, 46). The fact that hypotensive treatment benefits these patients suggests that normal tension glaucoma is also linked to IOP (15).

Whilst there is consensus that elevated IOP is due to increased aqueous humour outflow resistance rather than increased aqueous production (47, 48), the precise mechanisms involved in altered outflow resistance remain unclear. Many theories exist, which are discussed in section 1.3.2, and elucidating the causes of increased outflow resistance forms a key area of active research in glaucoma. The precise link between elevated IOP and optic nerve damage is also yet to be determined. Several animal studies have demonstrated that elevation of IOP leads to RGC degeneration and optic nerve head damage (49-51), and it is thought that the pressure increase causes mechanical changes at the lamina cribrosa, leading to RGC axonal injury and death (52).

1.1.3.4 *Current treatment strategies*

To date, reduction of IOP remains the only proven treatment strategy for glaucoma (8), which is achieved by a range of topical or oral medications, laser trabeculoplasty, or incisional surgery, such as trabeculectomy or the placement of a drainage implant (reviewed in (53)). The topical treatments available alter IOP by either increasing uveoscleral outflow or reducing aqueous humour production. A new class of drugs called rho kinase inhibitors, which increase trans-trabecular outflow, have recently been approved for clinical use (54). The aqueous humour outflow pathways mentioned above are further discussed in section 1.2.2.

1.2 OCULAR ANATOMY AND AQUEOUS HUMOUR DYNAMICS

1.2.1 **Ocular anatomy - an overview**

The human eye is divided into two main compartments: the anterior segment and the posterior segment (Figure 1.3). The former consists of the lens and all the structures in front of it, whereas the latter comprises all structures that lie behind the lens. The anterior segment of the eye is further subdivided into the anterior and posterior chamber (Figure 1.3), both of which are filled with aqueous humour. The posterior chamber contains the lens and the ciliary body and is separated from the anterior chamber by the iris. The cornea, the anterior face of the iris, the trabecular meshwork (TM), and Schlemm's canal jointly form the anterior chamber (55, 56).

In the posterior segment, the inner surface of the eye, called the fundus, consists of the retina, the optic disc, the macula, and the fovea (Figure 1.4). RGCs and their axons form the retinal nerve fibre layer, which makes up the innermost layer of the fundus. The visual impulses generated by the photoreceptors in the retina are transmitted via bipolar cells to the RGCs. The signal is then relayed to the lateral geniculate nucleus in the brain via the RGC axons, which leave the eye at the optic disc to form the optic nerve. The optic disc is therefore also known as the optic nerve head (57). The base of the optic nerve head is formed by a mesh-like, collagenous structure called the lamina cribrosa, through which the optic nerve fibres pass as they exit the eye. The lamina cribrosa is thought to be the principal site of RGC axonal injury, leading to the characteristic optic disc cupping observed in glaucoma (58).

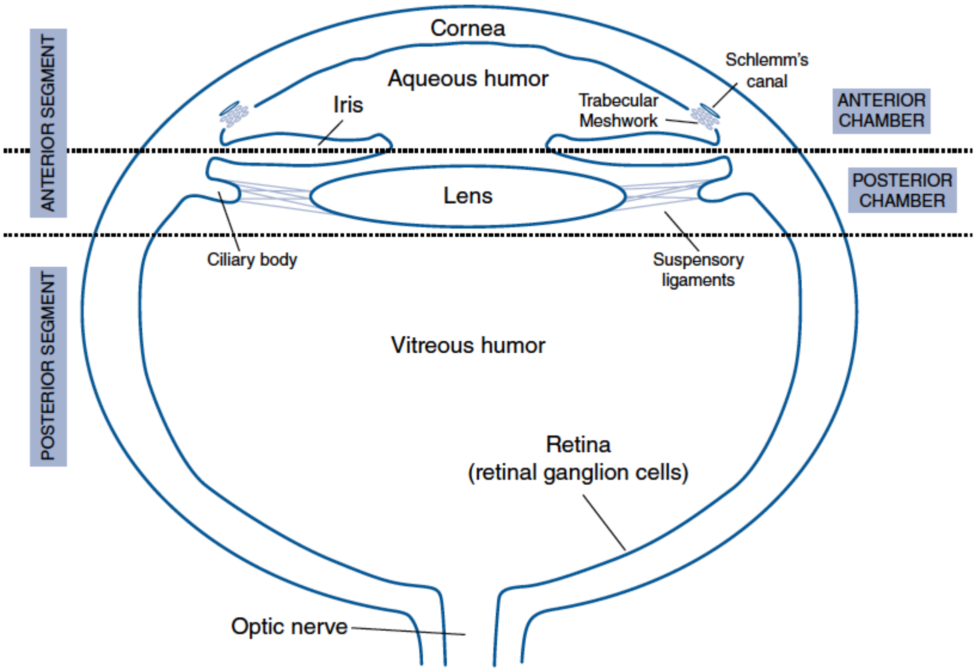

Figure 1.3 Anatomy of the human eye – subdivision into anterior and posterior segment. The anterior segment is further subdivided into the anterior and posterior chamber. Figure reproduced from (55).

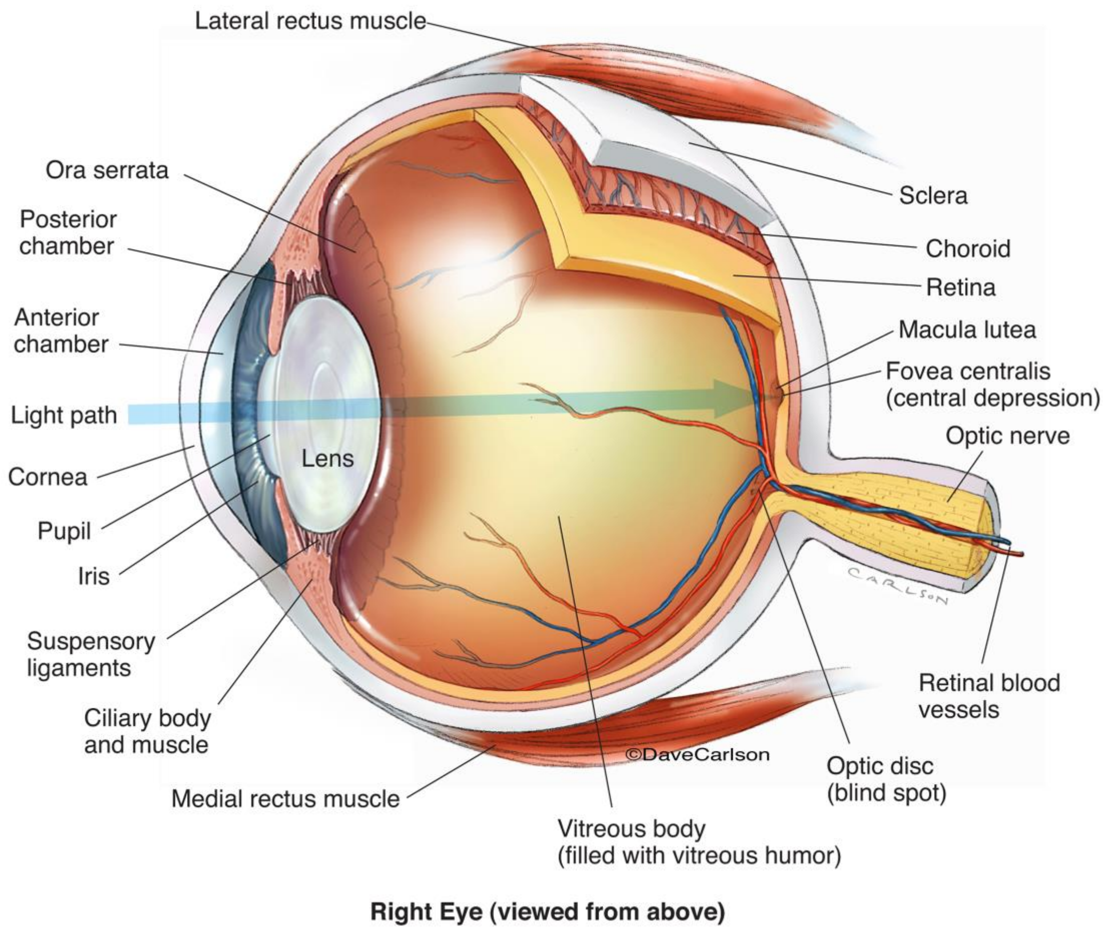

Figure 1.4 Anatomy of the human eye. Reproduced with permission from Carlson Stock Art.

1.2.2 Aqueous humour and the generation of intraocular pressure

Aqueous humour is the clear fluid secreted by the ciliary body (see Figure 1.4) that circulates through the anterior chamber to supply the avascular iris, lens, TM, and cornea with nutrients, as well as removing waste from these tissues (Figure 1.2). It consists of a complex mixture of organic solutes, ions, and proteins (59-62). In addition, the volume of aqueous humour determines IOP, which is critical for eye health, maintenance of correct ocular shape, and clear vision. IOP is closely regulated through the balance between aqueous humour secretion in the posterior chamber and drainage through the trabecular and uveoscleral pathways (63-66). The majority of aqueous humour drains through the trabecular pathway, which involves the TM and Schlemm's canal (67). As aqueous humour secretion is relatively constant and pressure-independent up to high levels of pressure, IOP is predominantly determined by outflow resistance through the trabecular pathway, which is modulated in order to enable IOP homeostasis (47, 68, 69). Whilst it is unclear exactly where and how outflow resistance is generated and regulated (47, 48, 70), there is consensus that the TM plays a key role in the regulation of IOP (71), which will be discussed in section 1.3.1.2.

1.2.3 Altered aqueous humour composition in primary open-angle glaucoma

Aqueous humour contains a vast range of proteins, including many growth factors and cytokines, and several studies have shown that the composition of aqueous humour is altered in POAG, as detailed below. In most cases, the comparison is made to aqueous humour from patients with cataract, as it can be sampled with ease during routine cataract surgery. Ideally, aqueous humour from healthy eyes would serve as the control, but such sample collection would be unethical. Whilst many studies of aqueous humour composition in animal models exist, this review focusses exclusively on human aqueous humour.

Due to the low protein concentration in aqueous humour and the small sample volumes available for testing, laboratory techniques with high sensitivity are preferential for composition analysis, in order to maximise the data generated (72, 73). Two main approaches have been used to date: mass spectrometry and multiplex immunoassay technology. Exploratory studies using mass spectrometry have provided insight into the composition of aqueous humour (74-76) and highlighted several proteins with altered abundance in POAG when compared to cataract control samples. The proteins identified include ones involved in oxidative stress, apoptosis, mitochondrial function, inflammation, metabolism, and proteolysis (77-82), highlighting these processes as potentially relevant to POAG pathogenesis. Whilst mass spectrometry has allowed researchers to take a global, unbiased view of the aqueous humour proteome, the technique's sensitivity limitations make the detection of low abundance proteins (ng/ml and lower), such as cytokines, growth factors, and soluble receptors challenging (72). Multiplex immunoassays on the other hand allow the simultaneous quantification of dozens of proteins per sample. These assays allow the determination of specific protein concentrations, yet the proteins to be tested need to be pre-selected, thus resulting in a biased view of the aqueous humour proteome. Despite the increased sensitivity compared to mass spectrometry techniques, many analytes still escape detection in multiplex immunoassay screens (72).

Of the many proteins present in aqueous humour, only a small number have been studied in some detail with regards to POAG. Several studies have shown significantly increased levels of TGF-β2 in POAG aqueous humour compared to non-glaucomatous cataract samples (summarised in (83)). The effects of TGF-β2 on the TM have been investigated extensively and studies have demonstrated a multitude of consequences on TM physiology, including increased ECM production, inhibition of ECM degradation, and a reduction in TM cellularity (reviewed in (83-85), further discussed in 1.3.2.4). Several *ex vivo* and *in vivo* studies have also indicated that elevated levels of TGF-β2 cause reduced aqueous humour outflow (86-88).

Two further protein families that have been investigated in detail are the matrix metalloproteinases (MMPs) and their endogenous tissue inhibitors (TIMPs). MMPs are proteolytic enzymes that degrade a variety of ECM molecules. Due to their destructive nature, MMP activity requires tight regulation. MMPs are secreted in a latent form and require extracellular cleavage of the pro-domain for activation (89). In addition, TIMPs reversibly bind to MMPs in a 1:1 stoichiometry to obstruct the MMP proteolytic site (90), thus inhibiting their activity. Several members of the MMP family and all four known TIMPs are expressed by TM cells and numerous MMPs and most TIMPs have been measured in human aqueous humour samples (reviewed extensively in (91)). Table 1.1 provides an overview of the reported changes in MMP and TIMP concentrations in POAG aqueous humour compared to cataract.

Table 1.1 Overview of published data regarding levels of MMPs and TIMPs found in human aqueous humour from POAG compared to cataract patients.

Isoform	Status	POAG levels (in comparison to cataract)	References
MMP2	Total	↑ Significant ↑ Non-significant	(92, 93) (94-97)
	Active	↑ Significant ↓ Significant	(92, 98) (97)
MMP3	Total	↑ Non-significant	(92, 97)
	Active	↑ Significant	(92)
	Latent	↑ Significant	(93)
TIMP1	n/a	↑ Significant ↑ Non-significant	(92, 93) (97)
TIMP2	n/a	↑ Significant ↑ Non-significant	(92-95) (96, 97)
TIMP3	n/a	No data available	
TIMP4	n/a	↑ Significant	(92)

Isoforms where only non-significant changes were reported have been excluded from the list. n/a: not applicable.

Whilst some previous publications include the calculation of direct MMP-to-TIMP ratios (ratio of concentrations measured) (92, 93, 97, 99, 100), none have considered the sizeable differences in molecular weight between MMPs and TIMPs. Given that MMPs and TIMPs interact at a 1:1 ratio, a stochiometric analysis that includes the molecular sizes would provide a more accurate indication of MMP-to-TIMP imbalances. Such imbalances are of interest due to the known role of MMPs in outflow facility (101) and the reported changes in TM ECM composition. Specifically, it has been suggested that the excessive accumulation of ECM material within the TM of POAG eyes may be due to imbalanced MMP-to-TIMP ratios (97).

The aqueous humour concentrations of numerous other growth factors and cytokines are also altered in POAG, although the effects of these changes on TM function remain to be elucidated. Increased levels of IL-8, IL-9, IL-10, IL-12, SAA, INFα, INFγ, TNFα, CCL2, and CXCL9 have been reported (102-106), although not all studies were able to detect these factors and only some adjusted their p-values to correct for multiple testing. On the other hand, IL-6 concentrations are reduced in POAG (103, 107). Collectively, these observations have led some researchers to suggest the involvement of inflammatory processes in TM dysfunction and POAG (104, 108, 109). Other specific proteins present in the aqueous humour that have been investigated in relation to POAG include CD44S (110), EPO (111, 112), fibronectin (113), HGF (114), myocilin (115), and VEGF (116).

For the most part, it is unclear how these changes in aqueous humour composition relate to clinical descriptors of POAG, as few studies have investigated correlations extensively. Studies that have assessed correlations have predominantly focussed on IOP, medication, and age (95, 96, 103, 104, 107, 117). Changes in protein abundance may still be relevant to TM dysfunction, even if they do not differ significantly from the concentrations found in cataract control samples. Thus, correlation with clinical descriptors offers an additional approach to analysing data gained from aqueous humour studies and may provide new insights into relevant disease mechanisms.

1.3 TRABECULAR MESHWORK DYSFUNCTION

1.3.1 Structure and function of the healthy trabecular meshwork

1.3.1.1 *Trabecular meshwork architecture - an overview*

The TM is a complex, connective tissue located in the iridocorneal angle, between the cornea, the sclera, and the iris (Figure 1.2). The anatomy of the TM has been reviewed in detail (71, 118). Briefly, the tissue consists of three different structural regions (Figure 1.5). As the aqueous humour leaves the eye via the trabecular pathway, it passes through the uveal meshwork, the corneoscleral meshwork, and finally the juxtacanalicular tissue (JCT), before entering Schlemm's canal. Subsequently, the aqueous humour drains into the episcleral veins. This fluid movement occurs as bulk flow driven by the pressure gradient rather than active transport (118).

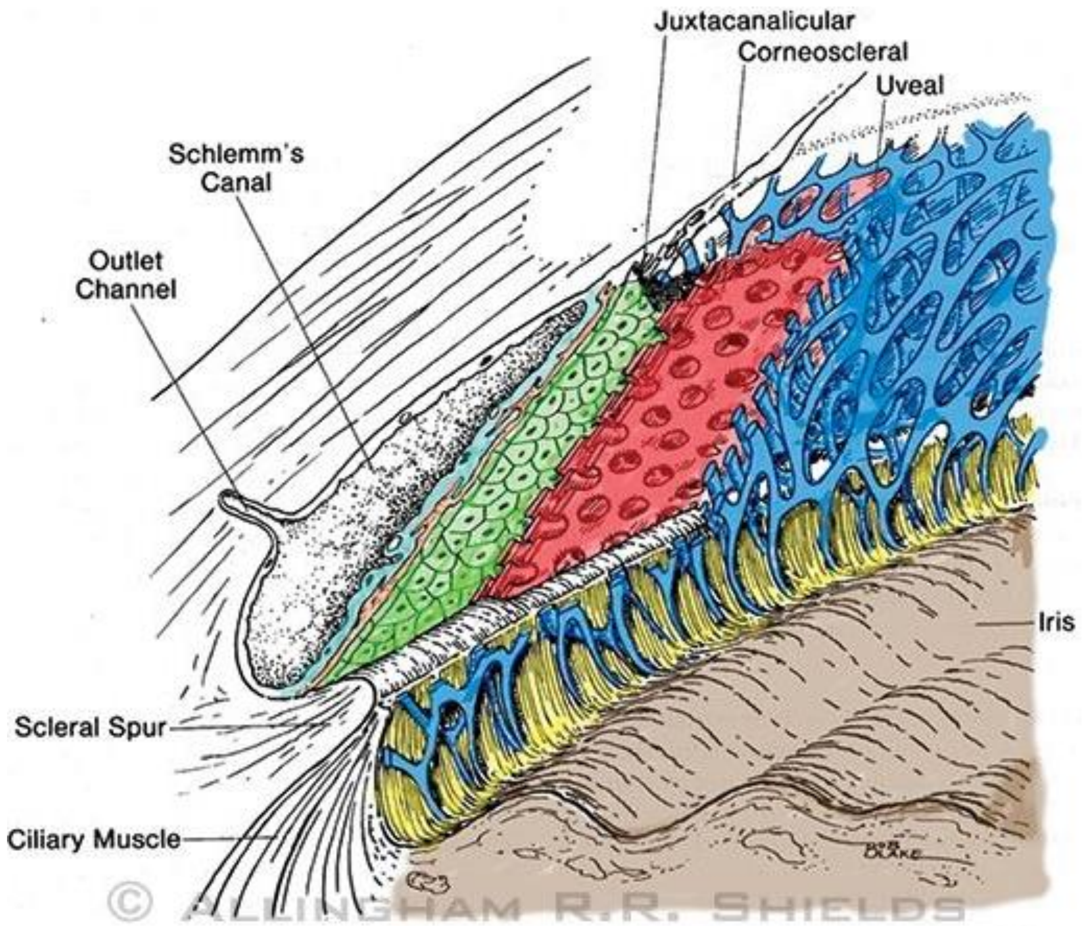

Figure 1.5 Anatomy of the trabecular meshwork. The trabecular meshwork consists of three layers: the uveal meshwork (blue), the corneoscleral meshwork (red), and the juxtacanalicular tissue (green). Figure reproduced from (119).

The uveal meshwork is comprised of a network of trabecular beams covered in a thin, continuous monolayer of flat TM cells. The beams contain densely packed collagen and elastic fibres and the TM cells are situated such that they bridge the intertrabecular spaces and connect adjacent beams. The corneoscleral meshwork, which forms the thickest layer of the TM, is made of perforated collagen and elastin sheets covered in TM cells. Both the uveal and the corneoscleral meshwork are highly porous and thus do not contribute significantly to outflow resistance (reviewed in (118, 120)). Instead, they function as a self-cleansing biological filter, responsible for clearing cellular debris and reactive oxygen species that could prevent the JCT from functioning (71). Unlike the uveal and corneoscleral meshwork, the JCT, which lies adjacent to the inner wall of Schlemm's canal, lacks trabecular beams and instead consists of TM cells loosely arranged in a fibrillar ECM forming an irregular network (120). The JCT, in combination with the inner wall endothelium of Schlemm's canal, is thought to be the site where outflow resistance is generated (47, 48).

1.3.1.2 *Biological properties of trabecular meshwork cells*

The TM has two primary roles: filtration of the aqueous humour and generation of outflow resistance. In order to fulfil these responsibilities, TM cells execute a diverse range of biological functions (summarized in Table 1.2). Due to their morphology, TM cells have often been referred to as endothelial-like cells (121-123). Whilst they do exhibit endothelial cell behaviours (see Table 1.2), this description fails to recognise many critical aspects of TM cells. Recently, Stamer and Clark published a comprehensive review of the TM cell's diverse biological properties (71), which highlighted that TM cells assume behaviours typical of macrophages, fibroblasts, endothelia and smooth muscle cells, in order to maintain outflow resistance and successfully respond to the wide-ranging stressors experienced by the TM, which include phagocytic, mechanical, metabolic, and oxidative stresses.

Table 1.2 The diverse biological functions of trabecular meshwork cells correspond to different cell phenotypes and behaviour. Table reproduced from (71).

Phenotype	Location	Cell behaviour	Responsibilities
Endothelial	Uveal/corneoscleral	Endothelia Macrophage	Maintain passageway patency Neutralize reactive oxygen species Biological filter/ phagocytosis Immune mediation
Fibroblastic	Juxtacanalicular tissue	Fibroblast Smooth muscle	ECM turnover/tissue repair Contractile tone Mechanotransduction

1.3.1.2.1 Resistance generation

The TM's central role is the generation and regulation of aqueous humour outflow resistance, in order to maintain IOP within an acceptable physiological range. Resistance generation is thought to occur in the JCT, in conjunction with the inner wall endothelium of Schlemm's canal and its basement membrane (47, 48, 124, 125). Specifically, the ECM of the JCT has been suggested to play a major role in determining aqueous humour outflow resistance (68, 120, 126-128), although other mechanisms have been proposed and resistance generation is yet to be fully understood (48, 129). The TM ECM and its components, which have been reviewed in detail (68, 118), are not static, as the ECM undergoes continuous remodelling to maintain open outflow pathways (120). In addition, elevated IOP is sensed in the JCT through mechanical stretch, triggering a cascade of events to alter ECM composition and thus outflow resistance. These processes, referred to as IOP homeostasis, involve the secretion of ECM proteins and their corresponding degradation enzymes (reviewed in (69, 130)). One major group of proteinases involved in ECM degradation are MMPs. Several MMPs are expressed by TM cells and mechanical stretching, increased pressure, and treatment with specific cytokines can lead to an increase in MMP expression levels (91, 130). The importance of MMPs, and thus ECM turnover, in controlling aqueous humour outflow was initially demonstrated by treating perfused anterior segments with MMPs or agents that stimulate MMP expression, which led to increased aqueous outflow. On the contrary, inhibition of MMP activity through the addition of TIMPs reduced outflow facility (101).

In addition to ECM composition, cellular contraction is also involved in regulating aqueous humour egress and the two are linked through integrin signalling. Thus, changes to the ECM are transmitted to the intracellular space and can affect cell contraction (131, 132). Both the TM and the JCT contain contractile cells, allowing them to alter the geometry of the outflow pathways (129). Specifically, contraction of TM cells leads to increased outflow resistance, whereas relaxation enhances aqueous humour egress (reviewed in (133, 134)). The contractile state of the ciliary muscle and the scleral spur cells (see Figure 1.5) further influence the geometry of the trabecular outflow pathways (reviewed in (129, 135)).

1.3.1.2.2 Aqueous humour filtration

Filtration of aqueous humour is thought to be critical for TM homeostasis, as the presence of debris in the JCT could obstruct aqueous humour outflow and prevent proper resistance generation (136-138). The TM cells in the uveal and corneoscleral meshwork are highly phagocytic (139-142), which allows them to clear cellular debris, reactive oxygen species, pigment granules, and pseudoexfoliative material present in the aqueous humour (reviewed in (71)). In addition, phagocytosis has been shown to affect the expression of ECM remodelling enzymes (143), suggesting it may also play a role in TM ECM homeostasis.

1.3.2 Trabecular meshwork dysfunction in primary open-angle glaucoma

Aqueous humour outflow resistance is elevated in glaucomatous eyes when compared to age-matched controls (144). The cause of increased outflow resistance in the TM is still unknown and many theories have been postulated. Rather than offering an exhaustive summary of each hypothesis presented in the literature, this section provides an overview of mechanisms that have been studied in considerable detail and that are relevant to the investigations contained in this thesis. The diverse range of processes studied in the field suggests that impaired regulation of outflow facility is likely due to a complex combination of changes, both at the cellular and tissue level, that lead to TM dysfunction.

Much of the current knowledge on TM cell dysfunction in POAG has come from studies using cultured TM cells. To date, no unique genetic marker or feature has been determined for TM cells, making identification of TM cells reliant on a combination of criteria. Due to a lack of consensus, different laboratories have used varying criteria to characterise TM cell cultures in the past, including morphology, the expression of various marker genes, corticosteroid induction of cross-linked actin networks (CLANs), phagocytic capacity, and Dexamethasone-stimulated myocilin upregulation (145-148). Further known cellular responses, as well as a list of positive and negative selection markers, are summarised in a recent review by Stamer and Clark (71). The lack of consensus for TM cell characterisation *in vitro* was recently addressed in a publication by Keller et al. (149), recommending the use of a panel of marker genes in combination with functional assays, in particular myocilin induction by Dexamethasone, which is considered the most reliable assay for functional TM characterisation.

1.3.2.1 *Reduced trabecular meshwork cellularity*

A gradual reduction in TM cell numbers is part of the aging process in healthy eyes (150, 151). Continuous TM cell loss occurs at a similar rate in POAG, but overall cellularity is lower than in age-matched controls (152). In addition, a greater number of senescent cells has been determined in the glaucomatous TM (153). The loss of TM cells leads to areas where trabecular beams are no longer covered, which has been suggested to cause the fused trabecular beams observed in eyes with advanced POAG (152, 154, 155). It has been hypothesised that reduced cell numbers affect the TM's ability to respond to increased pressure, which TM cells sense through mechanical distortion (120).

The mechanisms involved in TM cell death remain unclear. In a recent review, Green et al. (156) examined five cell death pathways (apoptosis, autophagy, necroptosis, pyroptosis, and immunogenic apoptosis), all of which may contribute to reduced TM cellularity, and suggested that immunogenic apoptosis is the most likely, due to the involvement of oxidative and ER stress in TM dysfunction. Based on animal studies, it has been suggested that phagocytic TM cells may leave the meshwork upon engulfing foreign particles, which could also contribute to reduced cellularity (140, 142, 157, 158). However, subsequent studies using human perfused anterior segments saw little to no cell loss in response to phagocytic challenge in single exposure experiments (139, 159).

1.3.2.2 *Abnormal extracellular matrix accumulation in the trabecular meshwork*

The composition of the TM ECM changes with age and POAG (155, 160-162) and characteristic structural alterations have been described in the JCT of POAG eyes (reviewed in (121, 155)). The quantity of sheath-derived plaques is significantly increased in POAG compared to age-matched controls (160, 161). Whilst the amount of plaque material in the JCT has been correlated with severity of optic nerve damage in POAG, no correlation was found with IOP (163), which may suggest that these changes are a consequence rather than a cause of POAG (135). In contrast to many ECM components, the amount of hyaluronic acid found in the TM is reduced in POAG (164). Treatment of TM cells with hyaluronic acid *in vitro* stimulated MMP2 and MMP9 expression (165). Inhibition of hyaluronic acid synthesis reduced outflow facility in perfused human anterior segments and led to decreased levels of ECM proteins fibronectin and versican (166, 167). Thus, the reduced hyaluronic acid levels seen in POAG may contribute to abnormal ECM accumulation. Some researchers have proposed that the ECM changes seen in the glaucomatous TM may be described as fibrosis (132, 168-170) and many have hypothesized that elevated outflow resistance is due to changes in the TM ECM. A key finding that supports the latter is that perfusion of anterior eye segments with MMPs increases outflow facility (101).

1.3.2.3 *Altered trabecular meshwork cell contraction state*

The discovery that TM cells are contractile (171) and that TM cell tone affects outflow facility (134) led to another hypothesis; increased outflow resistance in POAG may be due to an elevated TM cell contraction state, leading to increased rigidity and reduced outflow facility. Chemical disruption of the actin cytoskeleton leads to increased outflow facility (133, 172), an observation that supports the contraction hypothesis.

1.3.2.4 *Effects of elevated TGF-β2 in aqueous humour*

TGF-β2, which is elevated in aqueous humour samples from POAG patients (117, 173-176), is hypothesized to play a causative role in TM dysfunction (84, 177). Cultured TM cells treated with TGF-β2 increase their ECM synthesis, which is mediated through connective tissue growth factor (CTGF) (178). TGF-β2 also stimulates the expression of tissue transglutaminase (TGM2) and lysyl oxidases, which crosslink components of the ECM, thereby making them more resistant to degradation (179-181). TGF-β2 has been shown to further inhibit ECM proteolysis by reducing MMP activity (182) and perfusion of anterior segments with TGF-β2 led to reduced outflow facility (86, 183). These findings suggest that TGF-β2 is a key player in the ECM changes observed in the glaucomatous TM (129, 184).

The actin cytoskeleton of TM cells is also influenced by TGF-β2. Mediated through CTGF signalling (185), TGF-β2 causes elevated expression of α-smooth muscle actin (αSMA) and fibronectin, increased contractility of the actin cytoskeleton, and induction of actin stress fibres (185-187). Whilst it is unclear if elevated levels of TGF-β2 cause increased contractility and αSMA levels *in situ*, differences in the actin cytoskeleton of TM cells have been reported between POAG and control eyes (188). An increased number of CLANs have been observed in glaucomatous compared to healthy TM cells *in vitro* (189), a phenomenon that is inducible by TGF-β2 (190). However, CLANs appear to be mainly associated with steroid-induced glaucoma (191, 192). It is worth noting that the effects of TGF-β2 on TM cells are dependent on substrate stiffness (187), which is not reflected in *in vitro* studies where cells are grown as a monolayer on plastic ware.

1.3.2.5 *Increased trabecular meshwork stiffness*

TM tissue stiffness is increased in POAG eyes when compared to normal eyes (193). Increased stiffness is thought to be due to the reduction in TM cells (193-195), as well as altered ECM deposition, increased actin cytoskeleton, and enhanced ECM crosslinking (147, 181). The presence of pathological calcification in the glaucomatous TM has also been suggested, based on the observation that enzymatic activity of the calcification marker alkaline phosphatase is increased and levels of calcification inhibitor MGP are reduced in POAG (196), thus presenting another potential contributor to increased TM stiffness. In cell culture experiments, increased substratum stiffness was linked to an increase in actin stress fibres and altered expression levels of several proteins including myocilin, α-SMA, and TGM2 (197, 198). These data have led some researchers to hypothesise that the increase in stiffness may impair the ability of TM cells to sense IOP elevation, thus preventing the necessary outflow modulation required to bring IOP back to a physiological level (69, 129).

1.3.2.6 *Further potentially relevant mechanisms*

Many more mechanisms have been suggested to be causative of TM dysfunction, such as increased oxidative stress (125, 199), autophagy (200, 201), and inflammation (104, 108, 109). The many hypotheses that exist are not mutually exclusive and some attempts have been made to decipher how they relate to each other (see Figure 1.6) (202). Given the complex nature of POAG, it is unclear which of the observed changes in the TM and the aqueous humour are causal and which are a consequence of the disease. IOP dysregulation is yet to be fully understood and it is currently unclear how these mechanisms fit together, or indeed which are the most critical to POAG pathogenesis.

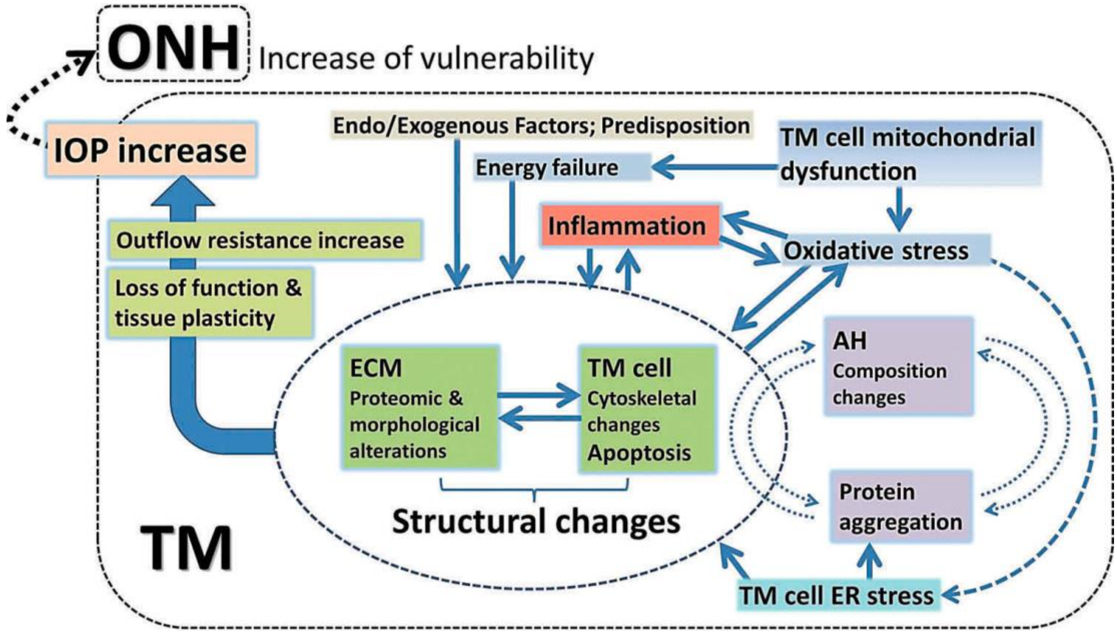

Figure 1.6 Model illustrating the wide range of factors thought to be involved in TM dysfunction, leading to increased outflow resistance and elevated IOP. Figure reproduced from (202). ONH: optic nerve head; IOP: intraocular pressure; TM: trabecular meshwork; ECM: extracellular matrix; AH: aqueous humour; ER: endoplasmic reticulum.

1.4 Specific Aims and Significance

1.4.1 Thesis objective and specific aims

The review of the literature has highlighted several gaps in our current knowledge regarding the changes in aqueous humour composition and how these relate to TM dysfunction and POAG. The objective of this thesis is to address some of these gaps, first by assessing changes in aqueous humour composition and relating these to disease descriptors, and secondly by applying this knowledge to an *in vitro* cell culture model to assess the effect of altered aqueous humour composition on TM cell function. In addition to enhancing our understanding of TM cell function, such *in vitro* functional studies may also help to explain the associations determined between specific aqueous humour proteins and clinical measures and may ultimately identify new treatments for POAG. Specifically, the aims of this thesis are as follows:

1) To quantify differences in aqueous humour composition between clinical samples from POAG and cataract control patients using multiplex assays and subsequently evaluate correlations with clinical parameters of POAG.
2) To characterise a commercial human TM cell line for use as a cell culture model, using gene expression and functional assays.
3) To determine the effect of a selected protein of interest (chosen from aim 1) on commercial human TM cells using a functional assay.

1.4.2 Significance

The mechanisms underlying TM dysfunction and IOP dysregulation remain unclear. In order to elucidate the disease aetiology (or potentially aetiologies), more information is required regarding the changes that occur in the aqueous humour and TM among other things. This thesis presents new insights with regards to aqueous humour composition, which may help to further our understanding of TM dysfunction and how different processes interact with each other. Furthermore, the information may prove to be useful in the search for biomarkers and the development of new diagnostic and treatment strategies. The *in vitro* study presented in chapter 4 forms a first step in the process of assessing the potential impact of specific aqueous humour proteins on TM function, in an attempt to understand how the TM responds to altered aqueous humour composition.

1.5 Thesis outline

Chapter 1 provides an overview of the literature and highlights areas where more research is needed.

Chapters 2 and 3 comprise two published studies, assessing a range of protein concentrations in aqueous humour samples from POAG and cataract control patients and investigating correlations with clinical descriptors including CDR, IOP, PSD, age, and disease duration (aim 1).

Chapter 2 is concerned with MMPs and TIMPs and assesses changes in aqueous humour concentrations as well as altered ratios between MMPs and TIMPs, which interact at a 1:1 ratio.

Chapter 3 investigates a series of proteins that have previously been identified in aqueous humour by means of discovery-based proteomic studies. This study highlighted HGF, FLRG and uteroglobin as proteins of interest in POAG.

Chapter 4 presents the final study of this thesis and consists of the characterisation of commercial primary TM cells as an *in vitro* model, followed by an assessment of recombinant uteroglobin treatment on TM cell function (aims 2 and 3).

Finally, a general discussion, conclusions, and future directions are presented in Chapter 5.

CHAPTER 2 TIMP1, TIMP2, AND TIMP4 ARE INCREASED IN AQUEOUS HUMOR FROM PRIMARY OPEN ANGLE GLAUCOMA PATIENTS

The research contained within this chapter is unedited and has been published as:

Ashworth Briggs EL, Toh TY, Eri R, Hewitt AW, and Cook AL. TIMP1, TIMP2, and TIMP4 are increased in aqueous humor from primary open angle glaucoma patients. *Mol Vis* 2015;21:1162-1172.

2.1 ABSTRACT

2.1.1 Purpose

Elevated intraocular pressure (IOP) is the only known modifiable risk factor for primary open-angle glaucoma (POAG), and it can be caused by reduced aqueous humour outflow from the anterior chamber. Outflow is predominantly regulated by the trabecular meshwork, consisting of specialised cells within a complex extracellular matrix (ECM). An imbalance between ECM-degrading matrix metalloproteinases (MMPs) and tissue inhibitors of MMPs (TIMPs) within the trabecular meshwork is thought to contribute to POAG. This study aimed to quantify levels of TIMPs and MMPs in aqueous humour samples from glaucomatous and non-glaucomatous eyes, analyse MMP/TIMP ratios, and correlate results with age, IOP and Humphrey's visual field pattern standard deviation (PSD).

2.1.2 Methods

Aqueous humour samples were collected from 26 non-glaucomatous control subjects prior to cataract surgery and 23 POAG patients undergoing trabeculectomy or cataract surgery. Analyte concentrations were measured using multiplexed

immunoassays. Statistical significance was tested with Mann-Whitney U tests, and Spearman's method was used to assess correlations with age, IOP and PSD.

2.1.3 Results

Concentrations of TIMP1 ($p=0.0008$), TIMP2 ($p=0.002$), TIMP4 ($p=0.002$) and MMP2 ($p=0.020$) were significantly increased in aqueous humour from POAG versus cataract samples. For the majority of MMP/TIMP molar ratios calculated for the cataract group, TIMPs outweighed MMPs. In POAG, molar ratios of MMP2/TIMP1 ($p=0.007$) and MMP9/TIMP1 ($p=0.005$) showed a significant decrease, corresponding to an elevated excess of TIMPs over MMPs in POAG compared to cataract samples. Conversely, MMP2/TIMP3 ($p=0.045$) and MMP3/TIMP3 ($p=0.032$) molar ratios increased. Several MMP/TIMP molar ratios correlated with IOP ($r=0.476$-0.609, $p=0.007$-0.034) and PSD ($r= -0.482$ to -0.655, $p=0.005$-0.046) in POAG samples and with age in cataract control samples.

2.1.4 Conclusions

An imbalance among MMPs and TIMPs was found in glaucomatous aqueous humour samples, with a shift towards raised TIMP levels. This may result in the inhibition of MMP activity, leading to an altered ECM composition in the TM and thereby contributing to increased outflow resistance.

2.2 Introduction

Glaucoma is a complex optic neuropathy involving loss of peripheral vision and ultimately leading to blindness if untreated (4). Worldwide, over 60 million people are affected by glaucoma, the majority of which can be classified as having primary open-angle glaucoma (POAG) (13, 203). Although the disease aetiology is not completely understood, an elevated intraocular pressure (IOP) is a major risk factor and is currently the sole target of drug intervention (36, 42).

Intraocular pressure is predominantly determined by the balance between aqueous humour production by the ciliary body and its outflow through the trabecular meshwork (TM) and uveoscleral pathways. The TM is a complex tissue located in the iridocorneal angle and consists of specialised cells embedded in an extracellular matrix (ECM) (68, 120, 204). Regulation of aqueous humour outflow resistance is one of the TM's key roles, which is achieved by modification of the ECM composition (130), along with contraction of the ciliary muscle and alteration of TM cell shape to modify the geometry and thus permeability of the TM (118, 133). TM composition is known to change with age, including a reduction in TM cellularity and an increase in ECM accumulation (205). These alterations appear to occur largely in patients with glaucoma and they are considered to result in a reduced outflow facility and consequently increased IOP (205).

ECM composition is regulated by the continual specific degradation of ECM components and the selective deposition of new ECM material produced by TM cells including collagens, glycosaminoglycans, proteoglycans, fibronectin and elastin-containing microfibrils (68, 206, 207). Interestingly, fibronectin is also present in the aqueous humour, and significantly elevated concentrations have been reported in the aqueous humour of POAG patients compared to cataract controls (113). The selective degradation of ECM components involves matrix metalloproteinases (MMPs), a family of secreted zinc-dependent proteinases with selective substrate specificity (208). MMP synthesis and activity are tightly regulated, with MMPs secreted as pro-enzymes and activated extracellularly, where their activity is controlled by endogenous inhibitors (89). Tissue inhibitors of metalloproteinases (TIMPs) are potent albeit non-selective inhibitors of active MMPs, inhibiting proteolytic activity by obstructing the active site in a tight, reversible interaction with a 1:1 stoichiometry (90).

It has been suggested that an imbalance in MMP-to-TIMP ratio could be involved in the development of glaucoma, due to reported changes in ECM composition and an increased deposition of ECM components in the TM of glaucoma patients (97). Several groups have also described altered MMP and TIMP concentrations in glaucomatous aqueous humour samples in comparison to non-glaucomatous cataract aqueous samples (92, 94, 97). However, the extent to which these imbalances correlate with any relevant clinical descriptors is not known. Thus, the aim of this study was to assess differences in TIMP and MMP concentrations in aqueous humour samples from POAG and non-glaucomatous cataract patients to evaluate changes in MMP-to-TIMP ratios by means of stoichiometric analyses. In addition, the study aimed to correlate these results with disease-associated parameters including age, IOP, optic cup-to-disc ratio (CDR), degree of visual field loss, quantified by Humphrey's visual field pattern standard deviation (PSD) score, and disease duration.

2.3 MATERIALS & METHODS

2.3.1 Patient eligibility and recruitment

This study was approved by the Health and Medical Human Research Ethics Committee Tasmania (EC00337) and executed in adherence to the tenets of the Declaration of Helsinki. All participants were recruited through the Launceston Eye Doctors and the Launceston Eye Institute and gave written consent with regards to the donation and use of aqueous humour samples.

2.3.2 Clinical assessment

Clinical descriptors including age, IOP, CDR, PSD, and disease duration were recorded for POAG patients. A diagnosis of POAG was made based on the characteristic optic disc cupping, corresponding visual field loss and thinning of the retinal nerve fibre layer recorded on the ocular coherence tomography (OCT), irrespective of the presenting IOP. A gonioscopic examination was also performed to classify the anatomy of the drainage angle. IOP was measured in all patients using a calibrated Goldmann Applanation tonometer. For this study, only the latest treated IOP measurement taken during the consultation prior to the surgery was used. Vertical CDR was estimated by one observer (TYT) using a 60D lens during indirect slit lamp fundoscopy and then confirmed with an optic disc profile scan on OCT. PSD was obtained from the SITA Fast 24-2 Humphrey Visual Field analyser, which was used under standard settings. PSD was chosen over mean deviation, as the latter did not permit a clear differentiation between any cataract effects on the field test and glaucoma-induced visual field loss, specifically in glaucoma patients undergoing cataract surgery or a combined procedure. The PSD score emphasises a focal variation in the visual field that highlights typical glaucomatous field loss. A greater PSD score indicates a denser field defect that correlates with disease severity. Disease duration was recorded as number of years since diagnosis at the time the aqueous humour samples were collected. All POAG patients recruited were receiving IOP-lowering medication, in the form of monotherapy or a combination of up to four of the following compounds: Timolol (β-blocker), Brimatoprost, Tafluprost, Latanoprost (prostaglandin derivatives), Brimonidine (α2 agonist), Dorzolamide and Brinzolamide (carbonic anhydrase inhibitors).

2.3.3 **Aqueous humour collection**

Aqueous humour samples (generally 50 – 100 μl) were obtained from 23 patients with POAG during either trabeculectomy or cataract surgery. POAG patients who had previously had a trabeculectomy or vitrectomy were excluded. To serve as a control, aqueous humour samples from 26 non-glaucomatous patients undergoing routine cataract surgery were collected. Case and control subjects were excluded if they had other retinal (such as diabetic retinopathy or age-related macular degeneration) or neurologic diseases. For all samples, aqueous humour was collected from the centre of the anterior chamber by paracentesis at the beginning of surgery, immediately frozen at -20°C, and transferred to -80°C within 48 hours, where they were stored for analysis.

2.3.4 **Quantification of MMPs and TIMPs**

Aqueous humour samples were analysed using the following magnetic bead-based multiplex assays: Magnetic Luminex Human TIMP multiplex kit (R&D Systems, Inc., Minneapolis, MN) and a custom Magnetic Luminex human premixed multi-analyte kit (R&D Systems). Using these kits, the concentrations of the following analytes were measured: TIMP1 (tissue inhibitor of metalloproteinase 1), TIMP2, TIMP3, TIMP4, MMP-1 (matrix metalloproteinase-1), MMP-2, MMP-3, MMP-7, MMP-8, MMP-9, MMP-12 and MMP-13. The assays were performed in accordance with the manufacturers' instructions on a Bio-Plex 200 System (Bio-Rad Laboratories, Inc., Hercules, CA). Aqueous humour samples were diluted 1:2.4 for the custom kit and 1:6 for the TIMP kit using the assay diluents provided, and 50 μl of diluted sample was added to each well. Fluorescence intensity (FI) was acquired and analysed using Bio-Plex Manager 6.0. Concentrations out of range were generally below the measurable concentration, with the exception of TIMP1 and TIMP2 (n=3 and 1 samples, respectively), which gave FI readings above the highest standard and thus were excluded from all analyses. The number of samples in range is given for each analyte concentration reported and median values were determined using only the measurable samples.

2.3.5 **Statistical analyses**

All statistical analyses were conducted with Prism 6 (GraphPad Software, San Diego, CA) using two-tailed tests with a p-value <0.05 regarded as statistically significant, unless otherwise noted. Differences with regards to age and gender were assessed using an unpaired t test and Fisher's exact test, respectively. The D'Agostino-Pearson omnibus normality test was used to assess normality of analyte concentration distributions, and subsequent comparison of analyte concentrations between POAG and cataract control samples was performed using the Mann-Whitney U test. Correction for multiple testing was performed using Bonferroni's method (adjusted $p=0.004$).

Further analyses included a calculation of molar MMP/TIMP ratios to assess potential imbalances, followed by correlation of analyte concentrations and MMP/TIMP ratios to clinical descriptors using Spearman's method. These analyses were performed only on analytes that were detected in at least 50% of cataract control and POAG samples.

Due to significant differences in size between MMPs (27.9 – 76.4 kDa) and TIMPs (20.7 – 22.4 kDa), molecular weight was taken into consideration for stoichiometric analysis of MMP-to-TIMP ratios. Thus, measured protein concentrations (pg/ml) were converted to mol/l using the amino acid sequence obtained from the UniProtKB database (www.uniprot.org; access date 18 June 2014) (209). The signal sequence, indicated in the database, was removed prior to molecular weight calculation (Appendix 1) using the ExPASy ProtParam tool (web.expasy.org/protparam; access date 18 June 2014) (210). Stoichiometric analyses combining each MMP with each TIMP were performed on individual samples and reported as median values with interquartile range. Because TIMPs are known to be non-selective in their MMP-inhibitory activity, we calculated all possible molar ratios using only the TIMPs and MMPs that were measured in more than 50% of cataract and POAG samples, with the number of molar ratio analyses precluding the adjustment of resulting p-values for multiple comparisons. Statistical significance was assessed using the Mann-Whitney U test ($p<0.05$ considered significant).

2.4 Results

In this study, a total of 23 POAG and 26 cataract control samples were analysed, measuring all four known TIMPs and several members of the MMP family. Clinical descriptors including age, IOP, PSD, CDR, and disease duration were collected for all POAG samples and are presented in Table 2.1. No significant differences were found between the cataract control and the POAG group with regards to age (p=0.226) or gender (p=0.245). However, a positive correlation was determined between PSD and CDR for the POAG group (r=0.654, p=0.0007). Correlations between all other clinical descriptors were non-significant. All POAG patients were treated with IOP-lowering medication; 95% were prescribed a prostaglandin derivative, of which 80% simultaneously received the β-blocker Timolol. Furthermore, 43% of POAG patients were treated with an α-2 agonist and 62% received a carbonic anhydrase inhibitor. The majority of POAG patients were treated with a combination of two or three compounds.

Table 2.1 Clinical data of non-glaucomatous cataract and POAG patients

Parameters	**Cataract**	**POAG**	**p-value**
Age (Mean ± SD)	74.8±7.0	72.2±7.8	0.226
Sample number (M/F)	26 (13/13)	23 (16/7)	0.245
IOP (Median, IQR)	N/A	22.0, 19.0-23.0	N/A
PSD (Median, IQR)	N/A	3.47, 2.16-8.36	N/A
CDR (Median, IQR)	N/A	0.85, 0.7-0.9	N/A
DD (Mean ± SD)	N/A	5.78±3.0	N/A

POAG: Primary open-angle glaucoma; SD: standard deviation; M: male; F: female; IOP: intraocular pressure in mmHg; PSD: pattern standard deviation; CDR: optic cup/disc ratio; DD: disease duration (years); IQR: interquartile range; N/A: not available. Statistical significance was assessed using unpaired *t* test (age) and Fischer's exact test (gender) and $p<0.05$ was considered significant. All POAG patients were receiving IOP-lowering medications and all IOPs reported correspond to treated IOPs.

2.4.1 The levels of TIMP1, TIMP2 and TIMP4 are significantly increased in glaucomatous aqueous humour samples

In both POAG and cataract control aqueous humour samples, TIMP1, TIMP2, TIMP3 and MMP2 were present at the highest concentrations, ranging from 4 to 25 ng/ml (Table 2.2). Concentrations measured for MMP3, MMP7, MMP8, MMP9 and MMP13 were between 100 and 660 pg/ml, whereas TIMP4, MMP1 and MMP12 were present at concentrations below 100 pg/ml. The analyte concentrations obtained in this study are broadly consistent with those reported in the existing literature (92, 94, 95, 97, 100). MMP7, MMP8, MMP12 and MMP13 could only be measured in a small number of samples (Table 2.2), with ≥50% of samples below the detection limits of the assay in both POAG and cataract control samples; consequently, these analytes were excluded from all subsequent analyses. Nevertheless, the proportion of samples in which MMP7, MMP8, MMP12 and MMP13 were out of range was not significantly different between the control and POAG groups (Fisher's exact test p=0.184 – 1.0).

A comparison of POAG aqueous humour samples to cataract control samples revealed higher concentrations in POAG for the majority of analytes, but for many this difference did not reach statistical significance. However, significant differences in concentration were seen for TIMP1 (p=0.0008), TIMP2 (p=0.002) and TIMP4 (p=0.002), with all three analytes presenting an increased median concentration in POAG (Table 2.2 and Figure 2.1). The increases in TIMP1, TIMP2 and TIMP4 remained significant after correction for multiple testing (adjusted p-value = 0.004). In addition, the median concentration of MMP2 was also increased in POAG (p=0.020; Table 2.2 and Figure 2.1). No sample was consistently above the 95th percentile across all analytes measured, and with regards to the statistically significant analytes, the highest concentrations plotted in Figure 2.1 stem from different individuals. Furthermore, the highest concentrations measured for TIMP1 and TIMP2 were outside the range of the assay standard curve and thus for TIMP1 and TIMP2, these samples were excluded prior to analysis.

Table 2.2 Aqueous humour analyte concentrations in cataract control versus POAG

	Cataract			**POAG**			
Analyte	**Median**	**IQR**	**In Range**	**Median**	**IQR**	**In Range**	**p-value**
TIMP1	7235	6062-8508	24/24	11226	8757-18434	17/20	**0.0008**
TIMP2	15298	13200-17767	24/24	20735	16167-30406	19/20	**0.002**
TIMP3	3967	2941-5380	24/24	4610	2941-6647	20/20	0.396
TIMP4	43.9	43.9-50.3	15/24	57.6	47.2-97.6	16/20	**0.002**
MMP1	25.0	18.5-34.4	25/26	31.5	16.9-99.0	22/23	0.406
MMP2	20641	16730-24127	26/26	24965	20458-36854	22/23	0.020
MMP3	418.3	293.4-644.5	25/26	660.3	318.8-1272.0	23/23	0.149
MMP7	261.8	230.2-270.5	3/26	361	178-637	8/23	0.606
MMP8	208.8	53.9-293.2	7/26	108.4	57.8-181.8	6/23	0.311
MMP9	187.6	129.4-347.4	26/26	179.6	114.6-376.5	22/23	0.778
MMP12	36.2	28.9-39.7	6/26	38.3	33.6-45.9	5/23	0.307
MMP13	140.9	107.8-206.0	10/26	199.2	155.2-205.8	6/23	0.367

Median and interquartile range (IQR) calculated for values in range reported as pg/ml. Significance was tested using the Mann-Whitney U test and a p-value <0.05 was considered significant. Correction for multiple testing was performed using Bonferroni's method (adjusted p-value= 0.004) and p-values that remained significant are highlighted in bold.

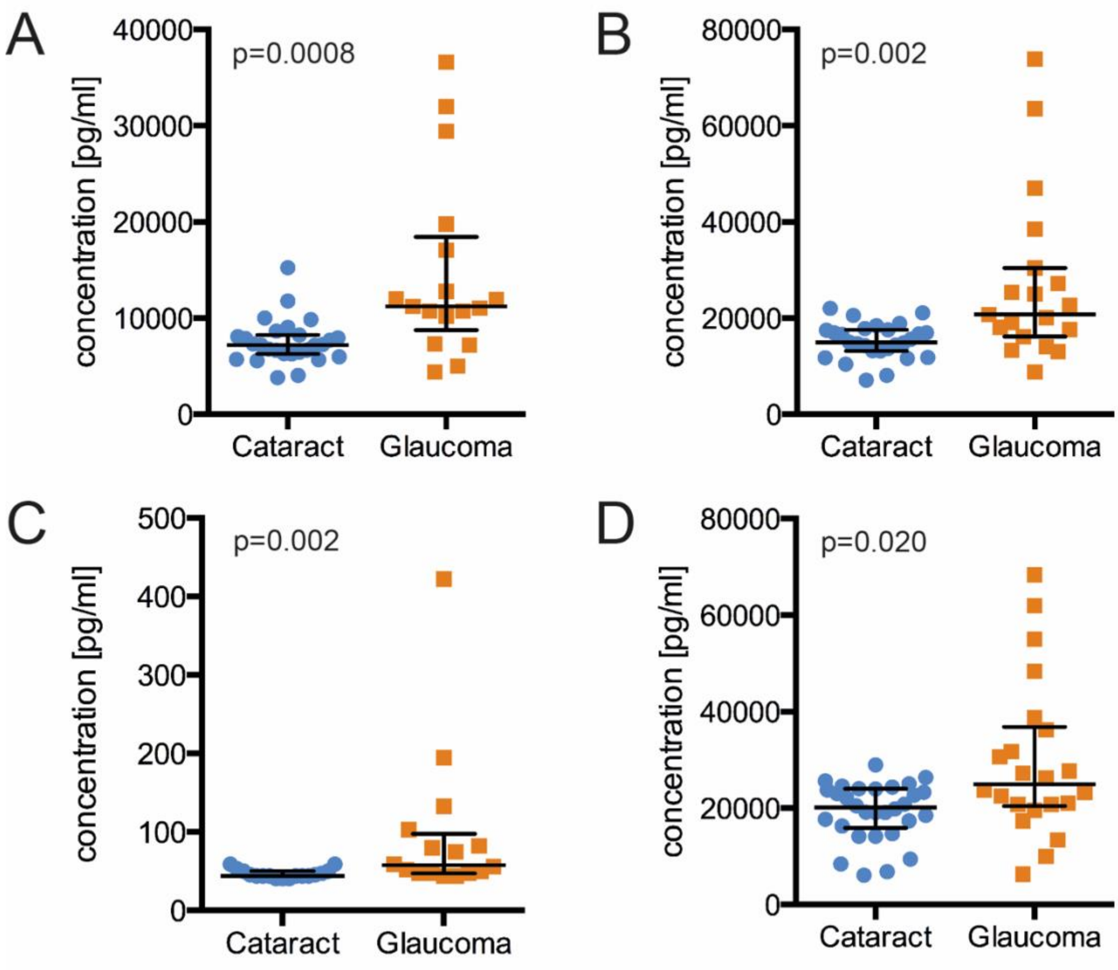

Figure 2.1 Distribution of TIMP1 (A), TIMP2 (B), TIMP4 (C) and MMP2 (D) concentrations in aqueous humor from non-glaucomatous cataract (blue) versus POAG (orange). Levels of all four analytes shown were significantly increased in POAG aqueous humor, as determined using Mann-Whitney U ($p<0.05$). Medians and interquartile ranges are indicated. See Table 2.2 for complete list of analyte concentrations measured.

Due to the known role of TIMPs as MMP inhibitors, we sought to determine the presence of an imbalance between specific MMP and TIMP proteins. Thus, MMP/TIMP stoichiometric ratios were calculated (Table 2.3 and Figure 2.2). With the exception of MMP2/TIMP3, MMP2/TIMP4, MMP3/TIMP4 and MMP9/TIMP4, the molar concentration of TIMP was higher than that of each MMP for all other median ratios presented in Table 2.3. When comparing the POAG group to cataract controls, the molar ratios of MMP2/TIMP1 ($p=0.007$) and MMP9/TIMP1 ($p=0.005$) showed a significant decrease in POAG samples, corresponding to an elevated excess of TIMPs over MMPs in POAG versus cataract samples. Conversely, the MMP2/TIMP3 ($p=0.045$) and MMP3/TIMP3 ($p=0.032$) molar ratios increased. These significant changes to MMP/TIMP molar ratios are likely due to the increase in TIMP1, TIMP2, and TIMP4 concentrations in POAG, as little difference was observed in MMP levels. Furthermore, the molar ratios demonstrate that in terms of total TIMP concentration, the increases in TIMP1, 2 and 4 outweigh the rise in total MMP2 concentration observed.

Table 2.3 Stoichiometric analysis of MMP and TIMP ratios in cataract control versus POAG samples

	Cataract			POAG			
Ratio	**Median**	**Interquartile range**	**N**	**Median**	**Interquartile range**	**N**	**p-value**
MMP1/TIMP1	1.28 $\times 10^{-3}$	8.68 $\times 10^{-4}$-2.07 $\times 10^{-3}$	23	1.20 $\times 10^{-3}$	6.17 $\times 10^{-4}$-1.96 $\times 10^{-3}$	16	0.353
MMP1/TIMP2	6.25 $\times 10^{-4}$	4.65 $\times 10^{-4}$-1.09 $\times 10^{-3}$	23	5.88 $\times 10^{-4}$	3.78 $\times 10^{-4}$-1.22 $\times 10^{-3}$	18	0.857
MMP1/TIMP3	2.46 $\times 10^{-3}$	1.57 $\times 10^{-3}$-3.40 $\times 10^{-3}$	23	2.69 $\times 10^{-3}$	1.58 $\times 10^{-3}$-1.47 $\times 10^{-2}$	19	0.193
MMP1/TIMP4	0.24	0.18-0.34	15	0.33	0.22-0.65	16	0.108
MMP2/TIMP1	0.74	0.69-1.04	24	0.64	0.46-0.77	16	**0.007**
MMP2/TIMP2	0.40	0.33-0.46	24	0.35	0.30-0.41	18	0.137
MMP2/TIMP3	1.32	1.06-1.88	24	2.01	1.48-2.29	19	**0.045**
MMP2/TIMP4	155.10	133.20-170.50	15	144.10	126.80-167.00	16	0.245
MMP3/TIMP1	2.40 $\times 10^{-2}$	1.66 $\times 10^{-2}$-3.97 $\times 10^{-2}$	23	2.52 $\times 10^{-2}$	1.27 $\times 10^{-2}$-2.91 $\times 10^{-2}$	17	0.492
MMP3/TIMP2	1.09 $\times 10^{-2}$	9.16 $\times 10^{-3}$-2.31 $\times 10^{-2}$	23	1.53 $\times 10^{-2}$	9.50 $\times 10^{-3}$-2.56 $\times 10^{-2}$	19	0.528
MMP3/TIMP3	4.26 $\times 10^{-2}$	3.04 $\times 10^{-2}$-8.22 $\times 10^{-2}$	23	7.10 $\times 10^{-2}$	4.29 $\times 10^{-2}$-2.24 $\times 10^{-1}$	20	**0.032**
MMP3/TIMP4	4.68	3.70-7.60	15	7.26	4.04-13.65	16	0.354
MMP9/TIMP1	8.55 $\times 10^{-3}$	4.91 $\times 10^{-3}$-1.25 $\times 10^{-2}$	24	4.64 $\times 10^{-3}$	2.20 $\times 10^{-3}$-9.11 $\times 10^{-3}$	16	**0.005**
MMP9/TIMP2	4.10 $\times 10^{-3}$	2.46 $\times 10^{-3}$-6.55 $\times 10^{-3}$	24	2.70 $\times 10^{-3}$	1.74 $\times 10^{-3}$-4.70 $\times 10^{-3}$	18	0.124
MMP9/TIMP3	1.45 $\times 10^{-2}$	8.05 $\times 10^{-3}$-2.88 $\times 10^{-2}$	24	1.42 $\times 10^{-2}$	7.96 $\times 10^{-3}$-2.74 $\times 10^{-2}$	19	0.631
MMP9/TIMP4	1.47	0.69-2.55	15	1.17	0.60-1.99	16	0.397

Values represent median stoichiometric ratio with interquartile range. Significance was tested by means of Mann-Whitney U and a p-value <0.05 was considered significant, as highlighted in bold. N: number of ratios calculated.

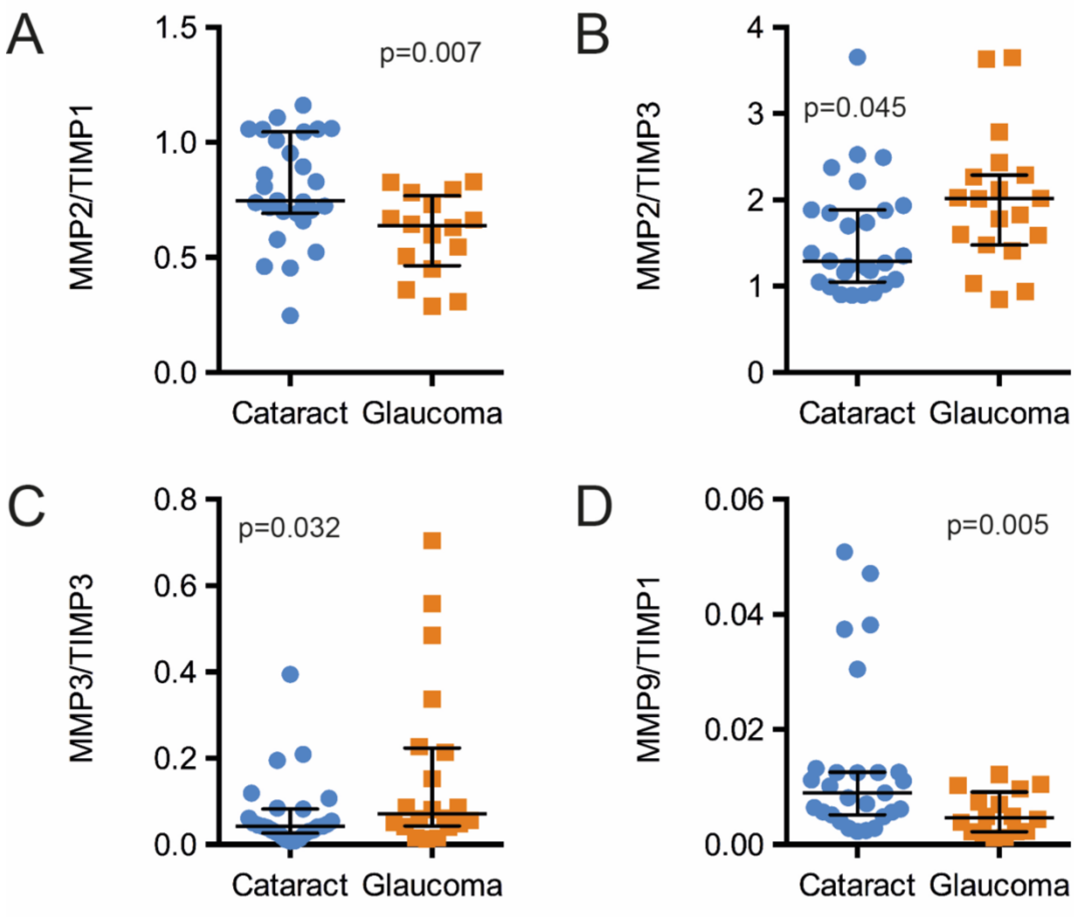

Figure 2.2 Distribution of MMP/TIMP ratios in cataract versus POAG patients. Stoichiometric ratios were calculated for individual aqueous humour samples from non-glaucomatous cataract (blue; N=23-24) and POAG (orange; N=16-20) patients. Median ratios and interquartile ranges are indicated. The ratios for MMP2/TIMP1 (A), MMP2/TIMP3 (B), MMP3/TIMP3 (C) and MMP9/TIMP1 (D) were significantly different between cataract and glaucoma ($p<0.05$), as determined using Mann-Whitney U. See Table 2.3 for full set of ratios calculated.

2.4.2 Several MMP/TIMP molar ratios correlate with IOP and PSD in glaucomatous aqueous humour samples

Spearman's rank correlation method was used to assess the correlation of each analyte concentration and MMP/TIMP ratio with age for both POAG and cataract samples (Table 2.4). Significant positive correlations were determined between age and TIMP1 (r=0.492, p=0.015), TIMP3 (r=0.413, p=0.045) and MMP3 (r=0.537, p=0.006). Furthermore, MMP3/TIMP1 (r=0.529, p=0.010) and MMP3/TIMP2 (r=0.492, p=0.017) also presented positive correlations with age in cataract samples. Nevertheless, none of these analytes or molar ratios correlated with age for POAG samples.

Table 2.4 Correlation of measured analytes and MMP/TIMP ratios to age for cataract control and POAG samples

	Cataract			POAG		
Analyte/ratio	**r_s**	**p-value**	**N**	**r_s**	**p-value**	**N**
TIMP1	0.492	**0.015**	24	-0.012	0.949	17
TIMP3	0.413	**0.045**	24	0.011	0.962	20
MMP1	0.388	0.055	25	0.115	0.612	22
MMP3	0.537	**0.006**	25	0.052	0.814	23
MMP2/TIMP4	-0.104	0.686	15	0.443	0.087	16
MMP3/TIMP1	0.529	**0.010**	23	0.346	0.173	17
MMP3/TIMP2	0.492	**0.017**	23	-0.045	0.855	19
MMP9/TIMP4	0.509	0.055	17	0.074	0.785	16

Correlation of analyte concentrations and MMP/TIMP ratios to age were determined using Spearman's rank correlation method. A p-value <0.05 was considered significant, as shown in bold. Only correlations with p<0.1 and their corresponding values for the other group are shown. r_s: Spearman correlation coefficient; N: number of correlation pairs.

Correlations with IOP, PSD, disease duration (Table 2.5) and CDR (Appendix 2) were determined for analyte concentrations and MMP/TIMP ratios for POAG samples.

Molar ratios for MMP1 in combination with any of the four TIMPs, as well as MMP3/TIMP3 and MMP9/TIMP3, correlated positively with IOP (p=0.007-0.034; Table 2.5). Several molar ratios also correlated negatively with PSD (p=0.005-0.046), and MMP9/TIMP1 correlated positively with disease duration (p=0.015), whereas no significant correlations were determined for CDR.

Table 2.5 Correlation of measured analytes and MMP/TIMP ratios to PSD, IOP and disease duration for POAG samples

	IOP		PSD		disease duration		
Analyte/ratio	**r_s**	**p-value**	**r_s**	**p-value**	**r_s**	**p-value**	**N**
MMP1	0.402	0.063	-0.147	0.516	0.134	0.553	22
MMP1/TIMP1	0.594	**0.017**	-0.538	**0.034**	0.368	0.161	16
MMP1/TIMP2	0.609	**0.007**	-0.482	**0.043**	0.240	0.338	18
MMP1/TIMP3	0.491	**0.033**	-0.407	0.084	0.215	0.378	19
MMP1/TIMP4	0.550	**0.029**	-0.556	**0.028**	0.005	0.976	16
MMP3/TIMP1	0.423	0.091	-0.655	**0.005**	0.316	0.216	17
MMP3/TIMP2	0.431	0.065	-0.492	**0.032**	0.050	0.838	19
MMP3/TIMP3	0.476	**0.034**	-0.348	0.133	0.166	0.484	20
MMP3/TIMP4	0.393	0.132	-0.509	**0.046**	-0.165	0.505	16
MMP9/TIMP1	0.247	0.353	-0.300	0.258	0.605	**0.015**	16
MMP9/TIMP2	0.334	0.175	-0.313	0.207	0.460	0.055	16
MMP9/TIMP3	0.527	**0.020**	-0.454	0.051	0.283	0.241	19
MMP9/TIMP4	0.467	0.070	-0.409	0.117	0.378	0.149	16

Correlation of analytes and MMP/TIMP ratios to IOP (intraocular pressure), PSD (Humphrey's visual field pattern standard deviation), and disease duration were determined using Spearman's rank correlation. A p-value of <0.05 was considered significant, as shown in bold. Only correlations with p<0.1 and their corresponding values for the other clinical descriptors are shown. r_s: Spearman correlation coefficient; N: number of correlation pairs (applies to all analyses).

2.5 Discussion

An imbalance between MMPs and TIMPs in aqueous humour has been suggested to play a role in the development of glaucoma (97). In this study, we quantified aqueous humour concentrations of TIMP 1-4 and several MMPs in POAG and cataract samples, assessed changes in MMP/TIMP molar ratios, and correlated these results with clinical descriptors. A significant increase in the concentrations of TIMP1, TIMP2 and TIMP4 was determined in POAG compared to cataract samples, which is broadly consistent with several reports in the literature (92, 94, 95, 97, 100). Unlike most other studies of MMP and TIMP levels in aqueous humour, we have included clinical data in our analyses and found that several of the MMP/TIMP molar ratios calculated for POAG aqueous humour samples correlated strongly with IOP, PSD or both.

Our results reveal an overall dominance of TIMPs over MMPs in cataract aqueous humour samples. However, the increased concentrations of TIMP1, TIMP2 and TIMP4 produce an MMP/TIMP molar ratio that is imbalanced in the aqueous humour of POAG patients compared to that of cataract patients and suggests that overall MMP activity may be decreased in POAG. All TIMPs are said to be able to inhibit all MMPs, with only a few exceptions. However, TIMP3 is more effective at inhibiting other enzymes such as ADAMs and ADAMTs compared to MMPs (208). Thus, in this study, all TIMPs relevant to MMP inhibition are upregulated in POAG aqueous humour, consistent with the reduction in active MMP levels reported for glaucomatous aqueous humour samples (97). This observation may contribute to a reduced clearance of ECM components and is in agreement with the reported increase in ECM deposition within the glaucomatous TM (205).

Several significant correlations with age were found for TIMPs, MMPs and MMP/TIMP molar ratios in cataract samples, which may contribute to the known age-associated increase in ECM deposition within the TM of healthy individuals (205). In contrast, no such associations with age were observed in POAG samples, despite the larger extent to which this occurs in the glaucomatous TM. However, a correlation was determined between the MMP9/TIMP1 molar ratio and disease duration in POAG samples.

Glaucoma has been described as a disease of early and accelerated cell senescence (153, 211, 212), a state in which cells permanently exit the cell cycle but remain metabolically active. A higher number of senescent cells in the TM of POAG patients compared to age-matched control individuals has been reported (153, 211, 212). Thus, changes in gene expression associated with senescence, which include increased secretion of TIMPs and MMPs (213), may contribute to the increased aqueous humour concentration of TIMPs reported here. It is possible that senescence-associated increases of MMP and TIMP secretion occur to varying extents in different POAG patients, and this may reduce the extent of correlation between these proteins and age. IOP may also modify the levels of MMPs and TIMPs by causing mechanical stretch of the TM, which alters the secretion of MMPs and TIMPs (214). This action has been suggested to involve TGFβ1 as a signalling intermediate (215). Thus, it is plausible that TM cells are directly involved in the change of MMP and TIMP levels in the aqueous humour.

In POAG samples, MMP/TIMP imbalances were correlated with an elevated PSD score and therefore deterioration of the visual field (indicated by negative correlations between several MMP/TIMP molar ratios and PSD). An association between elevated IOP and the progression of visual field defects has been shown (216), and the hypothesis that decreased MMP activity within the TM leads to elevated IOP is well described (130). Based on these findings, one may expect that the further imbalance of TIMPs over MMPs in POAG samples compared to cataract samples described here is likely to reduce ECM turnover, increase aqueous humour outflow resistance and thereby elevate IOP. However, we found that increased concentration of TIMPs altered the MMP/TIMP ratio such that a more pronounced imbalance correlated with a lower IOP. This may be due to treatment with hypotensive medication decreasing IOP to a variable extent between patients, or their impact on MMP and TIMP levels in the aqueous humour (217). Several IOP-lowering drugs have been tested in Sprague-Dawley rats and in cell cultures (human fibroblasts and keratocytes) and have been shown to affect the expression of some MMPs and TIMPs (218). Broadly, the prostaglandin derivative Latanoprost and α-2 agonist Brimonidine caused an increase in MMP3 and decreases in TIMP1 and TIMP3, whereas the β-blocker Timolol had the opposite effect. However, the effects of combinatorial treatments were not assessed in this study; therefore, such experiments do not fully reflect current treatment regimens, which often involve a combination of two or more compounds. In this present study, most POAG patients were being treated with a prostaglandin analogue (95%), of which 80% simultaneously received Timolol, and notably, no difference in MMP3 concentration between POAG and cataract samples was observed. Nevertheless, it is possible that the IOP-lowering treatments used in the care of the POAG study participants may have affected the MMP or TIMP concentrations reported here.

The positive correlations between MMP/TIMP ratios and IOP described in this study are also difficult to reconcile with current knowledge of TIMPs as potent MMP inhibitors. However, TIMPs have recently been shown to possess additional activities independent of their roles as MMP inhibitors, including regulation of cell growth, differentiation, migration, and apoptosis, mediated through direct interactions between TIMPs and cell surface receptors (219, 220). Increased TIMP expression in glaucomatous aqueous humour may therefore have as yet unrecognised MMP-independent effects, such as a direct inhibition of other TM cell functions, including contractibility and phagocytosis, which may affect aqueous humour outflow (118, 133), or contributing to the observed loss of cellularity within the TM of glaucomatous eyes, which may involve apoptotic signalling mechanisms (77, 152, 221, 222). Although the effect of TIMPs on apoptosis appears to be highly context-dependent (223), with several studies reporting pro- and anti-apoptotic responses to TIMP signalling (219), the positive correlations between MMP/TIMP ratios and IOP suggest that a higher IOP may be associated with a loss of anti-apoptotic (or pro-survival) TIMP signalling. This may lead to decreased cellularity within the TM and consequently insufficient drainage of aqueous humour.

The strong correlations determined between MMP/TIMP ratios and the clinical determinants IOP and PSD indicate that the imbalance between MMPs and TIMPs is likely of importance in POAG. Nevertheless, it remains unknown whether the changes observed in POAG aqueous humour composition are a cause or consequence of the disease, and whether TIMP levels increase as a response to altered MMP secretion or vice versa, or indeed as a response to other events occurring in the anterior chamber. In conclusion, this study suggests that further work should focus on TIMPs, not only with respect to changes in ECM composition, but also the cellularity of the TM in POAG.

2.6 Acknowledgements

The authors would like to thank the Clifford Craig Medical Research Trust (Grant Number 121), Tasmania, for funding this research, and the University of Tasmania for providing the APA scholarship supporting Esther Lara Ashworth Briggs. The authors thank the study participants for their generosity, and Sally Baxter at Launceston Eye Doctors for her assistance with sample collection and handling. The authors have no commercial interests to disclose in relation to this manuscript. An oral presentation of the data in this manuscript was given at the Australian Health and Medical Research Congress 2014.

CHAPTER 3 UTEROGLOBIN AND FLRG CONCENTRATIONS IN AQUEOUS HUMOUR ARE ASSOCIATED WITH AGE IN PRIMARY OPEN ANGLE GLAUCOMA PATIENTS

The research contained within this chapter is unedited and has been published as:

Ashworth Briggs EL, Toh TY, Eri R, Hewitt AW, and Cook AL. Uteroglobin and FLRG concentrations in aqueous humour are associated with age in primary open angle glaucoma patients. *BMC Ophthalmology* 2018;18:57-64.

3.1 ABSTRACT

3.1.1 Background

The pathophysiological changes occurring in the trabecular meshwork in primary open-angle glaucoma are poorly understood, but are thought to include increased extracellular matrix deposition, trabecular meshwork cell apoptosis, inflammation, trabecular meshwork calcification and altered protein composition of the aqueous humour. Although many proteins are present in aqueous humour, relatively few have been studied extensively, and their potential roles in primary open-angle glaucoma are unknown.

3.1.2 Methods

Analyte concentrations in aqueous humour from 19 primary open-angle glaucoma and 18 cataract patients were measured using a multiplex immunoassay. Fisher's exact test was used to assess statistical significance between groups, and correlations of analyte concentrations with age, intraocular pressure, pattern standard deviation,

mean deviation, cup-to-disc ratio and disease duration since commencing treatment were tested by Spearman's method.

3.1.3 **Results**

CHI3L1, FLRG, HGF, MIF, p-selectin and uteroglobin were detected in more than 50% of samples of one or both patient groups, some of which have not previously been quantified in aqueous humour. In the glaucoma but not the cataract group, significant correlations were determined with age for uteroglobin/SCGB1A1 (r_s=0.805, p<0.0001) and FLRG (r_s=0.706, p=0.0007). Furthermore, HGF correlated significantly with disease duration (r_s=-0.723, p=0.0007). There were no differences in analyte concentrations between groups, and no other significant associations with clinical descriptors that passed correction for multiple testing.

3.1.4 **Conclusions**

The correlations of uteroglobin and FLRG with age in primary open-angle glaucoma but not cataract may suggest a heightened requirement for anti-inflammatory (uteroglobin) or anti-calcification (FLRG) activity in the ageing glaucomatous trabecular meshwork.

3.2 INTRODUCTION

Aqueous humour is a clear fluid that circulates throughout the anterior chamber of the eye to provide nutrients to and remove metabolic waste products from the tissues it contacts, and thus contributes to the maintenance of normal eye function (4). The majority of aqueous humour drains from the eye via the trabecular meshwork (TM), a specialised porous tissue responsible for the regulation of intraocular pressure (IOP) (224). In primary open-angle glaucoma (POAG), decreased drainage of aqueous humour through a compromised TM leads to elevated IOP (4), causing optic nerve degeneration and thus a progressive loss of peripheral vision unless treated. Elevated IOP is the only modifiable risk factor for the development of glaucoma, and all current treatments for POAG are aimed at reducing IOP (224).

The molecular and cellular changes that contribute to TM dysfunction and elevated IOP in POAG are poorly understood. Several processes, including altered extracellular matrix (ECM) turnover (205), oxidative stress (225), inflammation (226), reduced TM cellularity (152), increased TM stiffness (193) and TM calcification (227) are all potential contributors to the pathological changes occurring in the TM during POAG. Many clinical studies of glaucomatous aqueous humour samples have reported alterations of multiple inflammatory mediators, including TGFβ2 (173, 174, 228), IL-8 (103), IL12, IFNγ and CXCL9 (104, 229) compared to controls, and a pro-inflammatory environment of the aqueous humour has been reported for an animal model of glaucoma (230). Furthermore, inflammation can cause TM cell apoptosis and lead to a dysfunctional TM, thus contributing to an elevated IOP (226).

Whilst many proteins have been detected in aqueous humour using discovery-based proteomics approaches (74, 75, 77, 231-234), detailed studies have been performed with regards to these proteins, and thus any potential role in eye physiology or diseases such as glaucoma remains undetermined. Increased knowledge of the proteins present in aqueous humour from POAG patients may provide clues to improve our understanding of the disease processes involved and how they interact with each other. Accordingly, the aims of this study were to compare the concentrations of selected proteins from these studies, including several not previously analysed in eye diseases, in aqueous humour samples obtained from a well-defined cohort of 19 POAG patients against 18 non-glaucomatous cataract samples. Subsequently, we sought to determine the extent of correlation between each of these proteins and relevant clinical descriptors including age, IOP, field of vision (quantified by Humphrey's visual field pattern standard deviation (PSD) score and mean deviation (MD)), optic cup/disc ratio (CDR) and disease duration since commencing treatment. Here, we report the concentrations of six aqueous humour proteins, and identify significant correlations of age with uteroglobin and FLRG specific to the POAG group, as well as a correlation of HGF with POAG disease duration.

3.3 MATERIALS & METHODS

3.3.1 Patient eligibility and recruitment

This study was approved by the Health and Medical Human Research Ethics Committee Tasmania (H0013264) and executed in adherence to the tenets of the Declaration of Helsinki. All participants were recruited through Tze'Yo Toh at the Launceston Eye Institute and gave written consent with regards to donation and use of aqueous humour samples. POAG was diagnosed based on characteristic optic disc cupping, corresponding visual field loss, and retinal nerve fibre layer thinning, regardless of the presenting IOP. The anatomy of the drainage angle was assessed by gonioscopic examination. Non-glaucomatous cataract patients (referred to herein as the cataract group) were recruited to serve as a control for this study. POAG patients who had previously had a trabeculectomy or vitrectomy were excluded from this study. Furthermore, POAG and cataract subjects were excluded if they had other retinal (such as diabetic retinopathy or age-related macular degeneration) or neurological disease.

Clinical descriptors including age, IOP and CDR were recorded for both patient groups. IOP was measured in all patients using a calibrated Goldmann Applanation tonometer. For POAG patients, only the latest treated IOP measurement taken during the consultation prior to the surgery was used for this study. Vertical CDR was estimated by one observer (Tze'Yo Toh), using a 60D lens during indirect slit lamp fundoscopy and further confirmed with an optic disc profile scan using optical coherence tomography. MD and PSD were included as measures for vision loss but were not available for all patients (MD was recorded for 13/19 POAG and 5/18 cataract patients, PSD for 19/19 POAG and 6/18 cataract patients). Furthermore, disease duration since commencing treatment was noted for POAG patients at the time aqueous humour samples were collected.

All POAG patients recruited were receiving IOP-lowering eye drops, in the form of monotherapy, or a combination of up to four of the following compounds: Timolol (β-blocker), Bimatoprost, Tafluprost, Latanoprost, Travoprost (prostaglandin derivatives), Brimonidine (α-2 agonist) and Brinzolamide (carbonic anhydrase inhibitor).

3.3.2 Aqueous humour collection

Aqueous humour samples (50–100 μl) were collected from 19 patients with POAG during routine cataract surgery. Aqueous humour was also collected from 18 non-glaucomatous patients undergoing routine cataract surgery to serve as a control for this study (75, 235). For all samples, aqueous humour was collected from the centre of the anterior chamber by paracentesis at the beginning of surgery, immediately frozen at -20°C, and transferred to -80°C within 48 hours, where they were stored for analysis.

3.3.3 Multiplex immunoassay

We used discovery-based proteomic studies of aqueous humour in combination with other relevant scientific literature to select 30 proteins for inclusion in a custom magnetic bead-based multiplex immunoassay (R&D Systems, Inc., Minneapolis, MN) to enable simultaneous measurement of each protein in aqueous humour samples from. The 30 proteins included were: angiopoietin-1, angiopoietin-2, BMP2, BMP4, BMP9, CCL27/CTACK, CHI3L1/YKL-40, collagen IV alpha 1, cripto-1, DcR3, EGF, endoglin/CD105, endothelin-1, EPO, FLRG, follistatin, growth hormone, HGF, IGFBP-1, IGFBP-3, IL-6, IL-9, LIF, MFG-E8, MIF, p-Selectin, thrombospondin-2, uteroglobin, VCAM-1 and vWF-A2. Some of these proteins (endothelin-1, HGF, EPO, MIF) have previously been shown to be present in aqueous humour using immunoassay techniques, but there are scant or no subsequent studies reporting correlation to clinical descriptors (103, 111, 112, 114, 236, 237). Others (e.g. thromobospondin-2, follistatin) have been shown to be altered in animal (238) or cell culture-based (239) models of glaucoma, but there are no reports of their levels in aqueous humour. We also selected several proteins (e.g. CHI3L1, CTACK, cripto-1, DcR3, endoglin, uteroglobin, FLRG, MFG-E8, p-selectin) that have been identified as being present in aqueous humour (75), but for which there is a paucity of studies characterising their involvement in glaucoma.

The assay was performed in accordance with manufacturers' instructions on a Bio-Plex 200 System (Bio-Rad Laboratories, Inc., Hercules, CA). Aqueous humour dilutions with assay diluent were kept to a minimum, with dilution factors ranging from 1.5 – 5.5, sufficient to allow loading of 50 µl of diluted sample per assay well. Fluorescence intensity (FI) was measured and analysed using Bio-Plex Manager 6.0. The majority of concentrations out of range were below the detection limit for the relevant analyte, with the exception of MIF, which resulted in FIs above the highest standard for two cataract and three POAG samples. Readings out of range of the standard curve were excluded from all subsequent analyses. The concentration ranges of the standard curves and the number of samples in range for each analyte tested are given in Appendix 3.

3.3.4 **Normalisation to total protein concentration**

Total aqueous humour protein concentration was measured using a BCA protein assay (Thermo Fisher Scientific, Waltham, MA). Aqueous humour samples were diluted 6-fold in ultrapure water and assessed as described in the manufacturer's protocol. Individual analyte concentrations were normalised to total protein concentration for each sample prior to calculation of correlations as described below.

3.3.5 Statistical analyses

All statistical analyses were conducted with Prism 6 (GraphPad Software, San Diego, CA), using unpaired two-tailed tests with a significance threshold of $p=0.05$. Differences in age, IOP, CDR and total protein concentration were assessed using unpaired T-tests, MD and PSD were evaluated with a Mann-Whitney U test due to non-Gaussian data distribution, and gender was tested using Fisher's exact test. Analyte concentrations measured for POAG and cataract samples were grouped and the number of samples within range versus out of range of the standard curve were compared using Fisher's exact. Due to the non-normal distributions obtained for some analyte data sets, correlations with clinical descriptors were calculated using the non-parametric Spearman's method (r_S: Spearman's correlation coefficient). To minimise identification of false associations in our data, Bonferroni's method was used to correct for multiple testing of the analyte concentration data set across different analyses, resulting in an adjusted significance threshold of $p = 0.0017$ (conventional threshold of 0.05/30 protein analytes = adjusted threshold of $p = 0.0017$).

3.4 RESULTS

In this study, aqueous humour samples from 19 POAG and 18 non-glaucomatous cataract patients were analysed using a multiplex assay, to quantify the concentrations of 30 proteins reported to be present in aqueous humour (75, 77). Clinical descriptors including age, IOP and CDR were collected for all patients and are presented in Table 3.1. MD and PSD were included as measures of vision loss; however, MD data was only available for 13 POAG and 5 cataract patients, and PSD for 6 cataract patients (Table 3.1). In addition, disease duration since commencing treatment was recorded for the POAG group (Table 3.1). There were no significant differences between cataract and POAG groups with regards to age ($p=0.335$), gender ($p=0.313$), IOP ($p=0.783$) or total aqueous protein concentration ($p=0.077$). Whilst the differences in MD and PSD were also non-significant ($p=0.846$ and $p=0.0818$, respectively), this is likely due to the lack of data for the majority of cataract patients. The difference in CDR was statistically significant, with a mean CDR of 0.78 in POAG compared to 0.40 in the cataract group ($p<0.0001$). All patients in the POAG cohort were receiving IOP-lowering medication, with 63% (12/19) on a monotherapy regime of one prostaglandin derivative. The remaining patients received a combination of up to four compounds. All POAG patients were treated with a prostaglandin derivative, and 32% (6/19) were simultaneously prescribed with Timolol (β-blocker). A small percentage of patients received an α-2 agonist (1/19) and/or a carbonic anhydrase inhibitor (2/19) in addition to the prostaglandin derivative and β-blocker. In this initial study, we have not attempted to assess differences in analyte concentrations due to specific medication regimes.

Table 3.1 Clinical data for non-glaucomatous cataract and POAG patients

Parameters	**Cataract**	**POAG**	**p-value**
Age (years; Mean ± SD)	66.5±7.0	68.9±7.9	0.335
Sample number (M/F)	18 (5/13)	19 (9/10)	0.313
IOP (Mean, ± SD)	17.9±3.5	17.6±3.4	0.783
MD (Median, IQR)	-3.1, -4.8 to -0.9	-3.6, -4.8 to -2.0	0.846
PSD (Median, IQR)	1.63, 1.40 - 2.95	2.11, 1.69 – 5.26	0.082
CDR (Mean ± SD)	0.40, 0.22	0.78, 0.09	**<0.0001**
Disease duration (years; Mean ± SD)	N/A	2.59, 2.15	N/A
AH total protein (mg/ml; Mean ± SD)	3.21±0.88	3.77±0.97	0.077

POAG: Primary open-angle glaucoma; SD: standard deviation; M: male; F: female; IOP: intraocular pressure in mmHg; MD: mean deviation; IQR: interquartile range; PSD: Humphrey's visual field pattern standard deviation; CDR: optic cup/disc ratio; N/A: not applicable; AH: aqueous humour. Statistical significance was assessed using Fischer's exact test (gender), unpaired T-test (age, IOP, CDR, total protein) and Mann-Whitney U-test (MD, PSD) with $p<0.05$ considered significant.

Out of the 30 proteins tested, 6 were detectable in ≥50% of samples in one or both groups: CHI3L1, FLRG, HGF, MIF, p-selectin and uteroglobin (Table 3.2). The remaining 24 analytes were either not detected, or detected in only a small number of samples, and were therefore excluded from all subsequent analyses (see Appendix 3). Of those proteins analysed further, CHI3L1 was present at the highest levels, with median concentrations above 65 ng/ml. FLRG and MIF were detected at intermediate levels, with median concentrations ranging from 3.6 to 6 ng/ml, whereas HGF, p-selectin and uteroglobin were all quantified at median concentrations below 1 ng/ml.

Table 3.2 Aqueous humour analyte concentrations in non-glaucomatous cataract versus POAG

	Cataract			POAG			
Analyte	**Median**	**IQR**	**In Range**	**Median**	**IQR**	**In Range**	**p-value**
CHI3L1	65171	53191-91124	18/18	83122	65958-95018	19/19	1.000
FLRG	3614	2857-4412	16/18	4303	3679-5323	19/19	0.230
HGF	171.2	114-227	9/18	170.7	133-222	18/19	0.003
MIF	5592	4061-10039	15/18	4809	3697-5830	15/19	1.000
p-selectin	791	691-874	9/18	927	803-1193	15/19	0.091
uteroglobin	335	198-463	17/18	253	174-477	18/19	1.000

Median and interquartile range (IQR) calculated for data in range, reported as pg/ml. Significance was tested using the Fisher's exact test for comparison of number of detected vs. undetected samples in each group. Following correction for multiple testing using Bonferroni's method, a p-value of <0.0017 was considered significant.

The number of samples in range versus below the range of the standard curve were compared for each analyte using Fisher's exact test. Whilst analysis revealed a difference for HGF (p=0.003) between cataract (9/18 in range) and POAG (18/19 in range), the result did not pass correction for multiple testing (adjusted p-value threshold = 0.0017). In addition, no sample was consistently below the 5th or above the 95th percentile for all analytes reported.

3.4.1 Significant correlation of FLRG and uteroglobin with age in POAG but not cataract

Prior to calculating correlations, analyte concentrations were normalised using total aqueous humour protein concentration. The total protein concentrations determined for POAG and cataract samples (mean concentrations of 3.77 and 3.21 mg/ml, respectively) did not differ significantly between groups (p=0.077). Similarly, normalised analyte concentrations did not differ significantly between the POAG and cataract group (Figure 3.1).

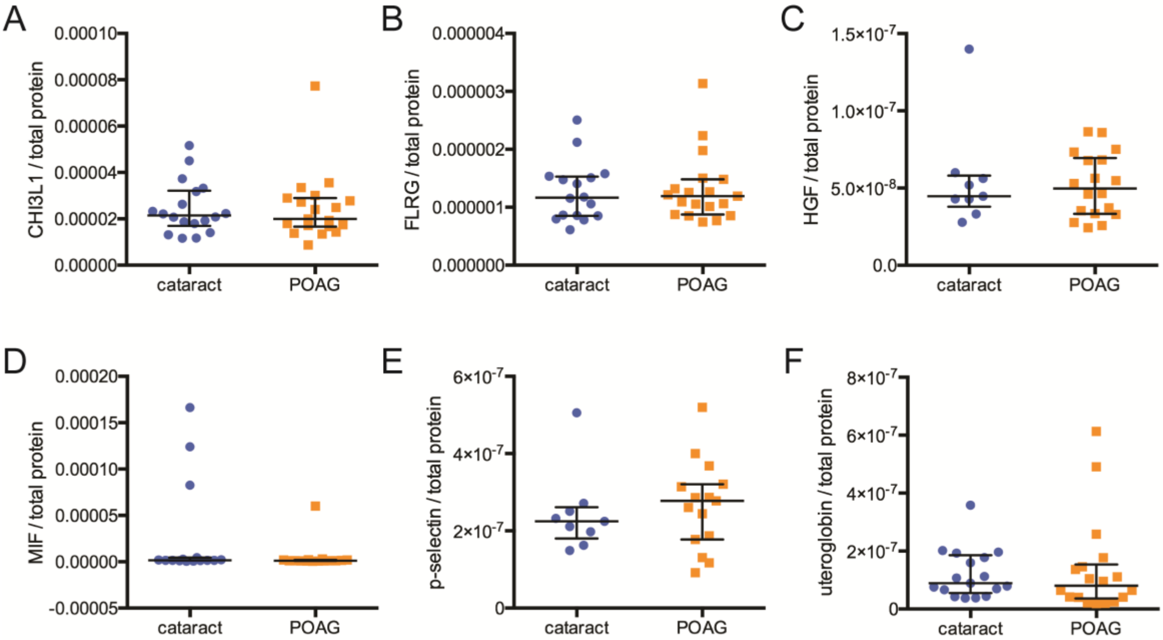

Figure 3.1 Normalised analyte distributions in cataract and primary open-angle glaucoma (POAG) samples. Distribution of CHI3L1 (A), FLRG (B), HGF (C), MIF (D), p-selectin (E) and uteroglobin (F) concentrations in aqueous humour normalised to total aqueous humour protein concentration from non-glaucomatous cataract (blue) and POAG (orange). Median and interquartile range are indicated.

Correlations between normalised analyte concentrations and age were assessed for both patient groups (Table 3.3). Significant positive correlations were obtained with FLRG (r_s=0.706, p=0.0007) and uteroglobin (r_s=0.805, p<0.0001) for POAG but not the cataract group (r_s=0.475, p=0.065 and r_s=0.555, p=0.022, respectively). Whilst further correlations were determined for CHI3L1 (r_s=0.566, p=0.012) and HGF

(r_s=0.642, p=0.004) in POAG, these did not pass correction for multiple testing. No significant correlations were obtained between age and other analytes (all p≥0.05).

Table 3.3 Correlation of measured analytes to age for non-glaucomatous cataract and POAG samples

	Cataract			POAG		
Analyte	r_s	**p-value**	**N**	r_s	**p-value**	**N**
CHI3L1	-0.066	0.794	18	0.566	0.012	19
FLRG	0.475	0.065	16	0.706	**0.0007**	19
HGF	0.170	0.662	9	0.642	0.004	18
MIF	0.404	0.135	15	0.159	0.570	15
p-selectin	-0.756	0.835	9	0.500	0.060	15
uteroglobin	0.555	0.022	17	0.805	**<0.0001**	18

Correlations of normalised analyte concentrations to age were determined using Spearman's rank correlation. Following correction for multiple testing using Bonferroni's method, a p-value of <0.0017 was considered significant (highlighted in bold). r_s: Spearman correlation coefficient. N: number of correlation pairs.

3.4.2 HGF correlated significantly with POAG disease duration since commencing treatment

Analyte concentrations were also assessed for correlations with CDR, IOP, PSD and MD for both patient groups, and with disease duration since commencing treatment in POAG only (Table 3.4 and Appendix 4-7). A significant correlation was determined between HGF and disease duration (r_s=-0.723, p=0.0007, Table 3.4). Further correlations with disease duration were determined for CHI3L1 and FLRG (r_s=-0.555, p=0.014 and r_s=-0.673, p<0.002, respectively, Table 3.4), and CHI3L1 correlated with CDR in cataract (r_s=-0.539, p=0.021, Appendix 5), however, they did not pass correction for multiple testing (adjusted p-value threshold =0.0017). No correlations were obtained between IOP (Appendix 4), MD (Appendix 6) or PSD (Appendix 7) and any analyte for either patient group.

Table 3.4 Correlation of measured analytes to disease duration for POAG samples

Analyte	r_s	p-value	N
CHI3L1	-0.555	0.014	19
FLRG	-0.673	0.002	19
HGF	-0.723	**0.0007**	18
MIF	-0.306	0.246	15
p-selectin	-0.312	0.226	15
uteroglobin	-0.377	0.123	18

Correlations of normalised analyte concentrations disease duration (in years since commencing treatment) were determined using Spearman's rank correlation. Following correction for multiple testing using Bonferroni's method, a p-value of <0.0017 was considered significant (highlighted in bold). r_S: Spearman correlation coefficient. N: number of correlation pairs

3.5 Discussion

In this present study, aqueous humour samples were collected and analysed from 19 POAG and 18 non-glaucomatous cataract patients as controls. Out of the 30 analytes measured, 6 were quantified in sufficient samples to allow for further analysis (CHI3L1, FLRG, HGF, MIF, p-selectin and uteroglobin), some of which have not previously been assessed with regards to eye physiology or disease. The concentrations obtained for HGF and MIF are consistent with existing literature (103, 114, 240) and to the best of our knowledge, no quantitative measures of CHI3L1, FLRG, p-selectin or uteroglobin have been reported in aqueous humour. Four of these proteins are directly linked to inflammation: p-selectin and MIF are both pro-inflammatory mediators, with p-selectin mediating leukocyte-endothelium adhesion (241), and MIF suppressing the anti-inflammatory and immunosuppressive effects of glucocorticoids (242). CHI3L1 exerts its pro-inflammatory effects at least in part by inhibiting apoptosis of T-cells, macrophages and eosinophils (243). In contrast, uteroglobin has anti-inflammatory effects (244, 245). Furthermore, HGF is involved in tissue repair (114) and FLRG acts as an inhibitor to members of the TGFβ superfamily (246). Whilst no significant differences were found between normalised analyte concentrations, significant correlations of specific analytes with disease descriptors were obtained, which are discussed below.

A positive correlation was determined for uteroglobin with age in POAG but not cataract samples, which may indicate an increased need for anti-inflammatory activity in the ageing glaucomatous TM. Uteroglobin is primarily known for its association with various allergic and inflammatory lung diseases (247), where it exerts an anti-inflammatory effect by supressing various inflammatory mediators, including INFγ, PLA_2 and TNFα (244, 245). In addition, uteroglobin plays a protective role against oxidative stress (248). In eosinophilic chronic rhinosinusitis, uteroglobin suppresses the expression of pro-inflammatory CHI3L1 (249). CHI3L1 is a commonly used TM cell marker (250-252), although it is only expressed by TM cells in the most anterior and posterior regions of the TM tissue (251), which may reflect areas subject to the greatest levels of tissue remodelling within the TM. Interestingly, in this study, uteroglobin and CHI3L1 correlated in the POAG group but not in the cataract group (POAG $p=0.006$, $r_s=0.624$; cataract $p=0.126$, $r_s=0.387$), which may suggest that a similar mechanism could be occurring in POAG, however, this correlation did not pass correction for multiple testing.

HGF levels were negatively associated with disease duration since commencing treatment in POAG samples, indicating a reduction of HGF over time, which may be linked to or independent from treatment for hypertension. HGF plays a role in tissue repair and is therefore closely linked to inflammation (114). HGF stimulates proliferation, migration and differentiation of many cell types, including TM cells (253), and can stimulate MMP activity in endothelial cells (254). In this study, the number of samples where HGF was above a set threshold of detection was analysed between the POAG and cataract group (Table 3.2, p=0.003); whilst this comparison did not pass correction for multiple testing, the result is in line with published literature, showing a significant increase in HGF in glaucomatous aqueous humour in relation to cataract samples (114). It has been suggested that elevated HGF levels in glaucomatous aqueous humour may play a compensatory role, by increasing aqueous humour outflow, or aiding in repairing TM damage (114). The correlation suggests that this compensation may be lost over time.

Similar to uteroglobin, FLRG correlated positively with age in POAG but not cataract. FLRG is a secreted glycoprotein highly homologous to follistatin (255) that binds to and thereby inactivates members of the TGFβ superfamily, including activin A and BMP2, by disabling their ability to interact with cell surface receptors (246). Interestingly, whilst FLRG was measurable, follistatin was not detected in any of the samples analysed in this study. Within the anterior segment, FLRG may be involved in the regulation of BMP2-induced calcification of the trabecular ECM, which has been suggested to occur with age and to be more prominent in glaucomatous TM (227). The correlation of FLRG with age may indicate a greater need for BMP2 inhibition, due to increased calcification. BMP2-induced calcification of the TM has been shown to directly lead to elevated IOP in a POAG rat model (227) and also agrees with existing reports of increased TM stiffness in POAG (193).

Whilst several correlations were determined between analytes and disease descriptors at a significance threshold of p=0.05, six out of nine did not pass correction for multiple testing (adjusted p=0.0017) but may do so in other appropriately powered studies. Although this study did not include a replication cohort, each analyte measured was selected from either discovery-based proteomic studies or immunoassay-based results reported by other groups (75, 103, 111, 112, 114, 236, 237). Despite this, we were unable to detect many of the proteins included in this study at levels above the lower limit of our standard curve. Aside from technical limitations of our chosen multiplex immunoassay, contributing factors may include the variation in proteins identified across multiple proteomic studies (75, 232), as well as the wide spread of specific analyte concentrations observed between aqueous humour samples from different individuals, as reported in some studies (256).

It is important to note that some topical treatments commonly used to treat ocular hypertension, such as Latanoprost and Brimonidine, may contribute to aqueous inflammation (257, 258). Whilst the potential effects of such medication on the protein concentrations discussed here are not specifically known, altered aqueous humour concentrations of other proteins have been reported (217). Although there were no differences between the normalised analyte concentrations measured in POAG and cataract for the six analytes studied here, the potential contributions from patient medications to the associations reported here cannot be excluded.

3.6 Conclusion

In conclusion, this study has expanded our knowledge of aqueous humour composition by providing quantitative measures for four proteins previously undetermined for aqueous humour. The correlations of uteroglobin and FLRG with age in POAG may suggest an increased need for compensation of inflammatory and calcifying activity in the ageing glaucomatous TM to maintain functionality, but at present it is unclear whether these proteins play a causative or compensatory role. If any or all of these proteins are to have clinical utility, be it as a diagnostic biomarker or therapeutic target, further research is needed to define their contributions to TM cell physiology, particularly in respect to aqueous humour inflammation and TM outflow resistance, and to determine if these proteins have roles in the onset and progression of POAG.

3.7 Acknowledgements

The authors thank the Clifford Craig Medical Research Trust Tasmania (Grant Number 121) and the Ophthalmic Research Institute of Australia for funding this work, and the University of Tasmania for supporting ELAB with an APA scholarship. We are grateful to the study participants for their generosity, to Sally Baxter for assistance with sample collection, to Aidan Bindoff for guidance with statistical analysis and to Laura Danderian and Courtney Brusamarello for technical assistance.

CHAPTER 4 MOLECULAR AND FUNCTIONAL CHARACTERISATION OF PRIMARY HUMAN TRABECULAR MESHWORK CELLS AND THE EFFECT OF UTEROGLOBIN ON TRABECULAR MESHWORK CONTRACTION *IN VITRO*

4.1 ABSTRACT

4.1.1 Purpose

Our previous study of aqueous humour composition in POAG identified uteroglobin as a protein of interest, due to the significant correlation determined between uteroglobin concentration and age in POAG but not cataract control aqueous humour samples. Whilst little is known about uteroglobin function, the literature indicates a possible role in the regulation of TM contraction, thus affecting aqueous humour outflow. We hypothesised that treating TM cells in a 3D collagen gel with recombinant uteroglobin would reduce their contractibility.

4.1.2 Methods

Commercial primary human TM cells (pHTMCs) were characterised by analysis of TM marker gene expression (*AQP1, CHI3L1, MGP, MMP3, MYOC* and *TIMP2*), increased myocilin expression in response to 3 and 5-day Dexamethasone exposure (100 and 500 nM) and collagen contraction. Expression of uteroglobin receptors *FPR2* and *LMBR1L* was assessed using quantitative polymerase chain reaction (qPCR) and immunofluorescence. pHTMCs treated with 1 or 2 μg/ml uteroglobin were embedded in collagen gels and contraction was monitored using photography at 6, 12, 24, 36, 48, 72 and 96 hours. Both subconfluent and 7-day contact-inhibited pHTMCs were tested. Treatment with ROCK inhibitor Y-27632 (100 μM) was used to inhibit contraction, and HeLa cells and human neonatal dermal fibroblasts (HDFn) were used as control

cell lines. Collagen gel contraction was quantified using ImageJ and significance was assessed using two-way ANOVA in Prism6. Experiments were conducted in triplicate and performed three times (n=3).

4.1.3 Results

All TM marker genes tested were expressed by pHTMCs and treatment with Dexamethasone led to a 25-fold increase in myocilin expression compared to vehicle control ($p<0.05$). Over the 96-hour period, subconfluent pHTMCs contracted the collagen gels by 67.0% and contact-inhibited pHTMCs by 62.7%, both comparable to HDFn at 71.3% contraction. Addition of Y-27632 significantly reduced contractibility of all cell types ($p\leq0.0001$) except HeLa cells. These assays confirmed known characteristics of pHTMCs. Of the uteroglobin receptors tested, *LMBR1L* was detected by qPCR and confirmed with immunofluorescence. The impact of uteroglobin treatment on contraction was not statistically significant at the concentrations tested.

4.1.4 Conclusions

No effect of uteroglobin on pHTMC contractibility was found under the conditions tested. Additional experiments such as phospholipase A2 (PLA_2) activity, TGM2 activity, and phagocytosis assays are needed to understand the effect of uteroglobin on TM cell function. Uteroglobin is a known inhibitor of PLA_2 activity, which is involved in TM contraction. Furthermore, uteroglobin has been shown to alter phagocytic activity of activated neutrophils and potentially inhibits TGM2's ability to cross-link ECM proteins.

4.2 INTRODUCTION

Elevated IOP is a primary risk factor for glaucoma (4) and the focal point of all current treatment strategies (259). The majority of aqueous humour drains through the conventional outflow pathway, which consists of the TM and Schlemm's canal (67). The TM is a complex connective tissue consisting of intricate ECM structures covered by TM cells (118). The TM's primary role is to regulate aqueous humour outflow resistance, which is achieved by continuous remodelling of the ECM (68, 69), alterations to TM cell tone and shape via the actomyosin system to affect the geometry of the outflow pathway (reviewed by Tian et al. (133)), and phagocytosis of debris to prevent pathway blockage (142, 158, 260). These actions are not stand alone, however, as contraction of scleral spur and ciliary muscle cells also affects the overall architecture of the TM and thus outflow resistance (129). In POAG, TM dysfunction causes impairment of the outflow facility, which results in increased aqueous humour outflow resistance and thus a build-up of IOP. Whilst many potential mechanisms have been investigated, the onset and progression of TM dysfunction and POAG are yet to be fully understood.

Uteroglobin, also known as clara cell protein, CC10, CC16 or CCSP, is a steroid-inducible, homodimeric protein of 16 kDa that contains a hydrophobic pocket (261). Whilst uteroglobin is best known for its presence in the uterus and lung, research has established that uteroglobin is secreted by many tissues (262). Uteroglobin has been well studied with regards to protein structure and gene expression regulation, yet its physiological roles are only partially understood.

Uteroglobin is a multifunctional protein that affects many cell processes. Known functions include binding and possibly sequestering a variety of hydrophobic ligands, inhibition of inflammation, and protection against oxidative stress (263-266). Uteroglobin's best studied function lies in its ability to inhibit PLA_2 activity (267-269), an enzyme that is present in the TM and affects aqueous humour outflow through TM contraction. Specifically, inhibition of calcium-independent PLA_2 results in cellular relaxation *in vitro* and increased aqueous humour outflow facility in perfused enucleated porcine eyes (270).

It is unclear how uteroglobin imparts its effects on cellular function. Several putative receptors and uteroglobin binding proteins have been identified (265, 271-274), and the detection of internalised uteroglobin in several studies (272, 275, 276) suggests cellular entry via receptor-mediated endocytosis as one mode of signalling. Uteroglobin has a high affinity for lipocalin-1 receptor (LMBR1L, also known as LIMR) (271), which presents itself as a potential endocytic receptor for uteroglobin. As LMBR1L mediates endocytosis of lipocalin-1 (277) and β-lactoglobulin (278), both of which share high structural similarity with uteroglobin, it is conceivable that LMBR1L may also mediate cellular uptake of uteroglobin. Specific uteroglobin interaction has also been demonstrated with membrane receptor FPR2 and research suggests that uteroglobin interaction with FPR2 may elicit an anti-inflammatory response (279).

Overall, whilst uteroglobin has been detected in aqueous humour samples from both glaucomatous and control subjects (280), the published literature contains no information regarding uteroglobin's potential role in ocular physiology. Based on the existing literature, we hypothesised that uteroglobin may inhibit TM cell contraction via PLA_2 inhibition. Thus, the aim of this study was to characterise a commercial human TM cell strain derived from non-glaucomatous post-mortem eyes and subsequently test whether application of exogenous uteroglobin affects cell contraction.

4.3 MATERIALS & METHODS

4.3.1 pHTMC culture

pHTMCs were obtained from ScienCell Research Laboratories (Carlsbad, CA). Plastic ware (Greiner Bio-one, Kremsmünster, Austria) used to culture pHTMCs was coated with a 0.1% gelatine solution (powdered porcine gelatine in sterile water; Sigma-Aldrich, St. Louis, MO) for 2 hours at room temperature prior to use (281). pHTMCs were cultured in glucose-free Dulbecco's modified Eagle's medium (DMEM) containing 4 mM glutamine, supplemented with 10% foetal bovine serum (FBS), D-glucose (final concentration 2.75 g/l) (282), and antibiotic-antimycotic (10'000 units/mL penicillin, 10'000 μg/ml streptomycin and 25 μg/ml Gibco amphotericin B), all from Thermo Fisher (Waltham, MA) (281, 283). This medium is referred to as TM growth medium below. Basic fibroblast growth factor (bFGF; Thermo Fisher) was added to daily media aliquots at 5 ng/ml (283). Cells were maintained at 37°C and 5% CO_2 and the medium was replaced every 2-3 days. Once 90% confluence was reached, cells were passaged using trypsin/EDTA and trypsin neutralising solution (both Lonza Walkersville Inc., Walkersville, MD) following the reagent protocol. Once resuspended, cells were plated at a minimum seeding density of 5'000 cells/cm^2. Cell cultures up to passage 6 were used for experimentation. For some experiments, as detailed below, pHTMCs were maintained at 100% confluence for seven days prior to the assay, as contact-inhibited pHTMCs have been reported to more closely reflect the behaviour of TM cells *in vivo* (71, 284). Supplementation with bFGF was omitted during this 7-day period and the medium was replaced every other day.

4.3.2 HDFn and HeLa cell culture

HDFn (Thermo Fisher) and HeLa cells (gift from Associate Professor Liza Snow) were grown in TM growth medium (glucose-free DMEM, 4 mM glutamine, 10% FBS, 2.75 g/l D-glucose, and antibiotic-antimycotic (10'000 units/ml penicillin, 10'000 µg/ml streptomycin and 25 µg/ml Gibco amphotericin B)) without bFGF supplementation and using uncoated plastic ware. The cells were maintained at 37°C and 5% CO_2 and the medium was replaced every 2-3 days. Cultures were passaged at 80-90% confluence using trypsin/EDTA and trypsin neutralising solution (both Lonza) and seeded at a split ratio of 1:4 to 1:8.

4.3.3 RNA extraction

RNA was extracted from subconfluent (approx. 90% confluence) and contact-inhibited pHTMCs, the latter of which were maintained at confluence in the absence of bFGF supplementation for seven days prior to RNA extraction. Cells were washed in Hank's balanced salt solution (HBSS; Thermo Fisher), disrupted in RLT buffer, and homogenised using the QIAshredder homogenizer (both Qiagen, Hilden, Germany). Total RNA was extracted in accordance with the manufacturer's instructions using the RNeasy Mini Kit with DNAse digestion (Qiagen). RNA was eluted in 30 µl RNase-free water and stored at -80°C. RNA extraction from each condition was performed three times (n=3).

4.3.4 cDNA synthesis

RNA purity was assessed using the Experion StdSens Analysis kit (Bio-Rad Laboratories, Inc. Hercules, CA) with a minimum RNA integrity number >9 considered acceptable. RNA concentration was measured with the Qubit RNA BR assay kit (Invitrogen). The Omniscript RT kit (Qiagen) was used to reverse transcribe one μg total RNA with random primer 9 (15.5 μM final concentration; New England Biolabs, Ipswich, MA) and RNase inhibitor (8 units/reaction; Qiagen). Prior to cDNA synthesis, RNA aliquots were heated to 65°C for 5 minutes to reduce secondary structure.

4.3.5 Quantitative PCR and analysis

qPCR experiments were performed using TaqMan fast advanced master mix and TaqMan gene expression probes (all Thermo Fisher). All probes used to assess TM marker gene expression, as well as *HPRT1* (used for normalisation), are listed in Appendix 8. Probes for uteroglobin, HGF, and their respective receptors are listed in Appendix 9. All cDNAs were diluted 1:10 with nuclease-free water prior to qPCR setup. Samples were run in triplicate on a StepOnePlus real-time PCR system (Thermo Fisher) and data points above 35 cycles (threshold cycle; C_T) were considered undetermined. Furthermore, values more than 0.2 C_T above or below the remaining readings were deemed outliers and removed prior to analysis. Mean C_T values from triplicate wells were normalised against *HPRT1* as the endogenous reference gene and the results were quantified using the comparative C_T method.

4.3.6 Immunocytofluorescence

pHTMCs were passaged as described above, resuspended in TM growth medium with bFGF supplementation, and seeded into 4-well chamber slides at a density of 5'000 cells/cm^2. The media was replaced every other day until a confluency of 60-80% was reached. All cells were fixed with 4% paraformaldehyde (Sigma-Aldrich) and cells probed for intracellular epitopes were permeabilised with cold methanol prior to immunostaining. The cells were blocked in 5% normal goat serum (Cell Signalling Technology, Inc., Danvers, MA) for one hour at room temperature, followed by overnight incubation with primary antibodies diluted in phosphate-buffered saline (PBS; extracellular epitope) or PBS/0.3% Triton X-100 (intracellular epitope) at 4°C (see Appendix 10 for details). Cells were then stained with fluorochrome-conjugated secondary antibodies (Appendix 11) at room temperature for two hours and counter-strained with Hoechst 33342 (Thermo Fisher) and in some instances Alexa Fluor 488 Phalloidin (Cell Signalling Technologies, Inc.) according to manufacturers' instructions prior to mounting with SlowFade Gold Antifade medium (Life Technologies). Negative control slides were prepared in the same manner but were incubated with PBS alone instead of the primary antibody. Images were taken on an Olympus FV1200 confocal microscope (Tokyo, Japan) and processed in Photoshop (version 12.0) to adjust global image brightness and contrast. Magnification and exposure times are indicated with each figure.

4.3.7 Dexamethasone-stimulated myocilin assay

The method for Dexamethasone-stimulated myocilin upregulation by cultured TM cells was adapted from Resch et al. (285). Briefly, pHTMC cultures were maintained at confluence for seven days prior to treatment with either 100 or 500 nM

Dexamethasone (Sigma-Aldrich), or 0.1% absolute ethanol (VWR, Radnor, PA) as a vehicle control, in TM growth medium without bFGF. Treatments were administered daily by direct addition to conditioned media. On the third and fifth day of treatment, total RNA was extracted and analysed as previously described to assess myocilin gene expression. The time points for sample collection were selected on the basis that myocilin protein upregulation is detectable after two days of Dex treatment (285, 286). In addition, conditioned medium was harvested and stored at -80°C for Western blot analysis. The Pierce BCA protein assay kit (Thermo Fisher) was used to determine sample protein concentrations. Equal amounts of protein (15 μg) were run on SDS-PAGE gels (4-15% Mini-PROTEAN TGX Precast gels; Bio-Rad) and transferred to PVDF membranes using the Trans-Blot Turbo transfer system (Bio-Rad). The Page Ruler Plus pre-stained protein ladder (Thermo Fisher) was run with the samples. The membrane was blocked in 5% skim milk powder in Tris-buffered saline pH7.6 + 0.1% Tween20 (TBST) at room temperature for 60 minutes, followed by overnight incubation with a polyclonal antibody to myocilin (PAH58Hu01; 1:1000 dilution; Cloud-Clone Corp., Katy, TX) in 5% skim milk powder in TBST at 4°C. Subsequently, the membrane was incubated with HRP-conjugated anti-rabbit antibody (CST# 7074; 1:2000 dilution; Cell Signalling Technology, Inc.) at room temperature for one hour. Chemiluminescent detection was performed after a 5-minute incubation with SuperSignal West Pico Chemiluminescent Substrate (Thermo Fisher).

4.3.8 MTT assay

Cell survival in the presence of recombinant uteroglobin (R&D Systems, Minneapolis, MN) was assessed with the 3-(4,5-dimethylthiazol-2-yl)-2,5-diphenyltetrazolium bromide (MTT) assay, using the Thermo Fisher Vybrant MTT cell proliferation assay kit protocol. pHTMCs were cultured in phenol-free media and optimal cell seeding density was determined by means of cell titration. For subsequent experiments, cells were seeded at 7.3 $x10^4$ cells/cm^2 in 96-well plates (75% confluence) in 100 μl phenol-free TM growth media and left to adhere overnight. Cells received a one-off treatment with recombinant uteroglobin at 0.05, 0.5, 1.0, 2.0, or 5 μg/ml, 1% HBSS as vehicle control, or 0.5% Triton X-100 (Sigma-Aldrich) as a negative control. Cell survival was assessed at 24, 48, and 72 hours of recombinant uteroglobin exposure. After incubation with 12 nM MTT, DMSO (Sigma-Aldrich) was added for 10 minutes at 37°C to dissolve the resulting formazan particles for measurement at 570 nm, with a reference wavelength of 650 nm, on a Tecan Infinite 200Pro (Tecan Trading AG, Männedorf, Switzerland). Cells treated with 0.5% Triton X-100 were used as a 100% death control and untreated cells as a 100% live control, which were used to calculate cell viability. Each variable was assessed in triplicate and the experiment was performed twice (n=2).

4.3.9 **Collagen gel contraction assay**

The collagen gel contraction assay was performed as previously described (287-289), with minor modifications. The wells of 24-well cell culture plates were coated with 1% bovine serum albumin (BSA) for one hour at 37°C. Cultured pHTMC, HDFn and HeLa cells were trypsinised as described above and resuspended in TM growth medium without bFGF at 2.2x10^6 cells/ml. Cell treatments with ROCK inhibitor Y-27632 (100 μM; StemCell Technologies, Inc., Vancouver, Canada), recombinant uteroglobin (1 and 2 μg/mL; R&D Systems), or 1% HBSS as vehicle control, were set up prior to preparing the collagen mix. Rat tail collagen type I (Thermo Fisher), 10x

DMEM (Sigma-Aldrich), 10x PBS (Thermo Fisher), cell suspension, and water were mixed on ice to obtain a final concentration of 1.9 mg/ml collagen and a final cell density of $2x10^5$ cells/ml. 1N sodium hydroxide was added as described in the manual for rat tail collagen. The mixture (0.5 ml) was added to each BSA-coated well and gel formation was induced at 37°C for 90 minutes. Subsequently, TM growth medium supplemented with the same concentrations of Y-27632, uteroglobin, and vehicle control as the cell treatments (0.5 ml, without bFGF) was added to the gels. After one hour, a microspatula was used to release the gels from the walls of the culture wells. The gels were photographed at 0, 6, 12, 24, 36, 48, 72 and 96 hours and a reduction in surface area was assessed using ImageJ (version 1.49v). A measurement scale was included in each photograph. Each experiment was performed in triplicate and repeated three times (n=3). HDFn and HeLa cells were used as a positive and negative control for contraction, respectively, and treatment with Y-27632 was used as a control for cell contraction inhibition.

4.3.10 Statistical analyses

All statistical analyses were conducted with Prism 6 (GraphPad Software, San Diego, CA). Gene expression was assessed with two-tailed, unpaired T-tests for individual markers and 2-way ANOVAs with Tukey post-test were used to test significance for myocilin PCR, contraction, and MTT assays. A p-value ≤ 0.05 was regarded as statistically significant.

4.4 RESULTS

4.4.1 Characterisation of commercial pHTMCs

Prior to testing the impact of uteroglobin on pHTMC behaviour *in vitro*, the suitability of commercial pHTMCs obtained from ScienCell Research Laboratories, Inc. was assessed. Expression of known TM marker genes *AQP1, CHI3L1, MGP, MMP3, MYOC* and *TIMP2* (71) was analysed, and Dexamethasone-stimulated myocilin secretion (285) and collagen contraction (287-289) assays were used to assess cell function.

4.4.1.1 *pHTMCs express known trabecular meshwork marker genes*

Expression of all TM markers tested was confirmed by means of qPCR in both subconfluent and contact-inhibited pHTMCs cultured *in vitro* (Figure 4.1A). Whilst gene expression did not differ significantly between the two growth conditions tested, greater variability between repeats was seen in subconfluent cultures. Expression of *AQP1* and *CHI3L1* was confirmed by immunofluorescent staining (Figure 4.1B), and both were expressed uniformly by all pHTMCs present. Immunofluorescence was performed using subconfluent cultures to allow the identification of individual cells.

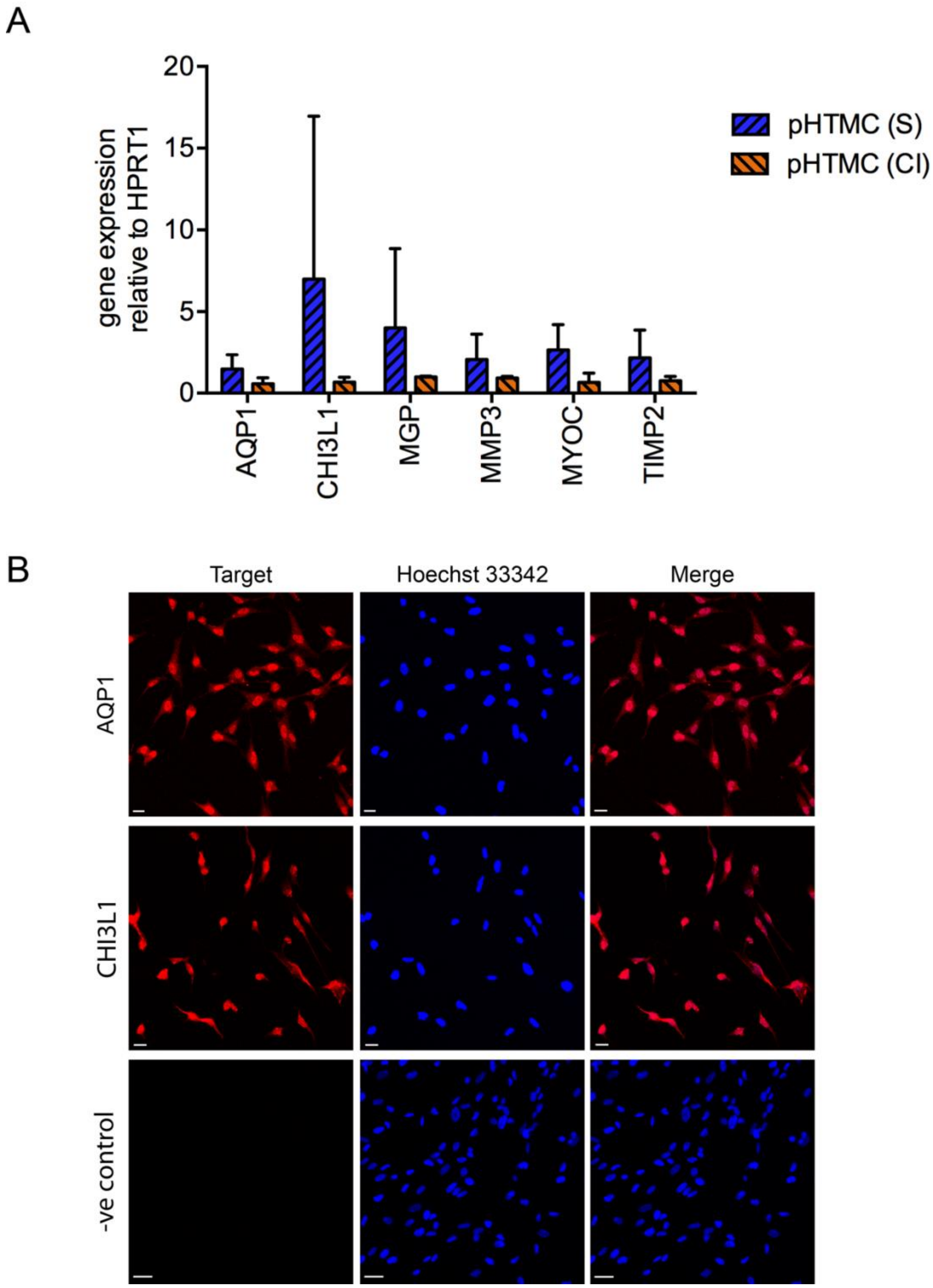

Figure 4.1 TM marker expression in pHTMCs in vitro. A) Subconfluent (S; blue) and contact-inhibited (CI; orange) pHTMCs were assessed for expression of TM markers relative to *HPRT1* using qPCR. Statistical significance was tested by unpaired T-tests for individual genes; no significant differences were determined. Gene expression was

measured in triplicate and the experiment was performed three times (n=3). Data shown as mean ± SD. B) Subconfluent pHTMCs were stained against selected TM markers (AQP1 and CHI3L1; red) and nuclei with Hoechst (blue). Images were taken on a confocal microscope using a 10x objective with 3.6x zoom and an exposure time of 2 μs/pixel. The scale bar corresponds to 20 μm.

4.4.1.2 *Stimulation with Dexamethasone increases myocilin expression in pHTMCs in vitro*

Contact-inhibited pHTMC cultures treated with 100 or 500 nM Dexamethasone for three days presented a statistically significant increase in myocilin gene expression ($p \leq 0.05$) compared to cultures treated with vehicle alone (0.1% ethanol; Figure 4.2). This increase in myocilin mRNA did not change significantly when Dexamethasone exposure was increased to five days. An attempt was made to detect secreted myocilin in conditioned media from Dexamethasone-treated pHTMC cultures by Western blotting (Appendix 12). However, a positive signal coinciding with the expected molecular weight of myocilin was obtained from naïve media making this analysis inconclusive.

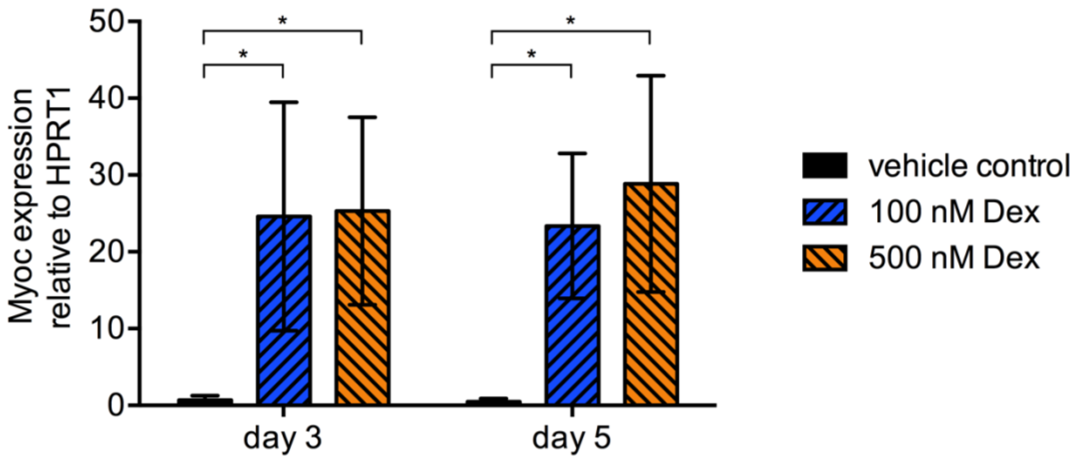

Figure 4.2 Effect of Dexamethasone (Dex) treatment on myocilin expression in pHTMCs in vitro. Myocilin gene expression levels relative to *HPRT1* in pHTMCs treated with vehicle control (0.1% ethanol, black), 100 nM Dex (blue), or 500 nM Dex (orange) *in vitro*. Gene expression was assessed by qPCR after 3 and 5 days of treatment. Statistical significance was assessed using two-way ANOVA with Tukey post-test, * indicates $p \leq 0.05$. The experiment was performed three times (n=3). Data are shown as mean ± SD.

4.4.1.3 *pHTMCs embedded in collagen I contract and treatment with ROCK inhibitor Y-27632 blocks this action*

Cellular contraction was assessed by seeding pHTMCs in a 3D gel made with collagen I and recording changes in surface area at 6, 12, 24, 36, 48, 72, and 96 hours. Both subconfluent and contact-inhibited pHTMCs were tested, and HDFn and HeLa cell cultures served as controls. Example photographs of gels at 0, 24, and 96 hours are shown in Figure 4.3A for all cell types assessed. Over the 96-hour period, subconfluent pHTMCs contracted the collagen gels by 67.0% ($p \leq 0.0001$) and contact-inhibited pHTMCs by 62.7% ($p \leq 0.0001$; Figure 4.4A) when compared to 0 hours. These results are comparable to HDFn cultures, which were used as a positive control and yielded

71.3% contraction ($p \leq 0.0001$). The contraction observed for HeLa cells, which served as a negative control, was negligible (4.0%; $p > 0.05$). By six hours, the level of contraction seen in both subconfluent and contact-inhibited pHTMCs differed significantly from HeLa cell contraction ($p \leq 0.05$). Furthermore, a statistically significant distinction between pHTMC and HDFn contraction was seen from 36 hours onwards ($p \leq 0.05$). At no time point did the extent of contraction differ significantly between subconfluent and contact-inhibited pHTMCs ($p > 0.05$).

With the exception of HeLa cells, the addition of 100 μM Y-27632 significantly reduced collagen gel contraction over the 96-hour period for all cell types tested (Figure 4.4B). Representative photographs of these gels are shown in Figure 4.3B. At 96 hours, in comparison to untreated cells, subconfluent pHTMCs reached just 15.0% contraction ($p=0.002$), contact-inhibited pHTMC contraction was 18.9% ($p=0.003$) and HDFn contraction was reduced to 15.3% ($p=0.003$). HeLa cells displayed no contraction when treated with Y-27632 ($p > 0.05$).

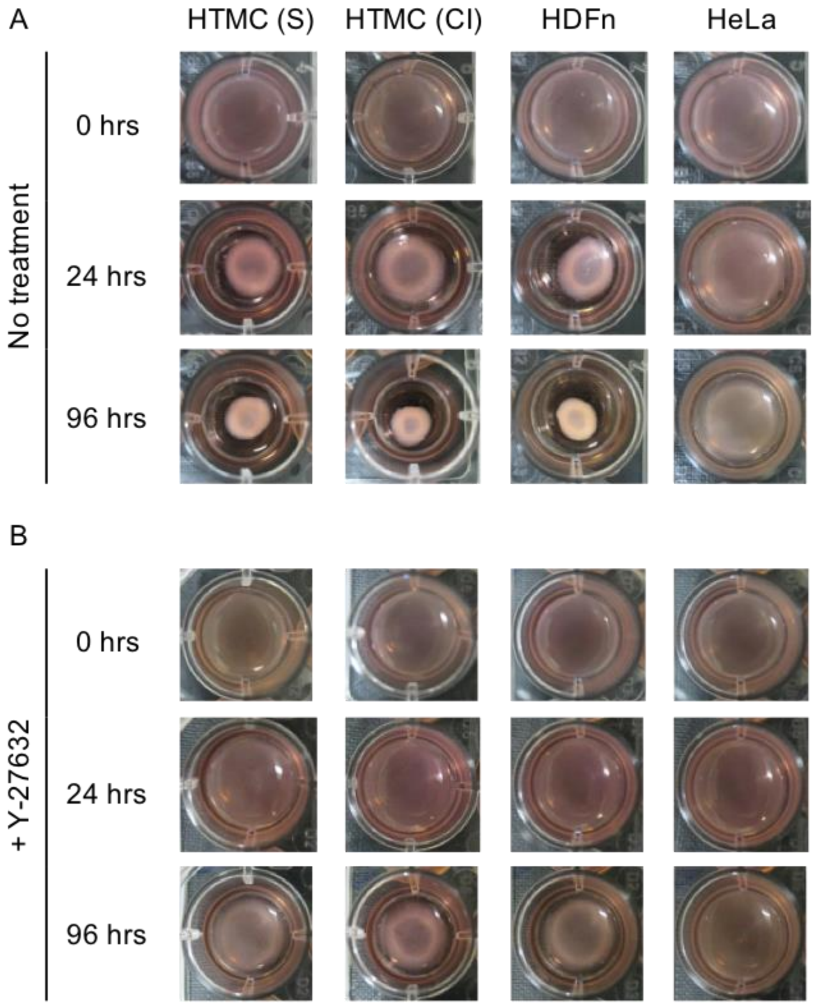

Figure 4.3 Representative photographs of pHTMC, HDFn, and HeLa cells contracting 3D collagen gels. Images of collagen gel contraction by subconfluent (S) and contact-inhibited (CI) pHTMCs, HDFn, and HeLa cells A) in the absence and B) presence of Y-27632 at 0, 24, and 96 hours.

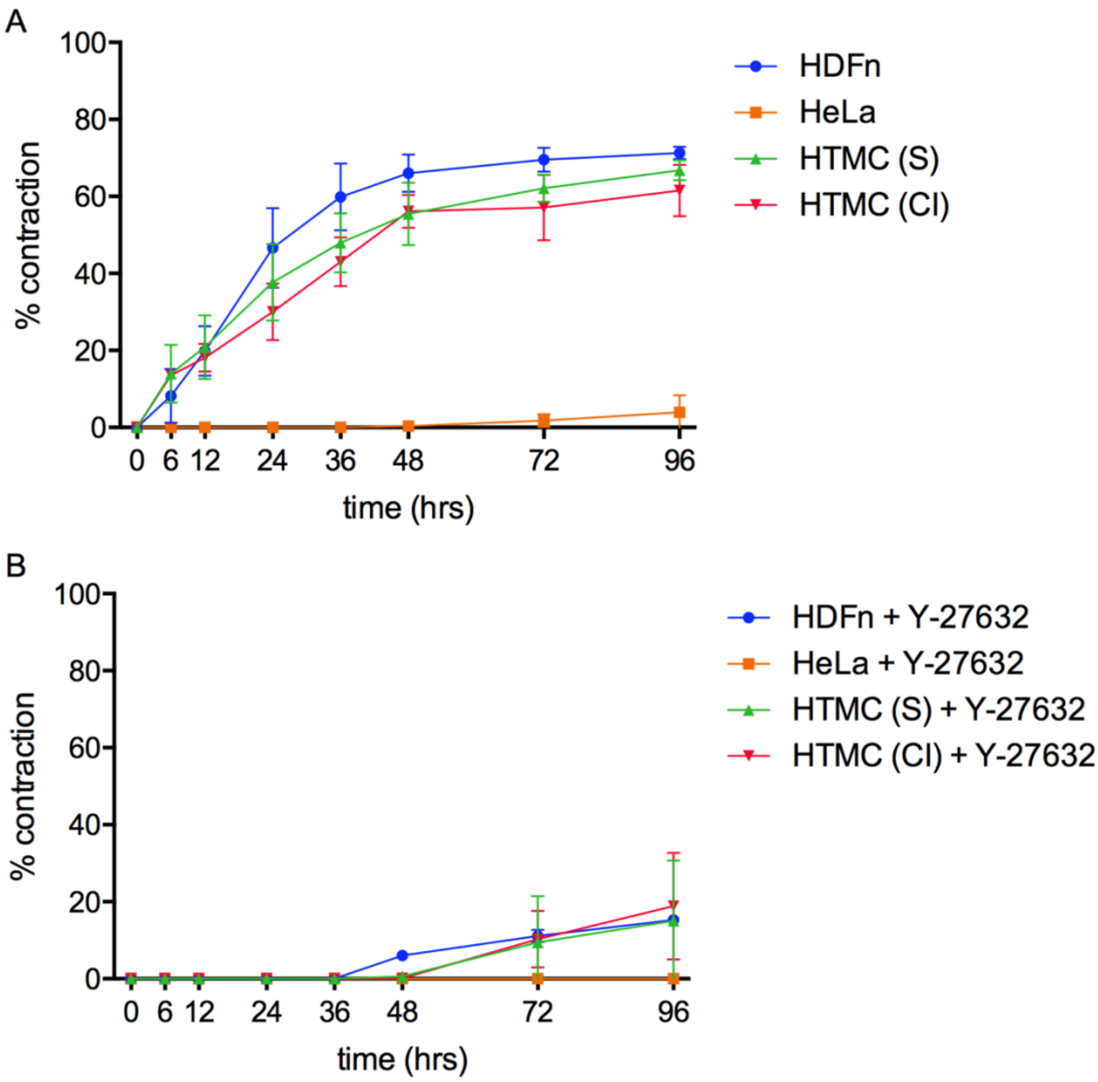

Figure 4.4 Contractibility of pHTMC, HDFn, and HeLa cells embedded in a 3D collagen gel. Collagen gel contraction by subconfluent (S) and contact-inhibited (CI) pHTMCs, HDFn, and HeLa cells A) in the absence and B) in the presence of 100 μM Y-27632 was determined by measuring changes in gel surface area over 96 hours, presented as % contraction relative to 0 hours. Data shown as mean ± SD (n=3). To minimize complexity, statistical significance has been omitted from the figure and is presented in the body of text.

4.4.2 Effect of exogenous uteroglobin on pHTMCs *in vitro*

Chapters 2 and 3 of this thesis involved the study of various protein concentrations in glaucomatous aqueous humour and correlation of these to POAG disease descriptors. Chapter 3 highlighted uteroglobin and HGF as two proteins of potential therapeutic or diagnostic use, based on the significant correlations determined with age and disease duration, respectively. To further investigate any potential roles in TM physiology, this study aimed to select HGF or uteroglobin, based on initial experiments, and investigate whether treatment of pHTMCs *in vitro* affects TM cell behaviour. To aid with the decision, pHTMCs were assessed for gene expression of both factors and their corresponding receptors to determine which protein would be more suitable for this study.

4.4.2.1 *pHTMCs cultured in vitro express HGF, its receptor MET, and uteroglobin receptor LMBR1L, but not uteroglobin or FPR2*

HGF is a well-known growth factor that signals through its receptor MET (290). With uteroglobin the signalling pathways appear more diverse and less clearly elucidated. Two receptors of interest for this study are LMBR1L and FPR2. LMBR1L has a high affinity for uteroglobin and is a potential endocytic receptor for uteroglobin (278). FPR2 presents another potential receptor for uteroglobin and this interaction results in a tonic inhibition of baseline PLA_2 activity (279), although it is unclear if this involves uteroglobin internalisation.

Both subconfluent and contact-inhibited pHTMCs were assessed for expression of *HGF* and its receptor *MET*, as well as uteroglobin and its putative receptors *LMBR1L* and *FRP2* using qPCR (Figure 4.5). In both cases, *HGF, MET*, and *LMBR1L* were expressed whereas uteroglobin and *FPR2* were undetected. No statistically significant differences were observed between the two culture conditions. To confirm these results, LMBR1L and MET expression were assessed by immunofluorescence using phalloidin to counterstain the actin cytoskeleton. Whilst LMBR1L uniformly stained all pHTMCs present (Figure 4.6A), the antibody used for MET yielded negative results under the conditions tested (Figure 4.6B). As with pHTMC characterisation, immunofluorescence was performed using subconfluent cultures to allow for identification of individual cells. At this point, a decision was made to focus on uteroglobin and subsequent experiments were planned accordingly.

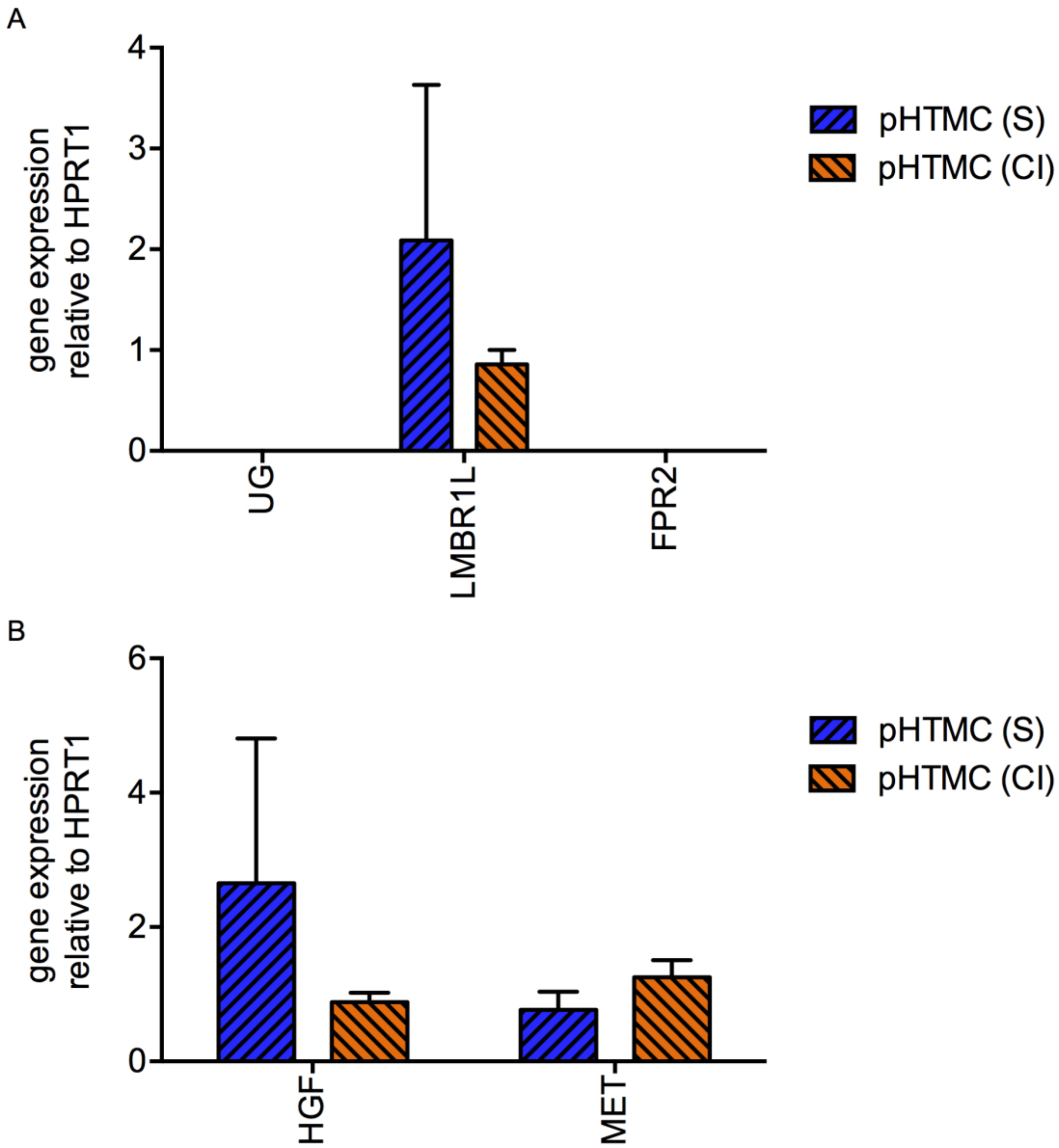

Figure 4.5 Gene expression of uteroglobin, *HGF*, and their respective receptors in pHTMCs *in vitro*. Subconfluent (S; blue) and contact-inhibited (CI; orange) pHTMCs were assessed for expression of A) *HGF* and its receptor *MET* and B) uteroglobin (*UG*) and receptors *LMBR1L* and *FPR2*, relative to *HPRT1* using qPCR. Statistical significance was assessed using unpaired T-tests for individual genes, with $p \leq 0.05$ considered significant. No significant differences were determined. Gene expression was measured in triplicate and the experiment was performed three times (n=3). Data are shown as mean ± SD.

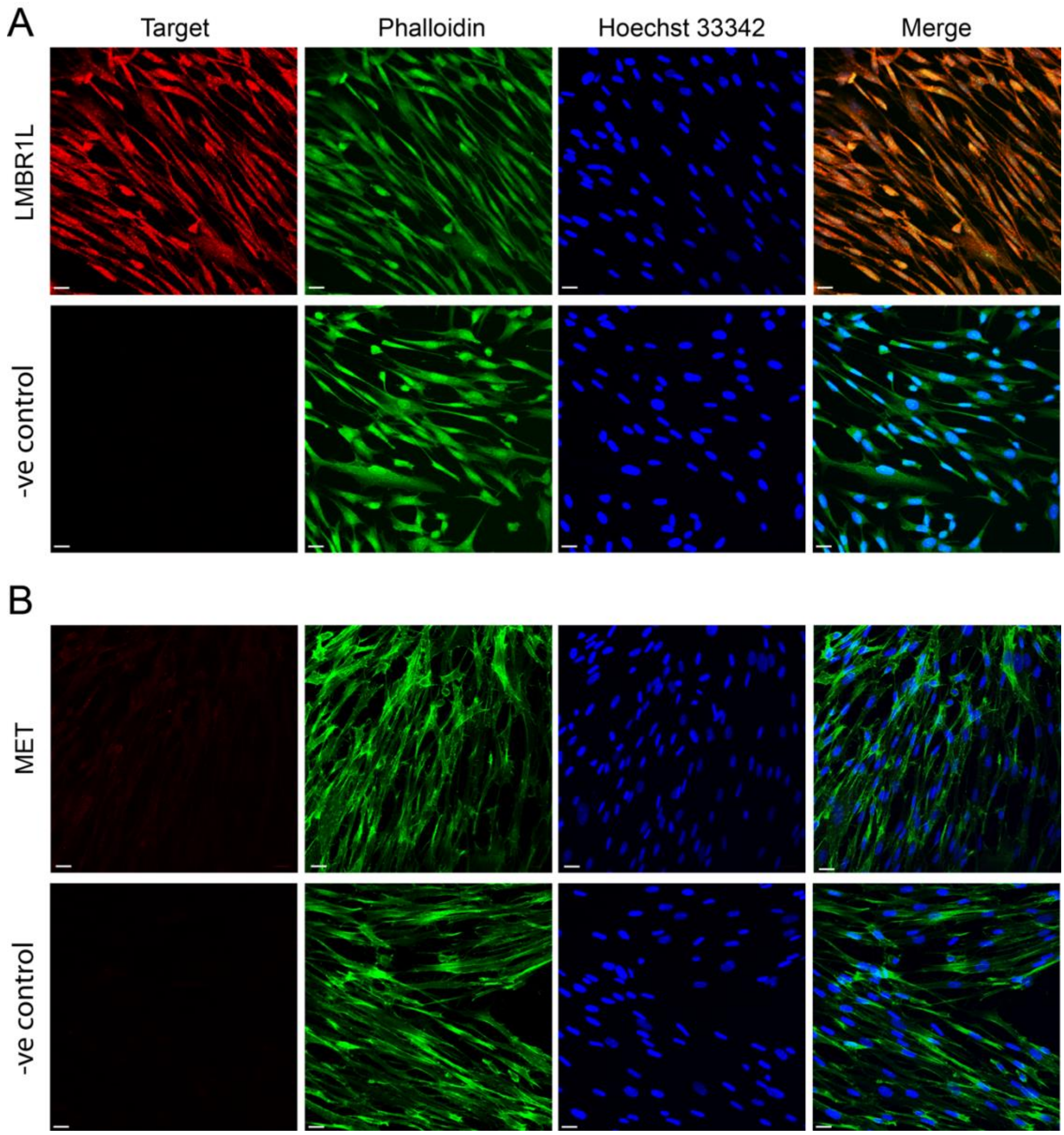

Figure 4.6 Immunofluorescent staining for MET and LMBR1L in pHTMCs *in vitro*. Subconfluent pHTMCs were stained for A) LMBR1L (red) and B) MET (red). Phalloidin (green) was used to stain actin and nuclei were stained using Hoechst (blue). Images were taken on a confocal microscope with a 40x objective and an exposure time of 8 μs/pixel. The scale bar corresponds to 20 μm.

4.4.2.2 *Exogenous uteroglobin does not affect pHTMC viability*

MTT assays were performed to assess the impact of uteroglobin treatment on pHTMC viability *in vitro*. Uteroglobin was tested at 0.05, 0.5, 1.0, 2.0, and 5.0 μg/ml in a single dose treatment at the start of the assay. No significant negative impact on pHTMC viability was observed over the 72-hour period tested (Figure 4.7). Equally, no significant differences were determined between the different uteroglobin concentrations at any of the time points tested ($p > 0.05$). The only statistically significant differences observed were for pHTMCs treated with 5 μg/ml, where MTT metabolism was increased at 48 hours and subsequently returned to its previous level by 72 hours. Both the difference between 24 and 48 hours and between 48 and 72 hours resulted in a p-value ≤ 0.05.

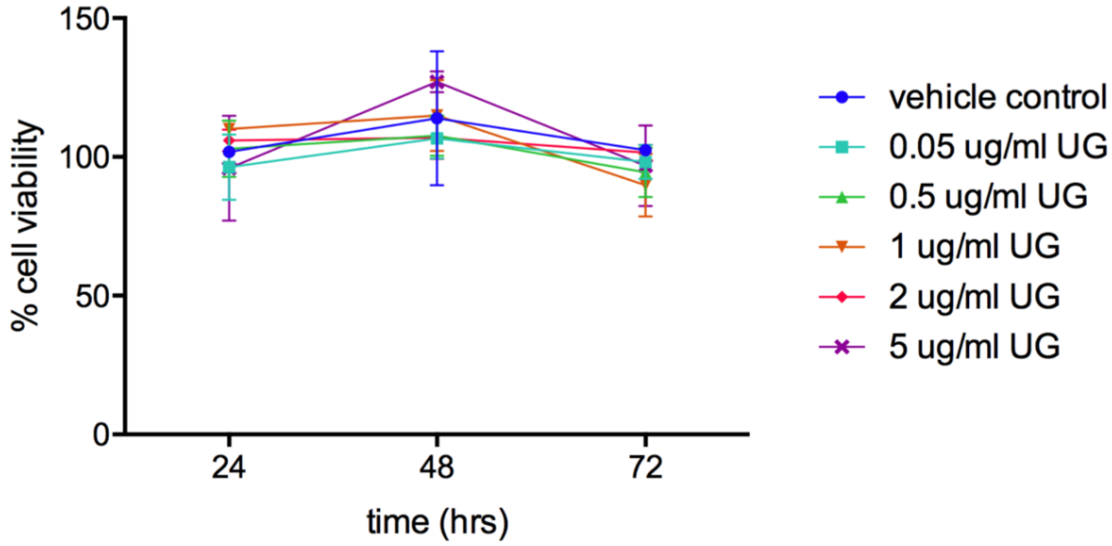

Figure 4.7 Effect of exogenous uteroglobin on pHTMC viability *in vitro* as determined by MTT assays. Subconfluent pHTMCs were treated with vehicle control (1% HBSS) or 0.05, 0.5, 1.0, 2.0, or 5.0 µg/ml uteroglobin (UG). Viability was assessed at 24, 48, and 72 hours. Each variable was tested in triplicate and the experiment was performed twice (n=2). Data are shown as mean ± SD. To minimize complexity, statistical significance has been omitted from the figure and is presented in the body of text.

4.4.2.3 *Effect of exogenous uteroglobin on pHTMC contraction*

The primary aim of this study was to determine whether uteroglobin affects pHTMC contraction by inhibiting PLA_2. As pHTMCs do not express uteroglobin (Figure 4.5A), any effects seen would be the result of extracellular uteroglobin either transmitting a signal via a cell surface receptor or entering the cell via receptor-mediated endocytosis. To test our hypothesis, subconfluent and contact-inhibited pHTMCs were treated with vehicle control, 1.0, or 2.0 µg/ml uteroglobin and then seeded in 3D gels containing collagen I. Gels were photographed at 6, 12, 24, 36, 48, 72, and 96 hours to record changes in surface area. Representative images of gels at 0, 24, and 96 hours are shown in Figure 4.8.

Over the 96-hour period, subconfluent pHTMCs treated with vehicle control, 1.0, and 2.0 μg/ml uteroglobin contracted the collagen gels by 65.1, 68.9, and 72.3%, respectively (Figure 4.9A), whereas contact-inhibited pHTMCs treated with vehicle control, 1.0, and 2.0 μg/ml uteroglobin resulted in 55.8, 58.2, and 56.3% contraction, respectively (Figure 4.9B). Neither subconfluent nor contact-inhibited pHTMCs gave rise to statistically significant differences between the treatments at any time point tested ($p > 0.05$).

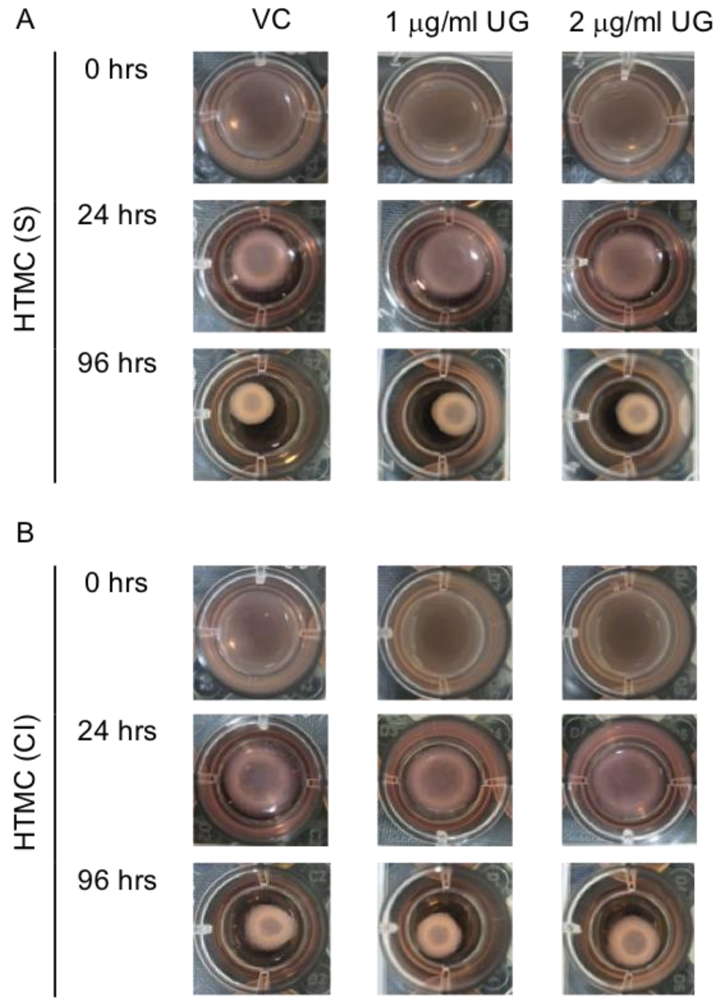

Figure 4.8 Representative photographs of collagen contraction by pHTMCs treated with uteroglobin. Images of collagen gel contraction by A) subconfluent (S) and B) contact-inhibited (CI) pHTMCs treated with vehicle control (VC; 1% HBSS), 1.0, or 2.0 μg/ml uteroglobin (UG) at 0, 24, and 96 hours.

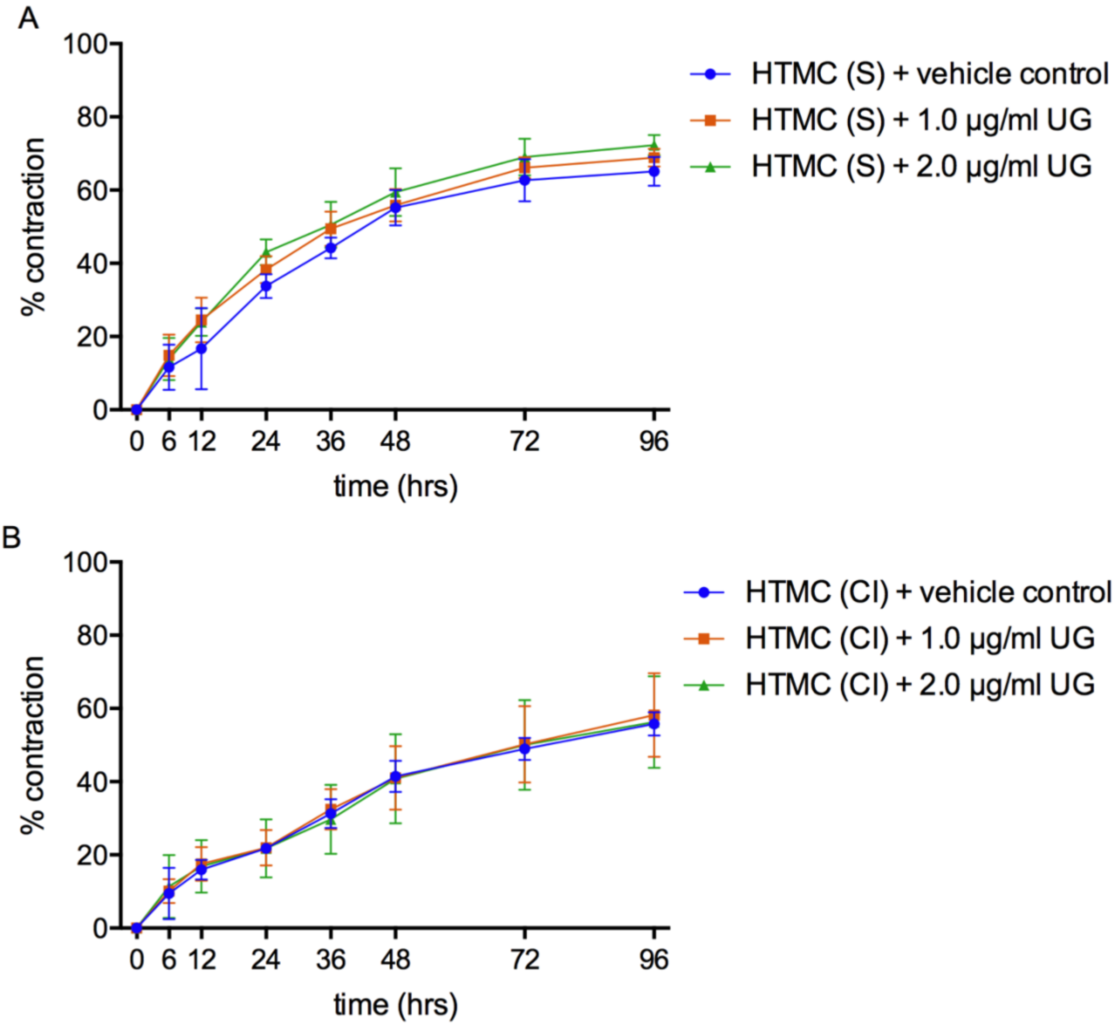

Figure 4.9 Effect of exogenous uteroglobin on pHTMC contraction. Collagen gel contraction by A) subconfluent (S) and B) contact-inhibited (CI) pHTMCs treated with vehicle control (1% HBSS), 1.0, or 2.0 µg/ml uteroglobin (UG) was determined by measuring changes in gel surface area over 96 hours, presented as % contraction relative to 0 hours. The experiment was performed in triplicate and repeated three times (n=3). Data are shown as mean ± SD. No statistically significant differences were found (assessed by 2-way ANOVAs with Tukey's post-test).

4.5 Discussion

TM cell contraction is one mechanism involved in the control of aqueous humour outflow resistance and thus IOP. Specifically, TM cell relaxation leads to an increase in aqueous humour drainage through the conventional outflow pathway (129, 133, 134). Consequently, chemicals that promote TM cell relaxation present a potential strategy for relieving ocular hypertension (291), an avenue that has been pursued more recently with the development of ROCK inhibitors for therapeutic use (292, 293).

Prior to assessing the potential effects of uteroglobin on TM cells *in vitro*, the cell strain to be tested was characterised for TM behaviour. Due to a lacking consensus regarding TM cell isolation, characterisation, and culture at the time of experimentation (recently addressed by Keller et al. (149)), a combination of previously described molecular and functional assays was employed to assess the suitability of the commercial pHTMC strain for use in this study. The pHTMCs expressed all TM markers tested and subconfluent versus contact-inhibited growth conditions did not significantly affect gene expression levels. Assessment of selected markers by immunofluorescence also indicated a high level of homogeneity within the cultures tested. Treatment with Dexamethasone to increase myocilin expression, an assay considered critical to TM cell characterisation (149), successfully induced myocilin gene expression. However, we were unable to show an increase in cell-secreted myocilin protein levels, due to a positive signal obtained for myocilin in the naïve media. It is unknown whether the immunoreactive signal is due to the presence of myocilin in naïve media or the result of a non-specific interaction with a protein of similar molecular weight.

The contraction assay successfully demonstrated the pHTMCs' contractile properties, which were significantly reduced when treated with Y-27632, an inhibitor that has previously been used to block TM cell contraction *in vitro* (289). While the level of contraction observed for pHTMCs was comparable to previously published work using human TM cells (289), an extended culturing time frame was required to achieve the same level of contraction, with 68% contraction reached by 96 hours in our study instead of 24 hours. In comparison, the extent of collagen contraction observed in studies using bovine TM cells was markedly lower (287, 288). Given this limited evidence in the literature regarding extent and duration of contraction, it is impossible to estimate a correct amount and duration for this assay and further evidence is required to determine the potential causes for the difference seen between Koga et al.'s and our study in regard to duration of contraction. In the presence of 100 μM Y-27632, no contraction was detectable at 24 hours, matching previously published results (289).

Whilst the cell strain characterisation was successful, the juvenile source of these cells (24-week old donor) may impact on their behaviour. Thus, the results obtained from this study require verification in TM cell cultures derived from adult post-mortem eyes, ideally from POAG subjects and age-matched healthy controls.

In a previous study (280), analysis of aqueous humour samples from non-glaucomatous cataract and POAG patients highlighted several proteins of interest with regards to POAG, including HGF and uteroglobin. To determine which protein to focus on in this current study, pHTMCs were assessed for expression of these two factors and their receptors MET (HGF receptor), LMBR1L, and FPR2 (both uteroglobin receptors). The gene expression results obtained suggest that pHTMCs express *HGF* but not uteroglobin, which is in agreement with the results gained when analysing HGF and uteroglobin concentrations in pHTMC conditioned media (unpublished data) as part of our previous study (280). Confirmation of receptor expression using immunofluorescence was successful for LMBR1L but not MET. The absence of endogenous uteroglobin production and the presence of a potentially endocytic receptor for uteroglobin led us to focus on uteroglobin's potential effect on pHTMC behaviour.

One-off treatment with 1 or 2 μg/ml recombinant uteroglobin did not result in any significant differences in pHTMC contraction when compared to vehicle control treated cells and as such, the results of this study are inconclusive. It is possible that repeat treatments with uteroglobin or a different concentration are necessary to see an effect on cell contraction. The concentrations tested have previously been used successfully in an *in vitro* phagocytosis study using neutrophils (275). Whilst these concentrations (equivalent to 62.5 and 125 nM) are substantially lower than the micromolar uteroglobin concentration determined by Levin et al. for *in vitro* PLA_2 inhibition (267), the concentrations of uteroglobin measured in aqueous humour (280) are even lower, in the pg/ml range.

The lack of response to uteroglobin treatment may also be due to the cell strain used. The TM is a complex tissue consisting of three distinct layers, and questions exist as to whether the TM cells in these structures form distinct cell types, specifically the cells of the JCT versus the corneoscleral TM, or whether they represent one cell type in different biological environments (122, 149, 294, 295). Therefore, the location of

TM cell extraction needs to be considered when evaluating *in vitro* experimental data. According to the manufacturer, the cell strain used in this study was isolated from the corneoscleral and juxtacanalicular region of a healthy TM, thus potentially presenting a heterogeneous cell population. This may or may not be relevant with regards to the effects of uteroglobin on contraction. Ideally, the effects of uteroglobin would be tested on TM cell strains from adult healthy and POAG eyes. Whilst some laboratories have successfully grown TM cells from glaucomatous eyes (189, 296, 297), glaucomatous TM cells are generally difficult to culture, due to reduced cell numbers and the effects of prolonged treatment with glaucoma medications (149). As an alternative, patient-derived induced pluripotent stem cells (iPSCs) could be used to model TM cell function *in vitro*, although the necessary differentiation protocol is yet to be fully developed.

Cellular contraction may also be assessed by measuring the formation of actin stress fibres, focal adhesions, and phosphorylation of myosin light chain kinase (270). Due to the molecular nature of cellular contraction processes, these alternative assays would likely provide more sensitive measures for contraction and may thus be able to detect differences that are not measurable by means of a collagen gel contraction assay.

Further experiments are needed to support the data obtained in this study, including the *in vitro* cell-free testing of recombinant uteroglobin in a PLA_2 activity assay to ensure its bioactivity. Ideally, a contractile cell line that responds to uteroglobin treatment would be used as a positive control. However, this may prove difficult to achieve due to the lack of knowledge regarding uteroglobin's signalling pathway and detailed physiological function.

Three additional aspects of uteroglobin function are of potential interest with regards to POAG and TM dysfunction (summarised in Figure 4.10). Firstly, uteroglobin has been reported to enhance phagocytosis of fluorescently-labelled beads in activated neutrophils (275). Thus, a phagocytosis assay could be used to assess whether uteroglobin treatment has a stimulatory effect on the phagocytic activity of TM cells (139).

Secondly, uteroglobin has a high affinity for TGM2 (298), an enzyme which covalently crosslinks ECM proteins to increase rigidity and prevent degradation (299). According to one *in vitro* study, TGM2 protein levels and enzymatic activity are elevated in glaucomatous TM cells compared to normal TM cells (180). Antiflamin, a peptide derived from uteroglobin, has been shown to inhibit TGM2 (300). Thus, it is conceivable that uteroglobin may also have an inhibitory effect on TGM2 activity, which would be beneficial in POAG, where ECM crosslinking and rigidity contribute to TM dysfunction and IOP elevation. Furthermore, TGM2 can stimulate PLA_2 function (300), thus inhibition of TGM2 by uteroglobin would additionally provide an indirect pathway for PLA_2 inhibition, resulting in TM relaxation and enhanced aqueous humour outflow.

Thirdly, uteroglobin can bind to fibronectin in a highly specific manner through a heparin-binding site (301). Whilst two main heparin-binding sites are known within fibronectin (HepI and HepII), Chowdhury et al (301) did not specify which heparin-binding site uteroglobin interacts with. Fibronectin is an abundant component of the TM ECM (302) and the HepII domain in fibronectin has been shown to reduce TM contractility (303) and increase outflow facility in perfused anterior segments (304, 305), highlighting the relevance of HepII in the regulation of outflow resistance. This process is thought to involve members of the rho GTPase family (304), which control TM contractility (291). Fibronectins can be crosslinked to each other as well as to other elements of the ECM by TGM2, a process stimulated by TGFβ2 (179). Interestingly, TGM2-fibronectin complexes stimulate rho GTPase signalling (306, 307), suggesting that the interaction between TGM2 and fibronectin may cause TM cell contraction and consequently reduced outflow facility (291, 308). In addition, TGM2 can also covalently crosslink uteroglobin to fibronectin. The specific interaction between uteroglobin and fibronectin has been shown to inhibit adhesion and migration of human endothelial cells *in vitro* (309). Collectively, this information suggests that uteroglobin interaction with fibronectin could influence TM cell contraction and thus affect aqueous humour outflow.

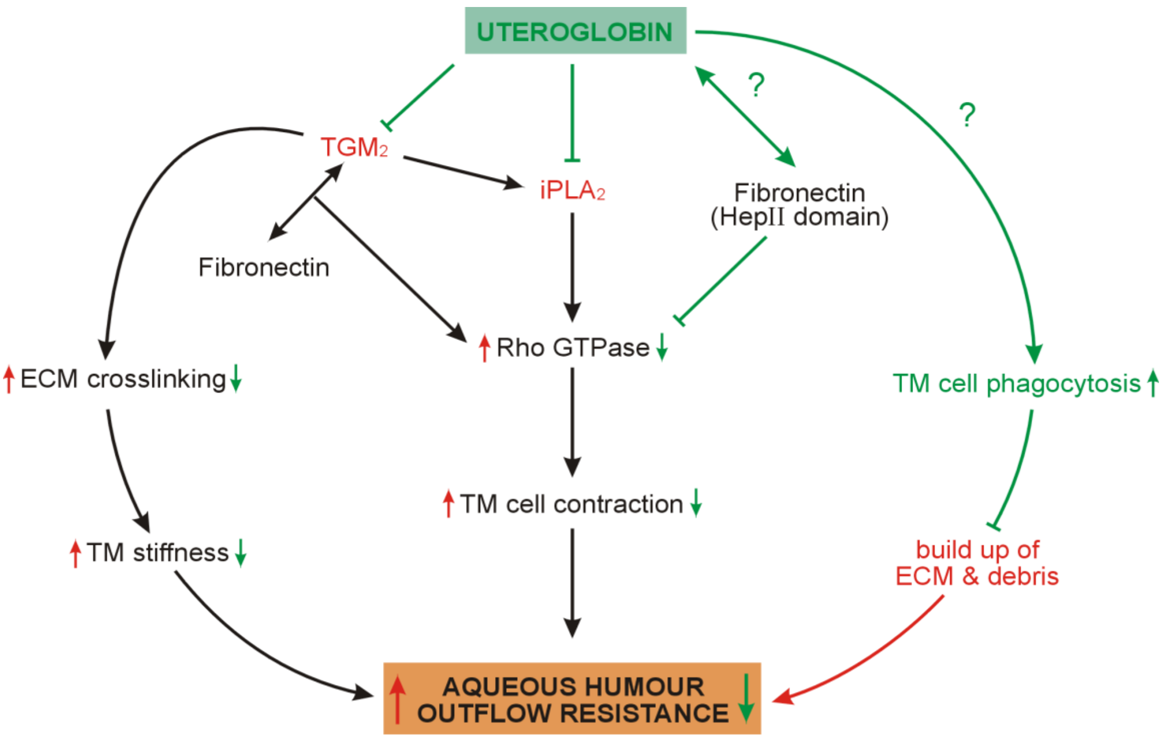

Figure 4.10 Diagram illustrating how uteroglobin may influence aqueous humour outflow through the trabecular meshwork, through interactions with tissue transglutaminase (TGM$_2$), calcium-independent phospholipase A2 (iPLA$_2$), fibronectin, and trabecular meshwork cell phagocytosis. Interactions that are uncertain are highlighted with a question mark (?).

In conclusion, treatment of pHTMCs with a single dose of exogenous uteroglobin did not affect cell contractibility at the concentrations tested. Additional experiments, such as PLA$_2$ activity, TGM2 activity, and phagocytosis assays, are needed to elucidate the role of uteroglobin in TM cell function.

4.6 Acknowledgements

The authors thank the Clifford Craig Medical Research Trust Tasmania (Grant Number 121) for funding this work, and the University of Tasmania for supporting

ELAB with an APA scholarship. We are grateful to Dr Dale Kunde and Nicole Ranson for technical assistance.

CHAPTER 5 GENERAL DISCUSSION AND CONCLUSION

5.1 PURPOSE AND AIMS OF THE RESEARCH

The TM plays a key role in regulating IOP, which in turn is critical for eye health and function. Whilst loss of appropriate pressure control is attributed to a dysfunctional TM, our knowledge of the cellular mechanisms involved is incomplete. The purpose of the research presented in this thesis was to increase our understanding of TM dysfunction in POAG, first by assessing changes in aqueous humour protein composition in clinical POAG and cataract control samples, and secondly by investigating the potential effects of one of the identified proteins on TM cell function using an *in vitro* cell model.

5.2 SUMMARY OF NOVEL FINDINGS AND IMPLICATIONS FOR THE FIELD

The aqueous humour studies presented in chapters 2 and 3 provide new insights into the altered protein composition of aqueous humour in POAG compared to cataract control samples. Whilst previous studies have quantified concentrations of various MMPs and TIMPs in aqueous humour and calculated direct ratios (pg/ml) (93, 97, 99, 100), none have performed a stochiometric analysis to investigate their molar ratios and determine potential relative imbalances in MMP inhibition. This is an important consideration, given that the ratio of enzyme to inhibitor determines enzyme activity and is thus more relevant than overall concentration. The imbalances determined in chapter 2, both in terms of concentration and molar ratios, are in agreement with the suggested dysfunctional ECM turnover in the glaucomatous TM (97, 121). The second aqueous humour study led to the successful quantification of CHI3L1, FLRG, HGF, MIF, p-selectin, and uteroglobin, of which only HGF and MIF had previously been measured in aqueous humour.

Previous studies on aqueous humour composition predominantly considered changes in protein concentrations. The few studies that did consider correlations with clinical factors did so in a limited fashion. To expand on the information gained through analysing protein concentrations and detect subtler yet potentially relevant changes, we also included correlation studies with a range of POAG disease descriptors, including IOP, CDR, age, and PSD. Several statistically significant correlations were determined in both studies, highlighting specific proteins for further investigation in regard to TM physiology and dysfunction. Further research on these proteins may reveal useful biomarkers or novel drug targets and enhance our understanding of the mechanisms involved in disease onset or progression.

Chapter 4 forms a first step in elucidating the relevance of one of these proteins, namely uteroglobin. Whilst no significant impact of uteroglobin on TM cell contraction was determined, possibly due to the cell model used, the chapter discusses four potential mechanisms by which uteroglobin may affect TM cell behaviour, namely cell contraction, phagocytosis, interaction with fibronectin, and ECM crosslinking (Figure 4.10). All of these processes influence aqueous humour outflow and thus warrant further investigation to determine if and how uteroglobin plays a role in their regulation.

5.3 STUDY LIMITATIONS

The limitations of each study contained in this thesis have been discussed in the respective chapter discussions (chapters 2-4). In summary, the main limitations of the aqueous humour studies presented in chapters 2 and 3 are the potential influence of hypotensive medication on aqueous humour composition and the limited sample volume, which prevented quantification of more analytes for each patient sample. Furthermore, the studies would benefit from repeat measurements in a separate cohort of participants to confirm the findings. While the use of samples from cataract patients as a control is not ideal, collection of aqueous humour from healthy eyes would be unethical, due to the invasive procedure required. Cataract samples are commonly used as a control for aqueous humour studies (79, 80, 92, 93, 99), given its routine availability and the estimated minimal impact of a cataract on aqueous humour protein concentration.

Many plausible reasons exist for the inconclusive results presented in chapter 4. It is possible that the cell strain used is not responsive to uteroglobin treatment and other TM cell strains should be tested to address this. The bioactivity of uteroglobin was not assessed, which presents an important limitation to this study. It is also possible that the contraction assay used is not sensitive enough to detect the effects of uteroglobin, thus requiring the use of alternative approaches to assess contraction.

5.4 Future directions

5.4.1 Improved trabecular meshwork cell models

As discussed in chapter 4, it would be preferable to test aqueous humour proteins on TM cells derived from POAG patients. However, primary TM cells strains can only be maintained for a limited time frame (149), requiring isolation from new eyes on a regular basis, and culturing glaucomatous TM cells presents additional challenges. The use of a stem cell-derived model could overcome these limitations by providing a large resource of genetically-relevant cells.

Patient-derived iPSCs present a promising avenue for *in vitro* disease modelling, as they can be differentiated into specific cell types of interest with a disease-relevant genetic background, which is particularly important for diseases that are genetically heterogenous and complex, as is the case with POAG. Disease modelling using iPSCs has been successfully used to study the molecular mechanisms underlying a variety of diseases, including neurodegenerative diseases such as Alzheimer's disease, Parkinson's disease, and amyotrophic lateral sclerosis. Differentiation of iPSCs to different retinal cell types has also enhanced our understanding of several ocular diseases, including glaucoma, age-related macular degeneration, Best disease, and retinitis pigmentosa (reviewed in (310)). With regards to the work presented in this thesis, iPSCs offer the opportunity to study the effects of different factors on TM cell behaviour, both in a healthy and a glaucomatous setting, using respective donor cells. Further benefits of developing such a model include the ability to investigate disease-relevant genetic mutations, use as a drug screening tool for personalized medicine and drug discovery, and development of patient-specific, cell-based therapy to overcome issues of graft rejection (311).

The TM develops from a cranial neural crest-derived structure known as the periocular mesenchyme (POM), which also gives rise to multiple other structures of the anterior segment, including the sclera, ciliary body, iris, Schlemm's canal, and cornea (312). Several methods have been published for generating neural crest cells from pluripotent stem cells (313-317) and studies of anterior segment dysgeneses have highlighted key transcription factors involved in the normal development of the POM and TM, namely *PAX6*, *PITX2, FOXC1,* and *LMX1B* (318-320) (see Figure 5.1). Whilst functional TM-like cells have been successfully derived from iPSCs using primary TM cell-derived ECM and conditioned medium to drive differentiation (252), a defined differentiation protocol with known factors would be the preferred method, especially in view of later clinical use. Recently, a protocol for defined differentiation of pluripotent stem cells to POM was published, using TGFβ and wnt inhibitors to drive the expression of *PITX2, FOXC1* and *LMX1B* (321). It remains to be determined what conditions are required to generate TM cells from POM, and whether these stem cell-derived POM cells are capable of differentiation to TM cells. It is likely that factors present in the aqueous humour are necessary for the final differentiation to TM, as aqueous humour has been shown to induce differentiation of resident adult stem cells in the TM (146).

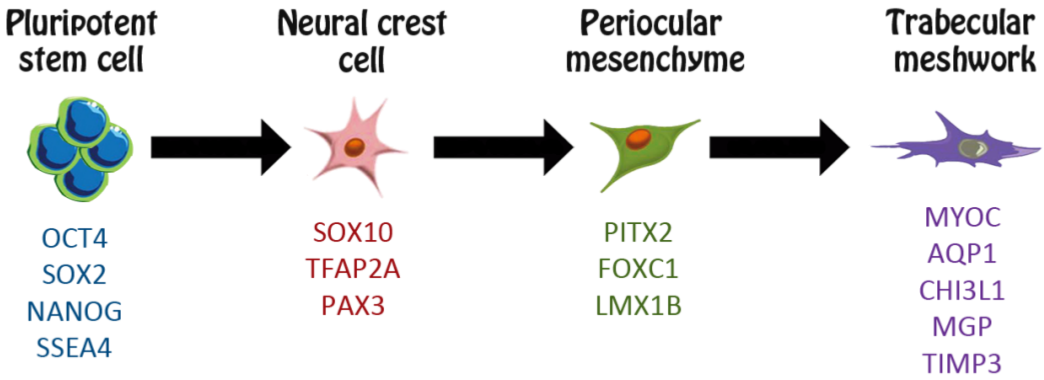

Figure 5.1 Differentiation of pluripotent stem cells to trabecular meshwork and associated markers. Figure adapted from LJ Danderian.

5.4.2 Further investigations of aqueous humour proteins

It is unclear whether the altered protein concentrations in glaucomatous aqueous humour result from changes in the TM or other tissues located along the aqueous humour pathway, but it is likely both are involved, as some of the proteins quantified are expressed by TM cells, whereas others, such as uteroglobin, are not. It also remains to be determined whether these changes are a cause, a consequence, or part of a compensatory mechanism in TM dysfunction. The results from the aqueous humour studies suggest TIMPs, uteroglobin, HGF, and FLRG as candidates for further investigation in relation to TM physiology and dysfunction. Future directions in relation to uteroglobin have been discussed extensively in chapter 4.

With regards to MMPs and TIMPs, the current literature focuses on MMPs and their impact on ECM turnover. However, given the significant increases in three out of four known TIMPs in glaucomatous aqueous humour shown in chapter 2 and the knowledge that TIMPs also possess MMP-independent functions (reviewed in (223)), TIMPs should be investigated in their own right with respect to TM physiology. The potential anti-apoptotic effect of TIMPs on TM cell apoptosis is of particular interest, as discussed in chapter 2. Treatment of TM cells *in vitro* with recombinant TIMP1 may reduce susceptibility to apoptosis induction, as previously observed in Burkitt's lymphoma cell lines (322). The use of a broad spectrum MMP inhibitor or inactivation of TIMP1's MMP-inhibitory activity via chemical reduction and alkylation, would permit exclusion of any MMP involvement in the resistance to apoptosis.

FLRG binds to members of the TGFβ superfamily, such as activin, myostatin, and BMP2, thereby blocking their interaction with cell surface receptors (246, 323, 324). The TM is thought to undergo a pathological calcification process with age, which is enhanced in POAG and induced by BMP2 (196, 325, 326). FLRG may therefore play a role in preventing calcification by inhibiting BMP2. Overexpression of BMP2 in TM cells *in vitro* increases calcification, as determined by alizarin red staining (227). If the above hypothesis is true, TM cells pre-treated with FLRG would be expected to show less calcification, unless FLRG interaction was blocked by an anti-FLRG antibody or a specific inhibitor. FLRG has also been shown to interact with fibronectin. Using hematopoietic UT-7 cells and primary human hematopoietic cells, enhanced cell adhesion to fibronectin was observed with increased FLRG concentrations (327). As fibronectin is abundant in the TM ECM, investigation of FLRG interaction with fibronectin may be of interest to TM physiology. Finally, follistatin, a BMP and activin inhibitor highly homologous to FLRG, is expressed by TM cells, and expression is upregulated by TGF-β2 (239). Given the structural and functional similarities between follistatin and FLRG, it is possible that TGF-β2 may also regulate FLRG expression.

HGF has been shown to enhance MMP activity in cultured endothelial cells (254). Treatment of perfused anterior segments with HGF may have a comparable effect to perfusion with MMPs, increasing aqueous humour outflow (101). In human keratinocytes, HGF inhibits UVB-induced apoptosis (328). Equally, HGF may protect TM cells from apoptosis, a process that has been suggested to be involved in TM cell loss (221, 222). Thus, treatment of TM cells *in vitro* with HGF followed by chemical induction of apoptosis may result in reduced levels of apoptosis.

5.5 Conclusion

In conclusion, the research findings presented in this thesis enhance our current understanding of aqueous humour imbalances in POAG, by providing quantitative measurements of several MMPs, TIMPs, growth factors, and cytokines. Comprehensive analysis of the data led to several significant correlations between these proteins and multiple disease descriptors, which may help to shed light on cellular processes relevant to POAG pathogenesis. Furthermore, analysis of MMP/TIMP ratios demonstrated imbalances in MMP inhibition in POAG aqueous humour, a process of known relevance to TM function. Finally, the research highlights uteroglobin as a potential protein of interest in TM dysfunction and discusses four distinct cellular processes that may be affected by uteroglobin, all of which impact on aqueous humour outflow.

REFERENCES

1. Tham YC, Li X, Wong TY, Quigley HA, Aung T, Cheng CY. Global prevalence of glaucoma and projections of glaucoma burden through 2040: a systematic review and meta-analysis. *Ophthalmology*. 2014;121:2081-2090.
2. Wensor MD, McCarty CA, Stanislavsky YL, Livingston PM, Taylor HR. The prevalence of glaucoma in the Melbourne Visual Impairment Project. *Ophthalmology*. 1998;105:733-739.
3. Mitchell P, Smith W, Attebo K, Healey PR. Prevalence of open-angle glaucoma in Australia. The Blue Mountains Eye Study. *Ophthalmology*. 1996;103:1661-1669.
4. Kwon YH, Fingert JH, Kuehn MH, Alward WL. Primary open-angle glaucoma. *N Engl J Med*. 2009;360:1113-1124.
5. Leske MC, Heijl A, Hussein M, et al. Factors for glaucoma progression and the effect of treatment: the early manifest glaucoma trial. *Arch Ophthalmol*. 2003;121:48-56.
6. Topouzis F, Coleman AL, Harris A, et al. Factors associated with undiagnosed open-angle glaucoma: the Thessaloniki Eye Study. *Am J Ophthalmol*. 2008;145:327-335.
7. Shaikh Y, Yu F, Coleman AL. Burden of undetected and untreated glaucoma in the United States. *Am J Ophthalmol*. 2014;158:1121-1129.
8. Jonas JB, Aung T, Bourne RR, Bron AM, Ritch R, Panda-Jonas S. Glaucoma. *Lancet*. 2017;390:2183-2193.
9. Varma R, Lee PP, Goldberg I, Kotak S. An assessment of the health and economic burdens of glaucoma. *Am J Ophthalmol*. 2011;152:515-522.

10. Tunnel Vision. The Ecomonic Impact of Primary Open Angle Glaucoma - A Dynamic Economic Model. Centre for Eye Research Australia, 2008.

11. Gaton D. Screening for glaucoma. *Isr Med Assoc J*. 2014;16:509-510.

12. Francis BA, Varma R, Vigen C, et al. Population and high-risk group screening for glaucoma: the Los Angeles Latino Eye Study. *Invest Ophthalmol Vis Sci*. 2011;52:6257-6264.

13. Quigley HA. Glaucoma. *Lancet*. 2011;377:1367-1377.

14. Weinreb RN, Khaw PT. Primary open-angle glaucoma. *Lancet*. 2004;363:1711-1720.

15. Casson RJ, Chidlow G, Wood JP, Crowston JG, Goldberg I. Definition of glaucoma: clinical and experimental concepts. *Clin Exp Ophthalmol*. 2012;40:341-349.

16. Wilson MR. The myth of "21". *J Glaucoma*. 1997;6:75-77.

17. Weinreb RN, Leung CK, Crowston JG, et al. Primary open-angle glaucoma. *Nat Rev Dis Primers*. 2016;2:1-19.

18. Gupta D, Chen PP. Glaucoma. *Am Fam Physician*. 2016;93:668-674.

19. Weinreb RN, Aung T, Medeiros FA. The pathophysiology and treatment of glaucoma: a review. *JAMA*. 2014;311:1901-1911.

20. Harwerth RS, Wheat JL, Fredette MJ, Anderson DR. Linking structure and function in glaucoma. *Prog Retin Eye Res*. 2010;29:249-271.

21. Quigley HA, Dunkelberger GR, Green WR. Retinal ganglion cell atrophy correlated with automated perimetry in human eyes with glaucoma. *Am J Ophthalmol*. 1989;107:453-464.

22. Nordmann JP, Mesbah M, Berdeaux G. Scoring of visual field measured through Humphrey perimetry: principal component varimax rotation followed by validated cluster analysis. *Invest Ophthalmol Vis Sci*. 2005;46:3169-3176.

23. Sample PA. Short-wavelength automated perimetry: it's role in the clinic and for understanding ganglion cell function. *Prog Retin Eye Res*. 2000;19:369-383.

24. Nouri-Mahdavi K. Selecting visual field tests and assessing visual field deterioration in glaucoma. *Can J Ophthalmol*. 2014;49:497-505.

25. Tombran-Tink J, Barnstable CJ, Shields MB. Epidemiology of and Risk Factors for Primary Open-Angle Glaucoma. In: Tombran-Tink J, Barnstable CJ, Shields MB, eds. *Mechanisms of the Glaucomas: Disease Processes and Therapeutic Modalities*. Totowa, NJ: Humana Press; 2008:19-33.

26. Wolfs RC, Klaver CC, Ramrattan RS, van Duijn CM, Hofman A, de Jong PT. Genetic risk of primary open-angle glaucoma. Population-based familial aggregation study. *Arch Ophthalmol*. 1998;116:1640-1645.

27. Janssen SF, Gorgels TG, Ramdas WD, et al. The vast complexity of primary open angle glaucoma: disease genes, risks, molecular mechanisms and pathobiology. *Prog Retin Eye Res*. 2013;37:31-67.

28. Fan BJ, Wang DY, Lam DS, Pang CP. Gene mapping for primary open angle glaucoma. *Clin Biochem*. 2006;39:249-258.

29. Wang R, Wiggs JL. Common and rare genetic risk factors for glaucoma. *Cold Spring Harb Perspect Med*. 2014;4:1-13.

30. Liu Y, Allingham RR. Major review: Molecular genetics of primary open-angle glaucoma. *Exp Eye Res*. 2017;160:62-84.

31. Iglesias AI, Springelkamp H, Ramdas WD, Klaver CC, Willemsen R, van Duijn CM. Genes, pathways, and animal models in primary open-angle glaucoma. *Eye (Lond)*. 2015;29:1285-1298.

32. Vajaranant TS, Nayak S, Wilensky JT, Joslin CE. Gender and glaucoma: what we know and what we need to know. *Curr Opin Ophthalmol*. 2010;21:91-99.

33. Rudnicka AR, Mt-Isa S, Owen CG, Cook DG, Ashby D. Variations in primary open-angle glaucoma prevalence by age, gender, and race: a Bayesian meta-analysis. *Invest Ophthalmol Vis Sci*. 2006;47:4254-4261.

34. Kapetanakis VV, Chan MP, Foster PJ, Cook DG, Owen CG, Rudnicka AR. Global variations and time trends in the prevalence of primary open angle glaucoma (POAG): a systematic review and meta-analysis. *Br J Ophthalmol*. 2016;100:86-93.

35. Hsu CH, Chen RI, Lin SC. Myopia and glaucoma: sorting out the difference. *Curr Opin Ophthalmol*. 2015;26:90-95.

36. Boland MV, Quigley HA. Risk factors and open-angle glaucoma: classification and application. *J Glaucoma*. 2007;16:406-418.

37. Evangelho K, Mogilevskaya M, Losada-Barragan M, Vargas-Sanchez JK. Pathophysiology of primary open-angle glaucoma from a neuroinflammatory and neurotoxicity perspective: a review of the literature. *Int Ophthalmol*. 2017:1-13.

38. Kuehn MH, Fingert JH, Kwon YH. Retinal ganglion cell death in glaucoma: mechanisms and neuroprotective strategies. *Ophthalmol Clin North Am*. 2005;18:383-395.

39. Friedman DS, Wilson MR, Liebmann JM, Fechtner RD, Weinreb RN. An evidence-based assessment of risk factors for the progression of ocular hypertension and glaucoma. *Am J Ophthalmol*. 2004;138:S19-31.

40. Quigley HA, Enger C, Katz J, Sommer A, Scott R, Gilbert D. Risk factors for the development of glaucomatous visual field loss in ocular hypertension. *Arch Ophthalmol*. 1994;112:644-649.

41. Bengtsson B, Heijl A. A long-term prospective study of risk factors for glaucomatous visual field loss in patients with ocular hypertension. *J Glaucoma*. 2005;14:135-138.

42. Kass MA, Heuer DK, Higginbotham EJ, et al. The Ocular Hypertension Treatment Study: a randomized trial determines that topical ocular hypotensive medication delays or prevents the onset of primary open-angle glaucoma. *Arch Ophthalmol*. 2002;120:701-713.

43. Heijl A, Leske MC, Bengtsson B, et al. Reduction of intraocular pressure and glaucoma progression: results from the Early Manifest Glaucoma Trial. *Arch Ophthalmol*. 2002;120:1268-1279.

44. The Advanced Glaucoma Intervention Study (AGIS): 7. The relationship between control of intraocular pressure and visual field deterioration. The AGIS Investigators. *Am J Ophthalmol*. 2000;130:429-440.

45. The effectiveness of intraocular pressure reduction in the treatment of normal-tension glaucoma. Collaborative Normal-Tension Glaucoma Study Group. *Am J Ophthalmol*. 1998;126:498-505.

46. Comparison of glaucomatous progression between untreated patients with normal-tension glaucoma and patients with therapeutically reduced

intraocular pressures. Collaborative Normal-Tension Glaucoma Study Group. *Am J Ophthalmol*. 1998;126:487-497.

47. Johnson M. 'What controls aqueous humour outflow resistance?'. *Exp Eye Res*. 2006;82:545-557.

48. Overby DR, Stamer WD, Johnson M. The changing paradigm of outflow resistance generation: towards synergistic models of the JCT and inner wall endothelium. *Exp Eye Res*. 2009;88:656-670.

49. Mabuchi F, Aihara M, Mackey MR, Lindsey JD, Weinreb RN. Optic nerve damage in experimental mouse ocular hypertension. *Invest Ophthalmol Vis Sci*. 2003;44:4321-4330.

50. Schaub JA, Kimball EC, Steinhart MR, et al. Regional Retinal Ganglion Cell Axon Loss in a Murine Glaucoma Model. *Invest Ophthalmol Vis Sci*. 2017;58:2765-2773.

51. Morrison JC, Cepurna WO, Johnson EC. Modeling glaucoma in rats by sclerosing aqueous outflow pathways to elevate intraocular pressure. *Exp Eye Res*. 2015;141:23-32.

52. Downs JC. Optic nerve head biomechanics in aging and disease. *Exp Eye Res*. 2015;133:19-29.

53. Cohen LP, Pasquale LR. Clinical characteristics and current treatment of glaucoma. *Cold Spring Harb Perspect Med*. 2014;4:1-16.

54. Tanna AP, Johnson M. Rho Kinase Inhibitors as a Novel Treatment for Glaucoma and Ocular Hypertension. *Ophthalmology*. 2018;125:1741-1756.

55. Ito YA, Walter MA. Genomics and anterior segment dysgenesis: a review. *Clin Exp Ophthalmol*. 2014;42:13-24.

56. Kels BD, Grzybowski A, Grant-Kels JM. Human ocular anatomy. *Clin Dermatol*. 2015;33:140-146.

57. Prasad S, Galetta SL. Anatomy and physiology of the afferent visual system. *Handb Clin Neurol*. 2011;102:3-19.

58. Abe RY, Gracitelli CP, Diniz-Filho A, Tatham AJ, Medeiros FA. Lamina Cribrosa in Glaucoma: Diagnosis and Monitoring. *Curr Ophthalmol Rep*. 2015;3:74-84.

59. De Berardinis E, Tieri O, Polzella A, Iuglio N. The chemical composition of the human aqueous humour in normal and pathological conditions. *Exp Eye Res*. 1965;4:179-186.

60. Consul BN, Taunk JP, Mathur GB. Human aqueous electrolytes (a study of sodium, potassium and chloride in normal and cataractous eyes). *J All India Ophthalmol Soc*. 1969;17:52-54.

61. Krause U, Raunio V. Proteins of the normal human aqueous humour. *Ophthalmologica*. 1969;159:178-185.

62. Krause U, Raunio V. Protein content of normal human aqueous humour in vivo. *Acta Ophthalmol (Copenh)*. 1969;47:215-221.

63. Bill A. The aqueous humor drainage mechanism in the cynomolgus monkey (Macaca irus) with evidence for unconventional routes. *Invest Ophthalmol*. 1965;4:911-919.

64. Bill A, Hellsing K. Production and drainage of aqueous humor in the cynomolgus monkey (Macaca irus). *Invest Ophthalmol*. 1965;4:920-926.

65. Toris CB, Yablonski ME, Wang YL, Camras CB. Aqueous humor dynamics in the aging human eye. *Am J Ophthalmol*. 1999;127:407-412.

66. Johnson M, McLaren JW, Overby DR. Unconventional aqueous humor outflow: A review. *Exp Eye Res*. 2017;158:94-111.

67. Bill A, Phillips CI. Uveoscleral drainage of aqueous humour in human eyes. *Experimental Eye Research*. 1971;12:275-281.

68. Acott TS, Kelley MJ. Extracellular matrix in the trabecular meshwork. *Exp Eye Res*. 2008;86:543-561.

69. Acott TS, Kelley MJ, Keller KE, et al. Intraocular pressure homeostasis: maintaining balance in a high-pressure environment. *J Ocul Pharmacol Ther*. 2014;30:94-101.

70. Carreon T, van der Merwe E, Fellman RL, Johnstone M, Bhattacharya SK. Aqueous outflow - A continuum from trabecular meshwork to episcleral veins. *Prog Retin Eye Res*. 2017;57:108-133.

71. Stamer WD, Clark AF. The many faces of the trabecular meshwork cell. *Exp Eye Res*. 2017;158:112-123.

72. Jones VS, Wu J, Zhu SW, Huang RP. Application of multiplex immunoassay technology to investigations of ocular disease. *Expert Rev Mol Med*. 2016;18:1-15.

73. Elsobky S, Crane AM, Margolis M, Carreon TA, Bhattacharya SK. Review of application of mass spectrometry for analyses of anterior eye proteome. *World J Biol Chem*. 2014;5:106-114.

74. Richardson MR, Price MO, Price FW, et al. Proteomic analysis of human aqueous humor using multidimensional protein identification technology. *Mol Vis*. 2009;15:2740-2750.

75. Chowdhury UR, Madden BJ, Charlesworth MC, Fautsch MP. Proteome analysis of human aqueous humor. *Invest Ophthalmol Vis Sci*. 2010;51:4921-4931.

76. Perumal N, Manicam C, Steinicke M, Funke S, Pfeiffer N, Grus FH. Characterization of the human aqueous humour proteome: A comparison of the genders. *PLoS One*. 2017;12.

77. Izzotti A, Longobardi M, Cartiglia C, Saccà SC. Proteome Alterations in Primary Open Angle Glaucoma Aqueous Humor. *Journal of Proteome Research*. 2010;9:4831-4838.

78. Duan X, Xue P, Wang N, Dong Z, Lu Q, Yang F. Proteomic analysis of aqueous humor from patients with primary open angle glaucoma. *Mol Vis*. 2010;16:2839-2846.

79. Kaeslin MA, Killer HE, Fuhrer CA, Zeleny N, Huber AR, Neutzner A. Changes to the Aqueous Humor Proteome during Glaucoma. *PLoS One*. 2016;11.

80. Sharma S, Bollinger KE, Kodeboyina SK, et al. Proteomic Alterations in Aqueous Humor From Patients With Primary Open Angle Glaucoma. *Invest Ophthalmol Vis Sci*. 2018;59:2635-2643.

81. Adav SS, Wei J, Terence Y, Ang BCH, Yip LWL, Sze SK. Proteomic Analysis of Aqueous Humor from Primary Open Angle Glaucoma Patients on Drug Treatment Revealed Altered Complement Activation Cascade. *J Proteome Res*. 2018;17:2499-2510.

82. Kaur I, Kaur J, Sooraj K, et al. Comparative evaluation of the aqueous humor proteome of primary angle closure and primary open angle glaucomas and age-related cataract eyes. *Int Ophthalmol*. 2018.

83. Prendes MA, Harris A, Wirostko BM, Gerber AL, Siesky B. The role of transforming growth factor beta in glaucoma and the therapeutic implications. *Br J Ophthalmol*. 2013;97:680-686.

84. Lutjen-Drecoll E. Morphological changes in glaucomatous eyes and the role of TGFbeta2 for the pathogenesis of the disease. *Exp Eye Res*. 2005;81:1-4.

85. Fuchshofer R, Tamm ER. Modulation of extracellular matrix turnover in the trabecular meshwork. *Experimental Eye Research*. 2009;88:683-688.

86. Bhattacharya SK, Gabelt BT, Ruiz J, Picciani R, Kaufman PL. Cochlin expression in anterior segment organ culture models after TGFbeta2 treatment. *Invest Ophthalmol Vis Sci*. 2009;50:551-559.

87. Birke MT, Birke K, Lutjen-Drecoll E, Schlotzer-Schrehardt U, Hammer CM. Cytokine-dependent ELAM-1 induction and concomitant intraocular pressure regulation in porcine anterior eye perfusion culture. *Invest Ophthalmol Vis Sci*. 2011;52:468-475.

88. Shepard AR, Millar JC, Pang IH, Jacobson N, Wang WH, Clark AF. Adenoviral gene transfer of active human transforming growth factor-{beta}2 elevates intraocular pressure and reduces outflow facility in rodent eyes. *Invest Ophthalmol Vis Sci*. 2010;51:2067-2076.

89. Sternlicht MD, Werb Z. How matrix metalloproteinases regulate cell behavior. *Annu Rev Cell Dev Biol*. 2001;17:463-516.

90. Gomis-Ruth FX, Maskos K, Betz M, et al. Mechanism of inhibition of the human matrix metalloproteinase stromelysin-1 by TIMP-1. *Nature*. 1997;389:77-81.

91. De Groef L, Van Hove I, Dekeyster E, Stalmans I, Moons L. MMPs in the trabecular meshwork: promising targets for future glaucoma therapies? *Invest Ophthalmol Vis Sci*. 2013;54:7756-7763.

92. Fountoulakis N, Labiris G, Aristeidou A, et al. Tissue inhibitor of metalloproteinase 4 in aqueous humor of patients with primary open angle

glaucoma, pseudoexfoliation syndrome and pseudoexfoliative glaucoma and its role in proteolysis imbalance. *BMC Ophthalmol*. 2013;13:69-75.

93. Nga AD, Yap SL, Samsudin A, Abdul-Rahman PS, Hashim OH, Mimiwati Z. Matrix metalloproteinases and tissue inhibitors of metalloproteinases in the aqueous humour of patients with primary angle closure glaucoma - a quantitative study. *BMC Ophthalmol*. 2014;14:33-38.

94. Maatta M, Tervahartiala T, Harju M, Airaksinen J, Autio-Harmainen H, Sorsa T. Matrix metalloproteinases and their tissue inhibitors in aqueous humor of patients with primary open-angle glaucoma, exfoliation syndrome, and exfoliation glaucoma. *J Glaucoma*. 2005;14:64-69.

95. Djordjevic-Jocic J, Zlatanovic G, Veselinovic D, et al. Transforming growth factor beta1, matrix-metalloproteinase-2 and its tissue inhibitor in patients with pseudoexfoliation glaucoma/syndrome. *Vojnosanit Pregl*. 2012;69:231-236.

96. Maatta M, Tervahartiala T, Vesti E, Airaksinen J, Sorsa T. Levels and activation of matrix metalloproteinases in aqueous humor are elevated in uveitis-related secondary glaucoma. *J Glaucoma*. 2006;15:229-237.

97. Schlotzer-Schrehardt U, Lommatzsch J, Kuchle M, Konstas AG, Naumann GO. Matrix metalloproteinases and their inhibitors in aqueous humor of patients with pseudoexfoliation syndrome/glaucoma and primary open-angle glaucoma. *Invest Ophthalmol Vis Sci*. 2003;44:1117-1125.

98. Kee C, Son S, Ahn BH. The relationship between gelatinase A activity in aqueous humor and glaucoma. *J Glaucoma*. 1999;8:51-55.

99. Kara S, Yildirim N, Ozer A, Colak O, Sahin A. Matrix metalloproteinase-2, tissue inhibitor of matrix metalloproteinase-2, and transforming growth factor beta

1 in the aqueous humor and serum of patients with pseudoexfoliation syndrome. *Clin Ophthalmol*. 2014;8:305-309.

100. Cellini M, Leonetti P, Strobbe E, Campos EC. Matrix metalloproteinases and their tissue inhibitors after selective laser trabeculoplasty in pseudoexfoliative secondary glaucoma. *BMC Ophthalmol*. 2008;8:20-24.

101. Bradley JM, Vranka J, Colvis CM, et al. Effect of matrix metalloproteinases activity on outflow in perfused human organ culture. *Invest Ophthalmol Vis Sci*. 1998;39:2649-2658.

102. Kuchtey J, Rezaei KA, Jaru-Ampornpan P, Sternberg P, Jr., Kuchtey RW. Multiplex cytokine analysis reveals elevated concentration of interleukin-8 in glaucomatous aqueous humor. *Invest Ophthalmol Vis Sci*. 2010;51:6441-6447.

103. Takai Y, Tanito M, Ohira A. Multiplex cytokine analysis of aqueous humor in eyes with primary open-angle glaucoma, exfoliation glaucoma, and cataract. *Invest Ophthalmol Vis Sci*. 2012;53:241-247.

104. Chua J, Vania M, Cheung CM, et al. Expression profile of inflammatory cytokines in aqueous from glaucomatous eyes. *Mol Vis*. 2012;18:431-438.

105. Freedman J, Iserovich P. Pro-inflammatory cytokines in glaucomatous aqueous and encysted Molteno implant blebs and their relationship to pressure. *Invest Ophthalmol Vis Sci*. 2013;54:4851-4855.

106. Balaiya S, Edwards J, Tillis T, Khetpal V, Chalam KV. Tumor necrosis factor-alpha (TNF-alpha) levels in aqueous humor of primary open angle glaucoma. *Clin Ophthalmol*. 2011;5:553-556.

107. Borkenstein A, Faschinger C, Maier R, et al. Measurement of tumor necrosis factor-alpha, interleukin-6, Fas ligand, interleukin-1alpha, and interleukin-

1beta in the aqueous humor of patients with open angle glaucoma using multiplex bead analysis. *Mol Vis*. 2013;19:2306-2311.

108. Wirtz MK, Keller KE. The Role of the IL-20 Subfamily in Glaucoma. *Mediators Inflamm*. 2016;2016:1-8.

109. Saccà SC, Centofanti M, Izzotti A. New Proteins as Vascular Biomarkers in Primary Open Angle Glaucomatous Aqueous Humor. *Investigative Ophthalmology & Visual Science*. 2012;53:4242-4253.

110. Knepper PA, Mayanil CS, Goossens W, et al. Aqueous humor in primary open-angle glaucoma contains an increased level of CD44S. *Invest Ophthalmol Vis Sci*. 2002;43:133-139.

111. Wang ZY, Zhao KK, Zhao PQ. Erythropoietin is increased in aqueous humor of glaucomatous eyes. *Curr Eye Res*. 2010;35:680-684.

112. Nassiri N, Nassiri N, Majdi M, et al. Erythropoietin levels in aqueous humor of patients with glaucoma. *Mol Vis*. 2012;18:1991-1995.

113. Kim KS, Lee BH, Kim IS. The measurement of fibronectin concentrations in human aqueous humor. *Korean J Ophthalmol*. 1992;6:1-5.

114. Hu DN, Ritch R. Hepatocyte growth factor is increased in the aqueous humor of glaucomatous eyes. *J Glaucoma*. 2001;10:152-157.

115. Howell KG, Vrabel AM, Chowdhury UR, Stamer WD, Fautsch MP. Myocilin levels in primary open-angle glaucoma and pseudoexfoliation glaucoma human aqueous humor. *J Glaucoma*. 2010;19:569-575.

116. Hu DN, Ritch R, Liebmann J, Liu Y, Cheng B, Hu MS. Vascular endothelial growth factor is increased in aqueous humor of glaucomatous eyes. *J Glaucoma*. 2002;11:406-410.

117. Picht G, Welge-Luessen U, Grehn F, Lutjen-Drecoll E. Transforming growth factor beta 2 levels in the aqueous humor in different types of glaucoma and the relation to filtering bleb development. *Graefes Arch Clin Exp Ophthalmol*. 2001;239:199-207.

118. Tamm ER. The trabecular meshwork outflow pathways: structural and functional aspects. *Exp Eye Res*. 2009;88:648-655.

119. Shields MB, Damji KF, Safranov G. *Shields' Textbook of Glaucoma*. 5th ed. Lippincott Willliams & Wilkins; 2005.

120. Keller KE, Acott TS. The Juxtacanalicular Region of Ocular Trabecular Meshwork: A Tissue with a Unique Extracellular Matrix and Specialized Function. *J Ocul Biol*. 2013;1:3.

121. Vranka JA, Kelley MJ, Acott TS, Keller KE. Extracellular matrix in the trabecular meshwork: intraocular pressure regulation and dysregulation in glaucoma. *Exp Eye Res*. 2015;133:112-125.

122. Ge P, Navarro ID, Kessler MM, et al. The Soluble Guanylate Cyclase Stimulator IWP-953 Increases Conventional Outflow Facility in Mouse Eyes. *Invest Ophthalmol Vis Sci*. 2016;57:1317-1326.

123. Cai S, Liu X, Glasser A, et al. Effect of latrunculin-A on morphology and actin-associated adhesions of cultured human trabecular meshwork cells. *Mol Vis*. 2000;6:132-143.

124. Ethier CR. The inner wall of Schlemm's canal. *Exp Eye Res*. 2002;74:161-172.

125. Stamer WD, Acott TS. Current understanding of conventional outflow dysfunction in glaucoma. *Curr Opin Ophthalmol*. 2012;23:135-143.

126. Swaminathan SS, Oh DJ, Kang MH, et al. Secreted protein acidic and rich in cysteine (SPARC)-null mice exhibit more uniform outflow. *Invest Ophthalmol Vis Sci*. 2013;54:2035-2047.

127. Keller KE, Bradley JM, Vranka JA, Acott TS. Segmental versican expression in the trabecular meshwork and involvement in outflow facility. *Invest Ophthalmol Vis Sci*. 2011;52:5049-5057.

128. Keller KE, Bradley JM, Kelley MJ, Acott TS. Effects of modifiers of glycosaminoglycan biosynthesis on outflow facility in perfusion culture. *Invest Ophthalmol Vis Sci*. 2008;49:2495-2505.

129. Tamm ER, Braunger BM, Fuchshofer R. Chapter Eighteen - Intraocular Pressure and the Mechanisms Involved in Resistance of the Aqueous Humor Flow in the Trabecular Meshwork Outflow Pathways. In: Hejtmancik JF, Nickerson JM, eds. *Progress in Molecular Biology and Translational Science*: Academic Press; 2015:301-314.

130. Keller KE, Aga M, Bradley JM, Kelley MJ, Acott TS. Extracellular matrix turnover and outflow resistance. *Exp Eye Res*. 2009;88:676-682.

131. Filla MS, Faralli JA, Peotter JL, Peters DM. The role of integrins in glaucoma. *Exp Eye Res*. 2017;158:124-136.

132. O'Callaghan J, Cassidy PS, Humphries P. Open-angle glaucoma: therapeutically targeting the extracellular matrix of the conventional outflow pathway. *Expert Opin Ther Targets*. 2017;21:1037-1050.

133. Tian B, Gabelt BT, Geiger B, Kaufman PL. The role of the actomyosin system in regulating trabecular fluid outflow. *Exp Eye Res*. 2009;88:713-717.

134. Wiederholt M, Thieme H, Stumpff F. The regulation of trabecular meshwork and ciliary muscle contractility. *Prog Retin Eye Res*. 2000;19:271-295.

135. Braunger BM, Fuchshofer R, Tamm ER. The aqueous humor outflow pathways in glaucoma: A unifying concept of disease mechanisms and causative treatment. *Eur J Pharm Biopharm*. 2015;95:173-181.

136. Epstein DL, Freddo TF, Anderson PJ, Patterson MM, Bassett-Chu S. Experimental obstruction to aqueous outflow by pigment particles in living monkeys. *Invest Ophthalmol Vis Sci*. 1986;27:387-395.

137. Grierson I, Lee WR. Erythrocyte phagocytosis in the human trabecular meshwork. *Br J Ophthalmol*. 1973;57:400-415.

138. Bill A. Editorial: The drainage of aqueous humor. *Invest Ophthalmol*. 1975;14:1-3.

139. Buller C, Johnson DH, Tschumper RC. Human trabecular meshwork phagocytosis. Observations in an organ culture system. *Invest Ophthalmol Vis Sci*. 1990;31:2156-2163.

140. Sherwood ME, Richardson TM. Phagocytosis by trabecular meshwork cells: sequence of events in cats and monkeys. *Exp Eye Res*. 1988;46:881-895.

141. Johnson DH, Richardson TM, Epstein DL. Trabecular meshwork recovery after phagocytic challenge. *Curr Eye Res*. 1989;8:1121-1130.

142. Rohen JW, van der Zypen E. The phagocytic activity of the trabecular meshwork endothelium. An electron-microscopic study of the vervet (Cercopithecus aethiops). *Albrecht Von Graefes Arch Klin Exp Ophthalmol* 1968;175:143-160.

143. Porter KM, Epstein DL, Liton PB. Up-regulated expression of extracellular matrix remodeling genes in phagocytically challenged trabecular meshwork cells. *PLoS One*. 2012;7.

144. Grant WM. Clinical measurements of aqueous outflow. *Am J Ophthalmol*. 1951;34:1603-1605.

145. Mao W, Liu Y, Mody A, Montecchi-Palmer M, Wordinger RJ, Clark AF. Characterization of a spontaneously immortalized bovine trabecular meshwork cell line. *Exp Eye Res*. 2012;105:53-59.

146. Du Y, Roh DS, Mann MM, Funderburgh ML, Funderburgh JL, Schuman JS. Multipotent stem cells from trabecular meshwork become phagocytic TM cells. *Invest Ophthalmol Vis Sci*. 2012;53:1566-1575.

147. Raghunathan VK, Morgan JT, Park SA, et al. Dexamethasone Stiffens Trabecular Meshwork, Trabecular Meshwork Cells, and Matrix. *Invest Ophthalmol Vis Sci*. 2015;56:4447-4459.

148. Mao W, Liu Y, Wordinger RJ, Clark AF. A magnetic bead-based method for mouse trabecular meshwork cell isolation. *Invest Ophthalmol Vis Sci*. 2013;54:3600-3606.

149. Keller KE, Bhattacharya SK, Borras T, et al. Consensus recommendations for trabecular meshwork cell isolation, characterization and culture. *Exp Eye Res*. 2018;171:164-173.

150. Grierson I, Howes RC. Age-related depletion of the cell population in the human trabecular meshwork. *Eye (Lond)*. 1987;1:204-210.

151. Alvarado J, Murphy C, Polansky J, Juster R. Age-related changes in trabecular meshwork cellularity. *Invest Ophthalmol Vis Sci*. 1981;21:714-727.

152. Alvarado J, Murphy C, Juster R. Trabecular meshwork cellularity in primary open-angle glaucoma and nonglaucomatous normals. *Ophthalmology*. 1984;91:564-579.

153. Liton PB, Challa P, Stinnett S, Luna C, Epstein DL, Gonzalez P. Cellular senescence in the glaucomatous outflow pathway. *Exp Gerontol*. 2005;40:745-748.

154. Gong H, Swain DL. The histopathological changes in the trabecular outflow pathway and their possible effects on aqueous outflow in eyes with primary open-angle glaucoma. In: Knepper PA, Samples JR, eds. *Glaucoma research and clinical advances 2016 to 2018*. *New concepts in glaucoma*. Amsterdam: Kugler Publications; 2016:17-40.

155. Tektas OY, Lutjen-Drecoll E. Structural changes of the trabecular meshwork in different kinds of glaucoma. *Exp Eye Res*. 2009;88:769-775.

156. Green KA, Yue BYJT, Samples JR, Knepper PA. Trabecular meshwork cell death in primary open-angle glaucoma. In: Knepper PA, Samples JR, eds. *Glaucoma research and clinical advances 2016 to 2018*. *New concepts in glaucoma*. Amsterdam: Kugler Publications; 2016:1-16.

157. Grierson I, Chisholm IA. Clearance of debris from the iris through the drainage angle of the rabbit's eye. *Br J Ophthalmol*. 1978;62:694-704.

158. Samuelson DA, Gelatt KN, Gum GG. Kinetics of phagocytosis in the normal canine iridocorneal angle. *Am J Vet Res*. 1984;45:2359-2366.

159. Matsumoto Y, Johnson DH. Trabecular meshwork phagocytosis in glaucomatous eyes. *Ophthalmologica*. 1997;211:147-152.

160. Rohen JW, Lutjen-Drecoll E, Flugel C, Meyer M, Grierson I. Ultrastructure of the trabecular meshwork in untreated cases of primary open-angle glaucoma (POAG). *Exp Eye Res*. 1993;56:683-692.

161. Lutjen-Drecoll E, Shimizu T, Rohrbach M, Rohen JW. Quantitative analysis of 'plaque material' in the inner- and outer wall of Schlemm's canal in normal- and glaucomatous eyes. *Exp Eye Res*. 1986;42:443-455.

162. Yue BY. The extracellular matrix and its modulation in the trabecular meshwork. *Surv Ophthalmol*. 1996;40:379-390.

163. Gottanka J, Johnson DH, Martus P, Lutjen-Drecoll E. Severity of optic nerve damage in eyes with POAG is correlated with changes in the trabecular meshwork. *J Glaucoma*. 1997;6:123-132.

164. Knepper PA, Goossens W, Hvizd M, Palmberg PF. Glycosaminoglycans of the human trabecular meshwork in primary open-angle glaucoma. *Invest Ophthalmol Vis Sci*. 1996;37:1360-1367.

165. Guo MS, Wu YY, Liang ZB. Hyaluronic acid increases MMP-2 and MMP-9 expressions in cultured trabecular meshwork cells from patients with primary open-angle glaucoma. *Mol Vis*. 2012;18:1175-1181.

166. Keller KE, Sun YY, Vranka JA, Hayashi L, Acott TS. Inhibition of hyaluronan synthesis reduces versican and fibronectin levels in trabecular meshwork cells. *PLoS One*. 2012;7.

167. Keller KE, Sun YY, Yang YF, Bradley JM, Acott TS. Perturbation of hyaluronan synthesis in the trabecular meshwork and the effects on outflow facility. *Invest Ophthalmol Vis Sci*. 2012;53:4616-4625.

168. Takahashi E, Inoue T, Fujimoto T, Kojima S, Tanihara H. Epithelial mesenchymal transition-like phenomenon in trabecular meshwork cells. *Exp Eye Res*. 2014;118:72-79.

169. McDonnell F, O'Brien C, Wallace D. The role of epigenetics in the fibrotic processes associated with glaucoma. *J Ophthalmol*. 2014;2014.

170. Wordinger RJ, Sharma T, Clark AF. The role of TGF-beta2 and bone morphogenetic proteins in the trabecular meshwork and glaucoma. *J Ocul Pharmacol Ther*. 2014;30:154-162.

171. Lepple-Wienhues A, Stahl F, Wiederholt M. Differential smooth muscle-like contractile properties of trabecular meshwork and ciliary muscle. 1991;53:33-38.

172. Tian B, Geiger B, Epstein DL, Kaufman PL. Cytoskeletal involvement in the regulation of aqueous humor outflow. *Invest Ophthalmol Vis Sci*. 2000;41:619-623.

173. Tripathi RC, Li J, Chan WF, Tripathi BJ. Aqueous humor in glaucomatous eyes contains an increased level of TGF-beta 2. *Exp Eye Res*. 1994;59:723-727.

174. Inatani M, Tanihara H, Katsuta H, Honjo M, Kido N, Honda Y. Transforming growth factor-beta 2 levels in aqueous humor of glaucomatous eyes. *Graefes Arch Clin Exp Ophthalmol*. 2001;239:109-113.

175. Min SH, Lee TI, Chung YS, Kim HK. Transforming growth factor-beta levels in human aqueous humor of glaucomatous, diabetic and uveitic eyes. *Korean J Ophthalmol*. 2006;20:162-165.

176. Ochiai Y, Ochiai H. Higher concentration of transforming growth factor-beta in aqueous humor of glaucomatous eyes and diabetic eyes. *Jpn J Ophthalmol*. 2002;46:249-253.

177. Tamm ER, Fuchshofer R. What increases outflow resistance in primary open-angle glaucoma? *Surv Ophthalmol*. 2007;52 S101-104.

178. Junglas B, Yu AH, Welge-Lussen U, Tamm ER, Fuchshofer R. Connective tissue growth factor induces extracellular matrix deposition in human trabecular meshwork cells. *Exp Eye Res*. 2009;88:1065-1075.

179. Welge-Lussen U, May CA, Lutjen-Drecoll E. Induction of tissue transglutaminase in the trabecular meshwork by TGF-beta1 and TGF-beta2. *Invest Ophthalmol Vis Sci*. 2000;41:2229-2238.

180. Tovar-Vidales T, Roque R, Clark AF, Wordinger RJ. Tissue transglutaminase expression and activity in normal and glaucomatous human trabecular meshwork cells and tissues. *Invest Ophthalmol Vis Sci*. 2008;49:622-628.

181. Sethi A, Mao W, Wordinger RJ, Clark AF. Transforming growth factor-beta induces extracellular matrix protein cross-linking lysyl oxidase (LOX) genes in human trabecular meshwork cells. *Invest Ophthalmol Vis Sci*. 2011;52:5240-5250.

182. Fuchshofer R, Welge-Lussen U, Lutjen-Drecoll E. The effect of TGF-beta2 on human trabecular meshwork extracellular proteolytic system. *Exp Eye Res*. 2003;77:757-765.

183. Gottanka J, Chan D, Eichhorn M, Lütjen-Drecoll E, Ethier CR. Effects of TGF-β2 in Perfused Human Eyes. *Invest Ophthalmol Vis Sci*. 2004;45:153-158.

184. Fuchshofer R, Tamm ER. The role of TGF-beta in the pathogenesis of primary open-angle glaucoma. *Cell and tissue research*. 2012;347:279-290.

185. Junglas B, Kuespert S, Seleem AA, et al. Connective tissue growth factor causes glaucoma by modifying the actin cytoskeleton of the trabecular meshwork. *Am J Pathol*. 2012;180:2386-2403.

186. Pattabiraman PP, Rao PV. Mechanistic basis of Rho GTPase-induced extracellular matrix synthesis in trabecular meshwork cells. *Am J Physiol Cell Physiol*. 2010;298:C749-763.

187. Han H, Wecker T, Grehn F, Schlunck G. Elasticity-Dependent Modulation of TGF-β Responses in Human Trabecular Meshwork Cells. *Invest Ophthalmol Vis Sci*. 2011;52:2889-2896.

188. Read AT, Chan DW, Ethier CR. Actin structure in the outflow tract of normal and glaucomatous eyes. *Exp Eye Res*. 2006;82:974-985.

189. Clark AF, Miggans ST, Wilson K, Browder S, McCartney MD. Cytoskeletal changes in cultured human glaucoma trabecular meshwork cells. *J Glaucoma*. 1995;4:183-188.

190. O'Reilly S, Pollock N, Currie L, Paraoan L, Clark AF, Grierson I. Inducers of cross-linked actin networks in trabecular meshwork cells. *Invest Ophthalmol Vis Sci*. 2011;52:7316-7324.

191. Clark AF, Wilson K, McCartney MD, Miggans ST, Kunkle M, Howe W. Glucocorticoid-induced formation of cross-linked actin networks in cultured human trabecular meshwork cells. *Invest Ophthalmol Vis Sci*. 1994;35:281-294.

192. Wordinger RJ, Clark AF. Effects of glucocorticoids on the trabecular meshwork: towards a better understanding of glaucoma. *Prog Retin Eye Res*. 1999;18:629-667.

193. Last JA, Pan T, Ding Y, et al. Elastic modulus determination of normal and glaucomatous human trabecular meshwork. *Invest Ophthalmol Vis Sci*. 2011;52:2147-2152.

194. Camras LJ, Stamer WD, Epstein D, Gonzalez P, Yuan F. Circumferential tensile stiffness of glaucomatous trabecular meshwork. *Invest Ophthalmol Vis Sci*. 2014;55:814-823.

195. Morgan JT, Raghunathan VK, Chang YR, Murphy CJ, Russell P. The intrinsic stiffness of human trabecular meshwork cells increases with senescence. *Oncotarget*. 2015;6:15362-15374.

196. Xue W, Comes N, Borras T. Presence of an established calcification marker in trabecular meshwork tissue of glaucoma donors. *Invest Ophthalmol Vis Sci*. 2007;48:3184-3194.

197. Schlunck G, Han H, Wecker T, Kampik D, Meyer-ter-Vehn T, Grehn F. Substrate rigidity modulates cell matrix interactions and protein expression in human trabecular meshwork cells. *Invest Ophthalmol Vis Sci*. 2008;49:262-269.

198. Thomasy SM, Wood JA, Kass PH, Murphy CJ, Russell P. Substratum stiffness and latrunculin B regulate matrix gene and protein expression in human trabecular meshwork cells. *Invest Ophthalmol Vis Sci*. 2012;53:952-958.

199. Liton PB, Gonzalez P. Stress response of the trabecular meshwork. *J Glaucoma*. 2008;17:378-385.

200. Liton PB. The autophagic lysosomal system in outflow pathway physiology and pathophysiology. *Exp Eye Res*. 2016;144:29-37.

201. Hirt J, Liton PB. Autophagy and mechanotransduction in outflow pathway cells. *Exp Eye Res*. 2017;158:146-153.

202. Funke S, Perumal N, Bell K, Pfeiffer N, Grus FH. The potential impact of recent insights into proteomic changes associated with glaucoma. *Expert Rev Proteomics*. 2017;14:311-334.

203. Quigley HA, Broman AT. The number of people with glaucoma worldwide in 2010 and 2020. *Br J Ophthalmol*. 2006;90:262-267.

204. Sacca SC, Pulliero A, Izzotti A. The dysfunction of the trabecular meshwork during glaucoma course. *J Cell Physiol*. 2015;230:510-525.

205. Gabelt BT, Kaufman PL. Changes in aqueous humor dynamics with age and glaucoma. *Prog Retin Eye Res*. 2005;24:612-637.

206. Tane N, Dhar S, Roy S, Pinheiro A, Ohira A, Roy S. Effect of excess synthesis of extracellular matrix components by trabecular meshwork cells: possible consequence on aqueous outflow. *Exp Eye Res*. 2007;84:832-842.

207. Keller KE, Kelley MJ, Acott TS. Extracellular matrix gene alternative splicing by trabecular meshwork cells in response to mechanical stretching. *Invest Ophthalmol Vis Sci*. 2007;48:1164-1172.

208. Visse R, Nagase H. Matrix metalloproteinases and tissue inhibitors of metalloproteinases: structure, function, and biochemistry. *Circ Res*. 2003;92:827-839.

209. The UniProt C. Activities at the Universal Protein Resource (UniProt). *Nucleic Acids Research*. 2014;42:D191-D198.

210. Gasteiger E, Gattiker A, Hoogland C, Ivanyi I, Appel RD, Bairoch A. ExPASy: the proteomics server for in-depth protein knowledge and analysis. *Nucleic Acids Research*. 2003;31:3784-3788.

211. Yu AL, Birke K, Moriniere J, Welge-Lussen U. TGF-beta 2 induces senescence-associated changes in human trabecular meshwork cells. *Invest Ophthalmol Vis Sci*. 2010;51:5718-5723.

212. Caprioli J. Glaucoma: a disease of early cellular senescence. *Invest Ophthalmol Vis Sci*. 2013;54:60-67.

213. Coppe JP, Desprez PY, Krtolica A, Campisi J. The senescence-associated secretory phenotype: the dark side of tumor suppression. *Annu Rev Pathol*. 2010;5:99-118.

214. Bradley JM, Kelley MJ, Zhu X, Anderssohn AM, Alexander JP, Acott TS. Effects of mechanical stretching on trabecular matrix metalloproteinases. *Invest Ophthalmol Vis Sci*. 2001;42:1505-1513.

215. Liton PB, Liu X, Challa P, Epstein DL, Gonzalez P. Induction of TGF-β1 in the trabecular meshwork under cyclic mechanical stress. *J Cell Physiol*. 2005;205:364-371.

216. Inatani M, Iwao K, Inoue T, et al. Long-term relationship between intraocular pressure and visual field loss in primary open-angle glaucoma. *J Glaucoma*. 2008;17:275-279.

217. Konstas AG, Koliakos GG, Karabatsas CH, et al. Latanoprost therapy reduces the levels of TGF beta 1 and gelatinases in the aqueous humour of patients with exfoliative glaucoma. *Exp Eye Res*. 2006;82:319-322.

218. Ito T, Ohguro H, Mamiya K, Ohguro I, Nakazawa M. Effects of antiglaucoma drops on MMP and TIMP balance in conjunctival and subconjunctival tissue. *Invest Ophthalmol Vis Sci*. 2006;47:823-830.

219. Brew K, Nagase H. The tissue inhibitors of metalloproteinases (TIMPs): an ancient family with structural and functional diversity. *Biochim Biophys Acta*. 2010;1803:55-71.

220. Moore CS, Crocker SJ. An alternate perspective on the roles of TIMPs and MMPs in pathology. *Am J Pathol*. 2012;180:12-16.

221. Aktas Z, Karaca EE, Gonul, II, Hasanreisoglu M, Onol M. Apoptosis in the iris and trabecular meshwork of medically treated and untreated primary open angle glaucoma patients. *Int J Ophthalmol*. 2013;6:827-830.

222. Baleriola J, Garcia-Feijoo J, Martinez-de-la-Casa JM, Fernandez-Cruz A, de la Rosa EJ, Fernandez-Durango R. Apoptosis in the trabecular meshwork of glaucomatous patients. *Mol Vis*. 2008;14:1513-1516.

223. Stetler-Stevenson WG. Tissue inhibitors of metalloproteinases in cell signaling: metalloproteinase-independent biological activities. *Sci Signal*. 2008;1.

224. Chowdhury UR, Hann CR, Stamer WD, Fautsch MP. Aqueous humor outflow: dynamics and disease. *Invest Ophthalmol Vis Sci*. 2015;56:2993-3003.

225. Izzotti A, Sacca SC, Cartiglia C, De Flora S. Oxidative deoxyribonucleic acid damage in the eyes of glaucoma patients. *Am J Med*. 2003;114:638-646.

226. Saccà SC, Gandolfi S, Bagnis A, et al. From DNA damage to functional changes of the trabecular meshwork in aging and glaucoma. *Ageing Research Reviews*. 2016;29:26-41.

227. Buie LK, Karim MZ, Smith MH, Borras T. Development of a model of elevated intraocular pressure in rats by gene transfer of bone morphogenetic protein 2. *Invest Ophthalmol Vis Sci*. 2013;54:5441-5455.

228. Ozcan AA, Ozdemir N, Canataroglu A. The aqueous levels of TGF-beta2 in patients with glaucoma. *Int Ophthalmol*. 2004;25:19-22.

229. Engel LA, Muether PS, Fauser S, Hueber A. The effect of previous surgery and topical eye drops for primary open-angle glaucoma on cytokine expression in aqueous humor. *Graefes Arch Clin Exp Ophthalmol*. 2014;252:791-799.

230. Zhou X, Li F, Kong L, Tomita H, Li C, Cao W. Involvement of inflammation, degradation, and apoptosis in a mouse model of glaucoma. *J Biol Chem*. 2005;280:31240-31248.

231. Bouhenni RA, Al Shahwan S, Morales J, et al. Identification of differentially expressed proteins in the aqueous humor of primary congenital glaucoma. *Exp Eye Res*. 2011;92:67-75.

232. Kim TW, Kang JW, Ahn J, et al. Proteomic analysis of the aqueous humor in age-related macular degeneration (AMD) patients. *J Proteome Res*. 2012;11:4034-4043.

233. Pollreisz A, Funk M, Breitwieser FP, et al. Quantitative proteomics of aqueous and vitreous fluid from patients with idiopathic epiretinal membranes. *Exp Eye Res*. 2013;108:48-58.

234. Richardson MR, Segu ZM, Price MO, et al. Alterations in the aqueous humor proteome in patients with Fuchs endothelial corneal dystrophy. *Mol Vis*. 2010;16:2376-2383.

235. Ashworth Briggs EL, Toh TY, Eri R, Hewitt AW, Cook AL. TIMP1, TIMP2, and TIMP4 are increased in aqueous humor from primary open angle glaucoma patients. *Mol Vis*. 2015;21:1162-1172.

236. Choritz L, Machert M, Thieme H. Correlation of endothelin-1 concentration in aqueous humor with intraocular pressure in primary open angle and pseudoexfoliation glaucoma. *Invest Ophthalmol Vis Sci*. 2012;53:7336-7342.

237. Lopez-Riquelme N, Villalba C, Tormo C, et al. Endothelin-1 levels and biomarkers of oxidative stress in glaucoma patients. *Int Ophthalmol*. 2015;35:527-532.

238. Haddadin RI, Oh DJ, Kang MH, et al. Thrombospondin-1 (TSP1)-null and TSP2-null mice exhibit lower intraocular pressures. *Invest Ophthalmol Vis Sci*. 2012;53:6708-6717.

239. Fitzgerald AM, Benz C, Clark AF, Wordinger RJ. The effects of transforming growth factor-beta2 on the expression of follistatin and activin A in normal and glaucomatous human trabecular meshwork cells and tissues. *Invest Ophthalmol Vis Sci*. 2012;53:7358-7369.

240. Alexander JP, Samples JR, Acott TS. Growth factor and cytokine modulation of trabecular meshwork matrix metalloproteinase and TIMP expression. *Curr Eye Res*. 1998;17:276-285.

241. McEver RP. Selectins: initiators of leucocyte adhesion and signalling at the vascular wall. *Cardiovasc Res*. 2015;107:331-339.

242. Lolis E, Bucala R. Macrophage migration inhibitory factor. *Expert Opin Ther Targets*. 2003;7:153-164.

243. Lee CG, Da Silva CA, Dela Cruz CS, et al. Role of chitin and chitinase/chitinase-like proteins in inflammation, tissue remodeling, and injury. *Annu Rev Physiol*. 2011;73:479-501.

244. Wang H, Liu Y, Liu Z. Clara cell 10-kD protein in inflammatory upper airway diseases. *Curr Opin Allergy Clin Immunol*. 2013;13:25-30.

245. Dierynck I, Bernard A, Roels H, De Ley M. Potent inhibition of both human interferon-gamma production and biologic activity by the Clara cell protein CC16. *Am J Respir Cell Mol Biol*. 1995;12:205-210.

246. Tsuchida K, Arai KY, Kuramoto Y, Yamakawa N, Hasegawa Y, Sugino H. Identification and characterization of a novel follistatin-like protein as a binding protein for the TGF-beta family. *J Biol Chem*. 2000;275:40788-40796.

247. Shijubo N, Kawabata I, Sato N, Itoh Y. Clinical aspects of Clara cell 10-kDa protein/ uteroglobin (secretoglobin 1A1). *Curr Pharm Des*. 2003;9:1139-1149.

248. Broeckaert F, Bernard A. Clara cell secretory protein (CC16): characteristics and perspectives as lung peripheral biomarker. *Clin Exp Allergy*. 2000;30:469-475.

249. Wang H, Long XB, Cao PP, et al. Clara cell 10-kD protein suppresses chitinase 3-like 1 expression associated with eosinophilic chronic rhinosinusitis. *Am J Respir Crit Care Med*. 2010;181:908-916.

250. Du Y, Yun H, Yang E, Schuman JS. Stem cells from trabecular meshwork home to TM tissue in vivo. *Invest Ophthalmol Vis Sci*. 2013;54:1450-1459.

251. Liton PB, Liu X, Stamer WD, Challa P, Epstein DL, Gonzalez P. Specific targeting of gene expression to a subset of human trabecular meshwork cells using the chitinase 3-like 1 promoter. *Invest Ophthalmol Vis Sci*. 2005;46:183-190.

252. Abu-Hassan DW, Li X, Ryan EI, Acott TS, Kelley MJ. Induced pluripotent stem cells restore function in a human cell loss model of open-angle glaucoma. *Stem Cells* 2015;33:751-761.

253. Wordinger RJ, Clark AF, Agarwal R, et al. Cultured human trabecular meshwork cells express functional growth factor receptors. *Invest Ophthalmol Vis Sci*. 1998;39:1575-1589.

254. Wang H, Keiser JA. Hepatocyte growth factor enhances MMP activity in human endothelial cells. *Biochem Biophys Res Commun*. 2000;272:900-905.

255. Forissier S, Razanajaona D, Ay AS, Martel S, Bartholin L, Rimokh R. AF10-dependent transcription is enhanced by its interaction with FLRG. *Biol Cell*. 2007;99:563-571.

256. Ohira S, Inoue T, Iwao K, Takahashi E, Tanihara H. Factors Influencing Aqueous Proinflammatory Cytokines and Growth Factors in Uveitic Glaucoma. *PLoS One*. 2016;11.

257. Fechtner RD, Khouri AS, Zimmerman TJ, et al. Anterior uveitis associated with latanoprost. *Am J Ophthalmol*. 1998;126:37-41.

258. Byles DB, Frith P, Salmon JF. Anterior uveitis as a side effect of topical brimonidine. *Am J Ophthalmol*. 2000;130:287-291.

259. Liebmann JM, Lee JK. Current therapeutic options and treatments in development for the management of primary open-angle glaucoma. *Am J Manag Care*. 2017;23:S279-S292.

260. Gasiorowski JZ, Russell P. Biological properties of trabecular meshwork cells. *Exp Eye Res*. 2009;88:671-675.

261. Umland TC, Swaminathan S, Singh G, et al. Structure of a human Clara cell phospholipid-binding protein-ligand complex at 1.9 A resolution. *Nat Struct Biol*. 1994;1:538-545.

262. Peri A, Cordella-Miele E, Miele L, Mukherjee AB. Tissue-specific expression of the gene coding for human Clara cell 10-kD protein, a phospholipase A2-inhibitory protein. *J Clin Invest*. 1993;92:2099-2109.

263. Harrod KS, Mounday AD, Stripp BR, Whitsett JA. Clara cell secretory protein decreases lung inflammation after acute virus infection. *Am J Physiol*. 1998;275:L924-930.

264. Dierynck I, Bernard A, Roels H, De Ley M. The human Clara cell protein: biochemical and biological characterisation of a natural immunosuppressor. *Mult Scler*. 1996;1:385-387.

265. Mukherjee AB, Zhang Z, Chilton BS. Uteroglobin: a steroid-inducible immunomodulatory protein that founded the Secretoglobin superfamily. *Endocr Rev*. 2007;28:707-725.

266. Mango GW, Johnston CJ, Reynolds SD, Finkelstein JN, Plopper CG, Stripp BR. Clara cell secretory protein deficiency increases oxidant stress response in conducting airways. *Am J Physiol*. 1998;275:L348-356.

267. Levin SW, Butler JD, Schumacher UK, Wightman PD, Mukherjee AB. Uteroglobin inhibits phospholipase A2 activity. *Life Sci*. 1986;38:1813-1819.

268. Singh G, Katyal SL, Brown WE, Kennedy AL, Singh U, Wong-Chong ML. Clara cell 10 kDa protein (CC10): comparison of structure and function to uteroglobin. *Biochim Biophys Acta*. 1990;1039:348-355.

269. Chowdhury B, Mantile-Selvaggi G, Miele L, Cordella-Miele E, Zhang Z, Mukherjee AB. Lys 43 and Asp 46 in alpha-helix 3 of uteroglobin are essential for its phospholipase A2 inhibitory activity. *Biochem Biophys Res Commun*. 2002;295:877-883.

270. Pattabiraman PP, Lih FB, Tomer KB, Rao PV. The role of calcium-independent phospholipase A2gamma in modulation of aqueous humor drainage and Ca2+ sensitization of trabecular meshwork contraction. *Am J Physiol Cell Physiol*. 2012;302:C979-991.

271. Zhang Z, Kim SJ, Chowdhury B, et al. Interaction of uteroglobin with lipocalin-1 receptor suppresses cancer cell motility and invasion. *Gene*. 2006;369:66-71.

272. Burmeister R, Boe IM, Nykjaer A, et al. A two-receptor pathway for catabolism of Clara cell secretory protein in the kidney. *J Biol Chem*. 2001;276:13295-13301.

273. Mandal AK, Zhang Z, Ray R, et al. Uteroglobin represses allergen-induced inflammatory response by blocking PGD2 receptor-mediated functions. *J Exp Med*. 2004;199:1317-1330.

274. Pang M, Yuan Y, Wang D, et al. Recombinant CC16 protein inhibits the production of pro-inflammatory cytokines via NF-kappaB and p38 MAPK pathways in LPS-activated RAW264.7 macrophages. *Acta Biochim Biophys Sin (Shanghai)*. 2017;49:435-443.

275. Katavolos P, Ackerley CA, Clark ME, Bienzle D. Clara cell secretory protein increases phagocytic and decreases oxidative activity of neutrophils. *Vet Immunol Immunopathol*. 2011;139:1-9.

276. Pang M, Wang H, Bai JZ, et al. Recombinant rat CC16 protein inhibits LPS-induced MMP-9 expression via NF-kappaB pathway in rat tracheal epithelial cells. *Exp Biol Med (Maywood)*. 2015;240:1266-1278.

277. Wojnar P, Lechner M, Redl B. Antisense down-regulation of lipocalin-interacting membrane receptor expression inhibits cellular internalization of lipocalin-1 in human NT2 cells. *J Biol Chem*. 2003;278:16209-16215.

278. Fluckinger M, Merschak P, Hermann M, Haertle T, Redl B. Lipocalin-interacting-membrane-receptor (LIMR) mediates cellular internalization of beta-lactoglobulin. *Biochim Biophys Acta*. 2008;1778:342-347.

279. Antico G, Aloman M, Lakota K, Miele L, Fiore S, Sodin-Semrl S. Uteroglobin, a possible ligand of the lipoxin receptor inhibits serum amyloid A-driven inflammation. *Mediators Inflamm*. 2014;2014:876395.

280. Ashworth Briggs EL, Toh T, Eri R, Hewitt AW, Cook AL. Uteroglobin and FLRG concentrations in aqueous humor are associated with age in primary open angle glaucoma patients. *BMC Ophthalmol*. 2018;18:57.

281. Polansky JR, Weinreb R, Alvarado JA. Studies on human trabecular cells propagated in vitro. *Vision research*. 1981;21:155-160.

282. Aga M, Bradley JM, Keller KE, Kelley MJ, Acott TS. Specialized podosome- or invadopodia-like structures (PILS) for focal trabecular meshwork extracellular matrix turnover. *Invest Ophthalmol Vis Sci*. 2008;49:5353-5365.

283. Alvarado JA, Wood I, Polansky JR. Human trabecular cells. II. Growth pattern and ultrastructural characteristics. *Invest Ophthalmol Vis Sci*. 1982;23:464-478.

284. Grierson I, Robins E, Unger W, Millar L, Ahmed A. The cells of the bovine outflow system in tissue culture. *Exp Eye Res*. 1985;40:35-46.

285. Resch ZT, Hann CR, Cook KA, Fautsch MP. Aqueous humor rapidly stimulates myocilin secretion from human trabecular meshwork cells. *Exp Eye Res*. 2010;91:901-908.

286. Faralli JA, Clark RW, Filla MS, Peters DM. NFATc1 activity regulates the expression of myocilin induced by dexamethasone. *Exp Eye Res*. 2015;130:9-16.

287. Nakamura Y, Hirano S, Suzuki K, Seki K, Sagara T, Nishida T. Signaling mechanism of TGF-beta1-induced collagen contraction mediated by bovine trabecular meshwork cells. *Invest Ophthalmol Vis Sci*. 2002;43:3465-3472.

288. Nakamura Y, Sagara T, Seki K, Hirano S, Nishida T. Permissive effect of fibronectin on collagen gel contraction mediated by bovine trabecular meshwork cells. *Invest Ophthalmol Vis Sci*. 2003;44:4331-4336.

289. Koga T, Koga T, Awai M, Tsutsui J, Yue BY, Tanihara H. Rho-associated protein kinase inhibitor, Y-27632, induces alterations in adhesion, contraction and motility in cultured human trabecular meshwork cells. *Exp Eye Res*. 2006;82:362-370.

290. Baldanzi G, Graziani A. Physiological Signaling and Structure of the HGF Receptor MET. *Biomedicines*. 2014;3:1-31.

291. Rao VP, Epstein DL. Rho GTPase/Rho kinase inhibition as a novel target for the treatment of glaucoma. *BioDrugs*. 2007;21:167-177.

292. Honjo M, Tanihara H. Impact of the clinical use of ROCK inhibitor on the pathogenesis and treatment of glaucoma. *Jpn J Ophthalmol*. 2018;62:109-126.

293. Lin CW, Sherman B, Moore LA, et al. Discovery and Preclinical Development of Netarsudil, a Novel Ocular Hypotensive Agent for the Treatment of Glaucoma. *J Ocul Pharmacol Ther*. 2018;34:40-51.

294. Coroneo MT, Korbmacher C, Flugel C, Stiemer B, Lutjen-Drecoll E, Wiederholt M. Electrical and morphological evidence for heterogeneous populations of cultured bovine trabecular meshwork cells. *Exp Eye Res*. 1991;52:375-388.

295. Flugel C, Tamm E, Lutjen-Drecoll E. Different cell populations in bovine trabecular meshwork: an ultrastructural and immunocytochemical study. *Exp Eye Res*. 1991;52:681-690.

296. Stamer DW, Roberts BC, Epstein DL, Allingham RR. Isolation of primary open-angle glaucomatous trabecular meshwork cells from whole eye tissue. *Curr Eye Res*. 2000;20:347-350.

297. Grant J, Tran V, Bhattacharya SK, Bianchi L. Ionic currents of human trabecular meshwork cells from control and glaucoma subjects. *J Membr Biol*. 2013;246:167-175.

298. Manjunath R, Chung SI, Mukherjee AB. Crosslinking of uteroglobin by transglutaminase. *Biochem Biophys Res Commun*. 1984;121:400-407.

299. Greenberg CS, Birckbichler PJ, Rice RH. Transglutaminases: multifunctional cross-linking enzymes that stabilize tissues. *FASEB J*. 1991;5:3071-3077.

300. Moreno JJ. Effects of antiflammins on transglutaminase and phospholipase A2 activation by transglutaminase. *Int Immunopharmacol*. 2006;6:300-303.

301. Chowdhury B, Zhang Z, Mukherjee AB. Uteroglobin interacts with the heparin-binding site of fibronectin and prevents fibronectin-IgA complex formation found in IgA-nephropathy. *FEBS Lett*. 2008;582:611-615.

302. Hann CR, Springett MJ, Wang X, Johnson DH. Ultrastructural localization of collagen IV, fibronectin, and laminin in the trabecular meshwork of normal and glaucomatous eyes. *Ophthalmic Res*. 2001;33:314-324.

303. Schwinn MK, Gonzalez JM, Jr., Gabelt BT, Sheibani N, Kaufman PL, Peters DM. Heparin II domain of fibronectin mediates contractility through an alpha4beta1 co-signaling pathway. *Exp Cell Res*. 2010;316:1500-1512.

304. Gonzalez JM, Jr., Hu Y, Gabelt BT, Kaufman PL, Peters DM. Identification of the active site in the heparin II domain of fibronectin that increases outflow facility in cultured monkey anterior segments. *Invest Ophthalmol Vis Sci*. 2009;50:235-241.

305. Santas AJ, Bahler C, Peterson JA, et al. Effect of heparin II domain of fibronectin on aqueous outflow in cultured anterior segments of human eyes. *Invest Ophthalmol Vis Sci*. 2003;44:4796-4804.

306. Janiak A, Zemskov EA, Belkin AM. Cell surface transglutaminase promotes RhoA activation via integrin clustering and suppression of the Src-p190RhoGAP signaling pathway. *Mol Biol Cell*. 2006;17:1606-1619.

307. Telci D, Wang Z, Li X, et al. Fibronectin-tissue transglutaminase matrix rescues RGD-impaired cell adhesion through syndecan-4 and beta1 integrin co-signaling. *J Biol Chem*. 2008;283:20937-20947.

308. Faralli JA, Schwinn MK, Gonzalez JM, Jr., Filla MS, Peters DM. Functional properties of fibronectin in the trabecular meshwork. *Exp Eye Res*. 2009;88:689-693.

309. Antico G, Lingen MW, Sassano A, et al. Recombinant human uteroglobin/CC10 inhibits the adhesion and migration of primary human endothelial cells via specific and saturable binding to fibronectin. *J Cell Physiol*. 2006;207:553-561.

310. Hung SSC, Khan S, Lo CY, Hewitt AW, Wong RCB. Drug discovery using induced pluripotent stem cell models of neurodegenerative and ocular diseases. *Pharmacol Ther*. 2017;177:32-43.

311. Avior Y, Sagi I, Benvenisty N. Pluripotent stem cells in disease modelling and drug discovery. *Nat Rev Mol Cell Biol*. 2016;17:170-182.

312. Gage PJ, Rhoades W, Prucka SK, Hjalt T. Fate maps of neural crest and mesoderm in the mammalian eye. *Invest Ophthalmol Vis Sci*. 2005;46:4200-4208.

313. Mica Y, Lee G, Chambers SM, Tomishima MJ, Studer L. Modeling neural crest induction, melanocyte specification, and disease-related pigmentation defects in hESCs and patient-specific iPSCs. *Cell Rep*. 2013;3:1140-1152.

314. Kreitzer FR, Salomonis N, Sheehan A, et al. A robust method to derive functional neural crest cells from human pluripotent stem cells. *American journal of stem cells*. 2013;2:119-131.

315. Menendez L, Kulik MJ, Page AT, et al. Directed differentiation of human pluripotent cells to neural crest stem cells. *Nat Protoc*. 2013;8:203-212.

316. Lee G, Kim H, Elkabetz Y, et al. Isolation and directed differentiation of neural crest stem cells derived from human embryonic stem cells. *Nat Biotechnol*. 2007;25:1468-1475.

317. Chambers SM, Mica Y, Lee G, Studer L, Tomishima MJ. Dual-SMAD Inhibition/WNT Activation-Based Methods to Induce Neural Crest and Derivatives from Human Pluripotent Stem Cells. *Methods Mol Biol*. 2016;1307:329-343.

318. Reis LM, Semina EV. Genetics of anterior segment dysgenesis disorders. *Curr Opin Ophthalmol*. 2011;22:314-324.

319. Pressman CL, Chen H, Johnson RL. LMX1B, a LIM homeodomain class transcription factor, is necessary for normal development of multiple tissues in the anterior segment of the murine eye. *Genesis*. 2000;26:15-25.

320. Cvekl A, Tamm ER. Anterior eye development and ocular mesenchyme: new insights from mouse models and human diseases. *Bioessays*. 2004;26:374-386.

321. Lovatt M, Yam GH, Peh GS, Colman A, Dunn NR, Mehta JS. Directed differentiation of periocular mesenchyme from human embryonic stem cells. *Differentiation*. 2018;99:62-69.

322. Guedez L, Stetler-Stevenson WG, Wolff L, et al. In vitro suppression of programmed cell death of B cells by tissue inhibitor of metalloproteinases-1. *J Clin Invest*. 1998;102:2002-2010.

323. Tsuchida K, Nakatani M, Matsuzaki T, et al. Novel factors in regulation of activin signaling. *Mol Cell Endocrinol*. 2004;225:1-8.

324. Maguer-Satta V, Rimokh R. FLRG, member of the follistatin family, a new player in hematopoiesis. *Mol Cell Endocrinol*. 2004;225:109-118.

325. Xue W, Wallin R, Olmsted-Davis EA, Borras T. Matrix GLA protein function in human trabecular meshwork cells: inhibition of BMP2-induced calcification process. *Invest Ophthalmol Vis Sci*. 2006;47:997-1007.

326. Borras T, Comes N. Evidence for a calcification process in the trabecular meshwork. *Exp Eye Res*. 2009;88:738-746.

327. Maguer-Satta V, Forissier S, Bartholin L, et al. A novel role for fibronectin type I domain in the regulation of human hematopoietic cell adhesiveness through binding to follistatin domains of FLRG and follistatin. *Exp Cell Res*. 2006;312:434-442.

328. Mildner M, Eckhart L, Lengauer B, Tschachler E. Hepatocyte growth factor/scatter factor inhibits UVB induced apoptosis of human keratinocytes via the PI-3-kinase pathway. *J Invest Dermatol*. 1999;113:1136-1137.

Appendix 1 Calculation of TIMP and MMP molecular weights for stoichiometric analysis

Protein	UniProtKB ID	AAs	MW (Da)
TIMP1	P01033	24-207	20708.8
TIMP2	P16035	27-220	21755.0
TIMP3	P35625	24-211	21690.1
TIMP4	Q99727	30-224	22441.8
MMP1	P03956	20-469	51844.2
MMP2	P08253	30-660	70975.7
MMP3	P08254	18-477	52221.0
MMP7	P09237	18-267	27934.6
MMP8	P22894	21-467	51130.2
MMP9	P14780	20-707	76370.5
MMP12	P39900	17-470	52329.4
MMP13	P45452	20-471	51680.2

Molecular weight (MW) given in Daltons (Da) was calculated using the amino acid sequence (AAs) stated (signal peptide sequence removed), retrieved from the UniProt database.

Appendix 2 Correlation of measured analytes & MMP/TIMP ratios to CDR for POAG samples

Analyte/ratio	r_S	p-value	N
MMP1	-0.080	0.724	22
MMP1/TIMP1	-0.257	0.270	16
MMP1/TIMP2	-0.151	0.549	18
MMP1/TIMP3	-0.285	0.237	19
MMP1/TIMP4	-0.365	0.122	16
MMP3/TIMP1	-0.201	0.352	17
MMP3/TIMP2	-0.086	0.725	19
MMP3/TIMP3	-0.202	0.393	20
MMP3/TIMP4	-0.359	0.128	16
MMP9/TIMP3	-0.267	0.269	19
MMP9/TIMP4	-0.046	0.756	16

Correlation of analytes and MMP/TIMP ratios to CDR (optic cup-to-disc ratio) was determined using Spearman's rank correlation. A p-value <0.05 was considered significant. Only correlations also shown in Table 2.5 are displayed. r_S: Spearman correlation coefficient; N: number of correlation pairs

Appendix 3 Standard curve ranges of multiplex assays

Analyte	HGNC code	Range	Cataract detected/total	POAG detected/total
Angiopoietin-1	ANGPT1	127.5 - 30980	0/18	0/19
Angiopoietin-2	ANGPT2	113.0 - 27450	0/18	0/19
BMP2	BMP2	32.4 - 7860	0/18	0/19
BMP4	BMP4	48.3 - 11730	0/18	0/19
BMP9	GDF2	5.0 - 1200	0/18	0/19
CCL27/CTACK	CCL27	7.5 - 1830	0/18	0/19
CHI3L1/YKL-40	**CHI3L1**	**368.2 - 89460**	**18/18**	**19/19**
Collagen IV alpha 1	COL4A1	122.9 - 29860	1/18	1/19
Cripto-1	CFC1	40.7 - 9900	0/18	0/19
DcR3	TNFRSF6B	1031.2 - 250580	0/18	0/19
EGF	EGF	17.8 - 4320	0/18	0/19
Endoglin/CD105	ENG	463.4 - 112610	0/18	0/19
Endothelin-1	EDN1	31.9 - 7760	0/18	0/19
Epo	EPO	456.8 - 111000	0/18	0/19
FLRG	**FSTL3**	**961.6 - 233660**	**16/18**	**19/19**
Follistatin	FST	2674.9 - 650000	0/18	0/19
Growth Hormone	GH1	76.1 - 18500	0/18	0/19
HGF	**HGF**	**43.2 - 10500**	**9/18**	**18/19**
IGFBP-1	IGFBP1	163.3 - 39690	6/18	8/19
IGFBP-3	IGFBP3	2824.7 - 686400	0/18	0/19
IL-6	IL6	13.9 - 3370	0/18	0/19
IL-9	IL9	3012.4 - 732000	0/18	0/19
LIF	LIF	68.1 - 16550	0/18	0/19
MFG-E8	MFGE8	391.8 - 95200	2/18	1/19
MIF	**MIF**	**781.9 - 190000**	**15/18**	**15/19**
P-Selectin	**SELP**	**223.3 - 54270**	**9/18**	**15/19**
Thrombospondin-2	THBS2	349.2 - 84860	0/18	0/19
Uteroglobin	**SCGB1A1**	**30.5 - 7400**	**17/18**	**18/19**
VCAM-1	VCAM1	7440.7 - 1808100	6/18	8/19
vWF-A2	VWF	97.1 - 23600	0/18	0/19

HGNC: HUGO Gene Nomenclature Committee. Range: Concentration range of standard curve in pg/ml. POAG: Primary open-angle glaucoma. Analytes detected in more than 50% of samples in at least one patient group are highlighted in bold and were further analysed (see Table 3.2, Table 3.3 and Table 3.4).

Appendix 4 Correlation of measured analytes to IOP for non-glaucomatous cataract and POAG samples

	Cataract			POAG		
Analyte/ratio	r_s	**p-value**	**N**	r_s	**p-value**	**N**
CHI3L1	0.050	0.845	18	-0.416	0.076	19
FLRG	-0.040	0.826	16	-0.044	0.857	19
HGF	-0.417	0.236	9	-0.402	0.098	18
MIF	-0.167	0.480	15	-0.326	0.183	15
P-selectin	-0.369	0.275	9	-0.398	0.106	15
Uteroglobin	-0.379	0.113	17	-0.055	0.827	18

Correlations of normalised analyte concentrations to intraocular pressure (IOP) were determined using Spearman's rank correlation. Following correction for multiple testing using Bonferroni's method, a p-value of <0.0017 was considered significant. r_s: Spearman correlation coefficient; N: number of correlation pairs.

Appendix 5 Correlation of measured analytes to CDR for non-glaucomatous cataract and POAG samples

	Cataract			POAG		
Analyte	r_s	**p-value**	**N**	r_s	**p-value**	**N**
CHI3L1	-0.539	0.021	18	-0.004	0.988	19
FLRG	-0.249	0.224	16	-0.091	0.711	19
HGF	-0.292	0.310	9	-0.110	0.665	18
MIF	-0.213	0.322	15	-0.139	0.560	15
P-selectin	-0.588	0.635	9	-0.091	0.648	15
Uteroglobin	-0.191	0.325	17	-0.163	0.520	18

Correlations of normalised analyte concentrations to cup-to-disc ratio (CDR) were determined using Spearman's rank correlation. Following correction for multiple testing using Bonferroni's method, a p-value of <0.0017 was considered significant. r_s: Spearman correlation coefficient; N: number of correlation pairs.

Appendix 6 Correlation of measured analytes to MD for non-glaucomatous cataract and POAG samples

	Cataract			POAG		
Analyte/ratio	**r_s**	**p-value**	**N**	**r_s**	**p-value**	**N**
CHI3L1	0.100	0.950	5	0.187	0.541	13
FLRG	0.400	0.750	4	-0.445	0.130	13
HGF	0.500	>0.999	3	-0.252	0.430	12
MIF	0.600	0.417	4	-0.050	0.912	9
P-selectin	N/A	N/A	1	-0.119	0.716	12
Uteroglobin	-0.200	0.783	5	-0.336	0.287	12

Correlations of normalised analyte concentrations to mean deviation (MD) were determined using Spearman's rank correlation. Following correction for multiple testing using Bonferroni's method, a p-value of <0.0017 was considered significant. r_s: Spearman correlation coefficient; N: number of correlation pairs; N/A: not available.

Appendix 7 Correlation of measured analytes to PSD for non-glaucomatous cataract and POAG samples

	Cataract			POAG		
Analyte/ratio	**r_s**	**p-value**	**N**	**r_s**	**p-value**	**N**
CHI3L1	0.086	0.919	6	0.260	0.283	19
FLRG	0.700	0.233	5	0.493	0.032	19
HGF	1.000	0.333	3	0.536	0.022	18
MIF	-0.600	0.350	5	0.136	0.630	15
P-selectin	N/A	N/A	2	0.186	0.504	15
Uteroglobin	-0.257	0.658	6	0.212	0.399	18

Correlations of normalised analyte concentrations to Humphrey's visual field pattern standard deviation (PSD) were determined using Spearman's rank correlation. Following correction for multiple testing using Bonferroni's method, a p-value of <0.0017 was considered significant. r_s: Spearman correlation coefficient; N: number of correlation pairs; N/A: not available.

Appendix 8 TaqMan probes used for TM marker and housekeeper gene expression analysis

Target symbol	HGNC-approved name	Reference (Thermo Fisher)
AQP1	aquaporin 1	Hs01028916_m1
CHI3L1	chitinase 3 like 1	Hs00609691_m1
HPRT1	hypoxanthine phosphoribosyltransferase 1	Hs99999909_m1
MGP	matrix GLA protein	Hs00969490_m1
MMP3	matrix metallopeptidase 3	Hs00968305_m1
MYOC	myocilin	Hs00165345_m1
TIMP2	TIMP metallopeptidase inhibitor 2	Hs00234278_m1

Appendix 9 TaqMan probes used for gene expression analysis of HGF, uteroglobin, and their respective receptors.

Target symbol	HGNC-approved name	Reference (Thermo Fisher)
FPR2	formyl peptide receptor 2	Hs02759175_s1
HGF	hepatocyte growth factor	Hs00300159_m1
LMBR1L	limb development membrane protein 1 like	Hs00216545_m1
MET	MET proto-oncogene	Hs01565576_m1
UG	secretoglobin family 1A member 1 (SCGB1A1)	Hs00171092_m1

Appendix 10 Primary antibodies used for immunocytofluorescence

Target	Type/Species	Location	Dilution	Manufacturer and reference
AQP1	polyclonal/rabbit	intracellular	1:50	Santa Cruz Biotechnology, Inc. (Dallas, TX) Ref# sc-20810
CHI3L1	polyclonal/rabbit	intracellular	1:50	Santa Cruz Biotechnology, Inc. Ref# sc-98955
MET	monoclonal/rabbit	extracellular	1:500	Cell Signaling Technology, Inc. Ref# 8198
LMBR1L	polyclonal/rabbit	intracellular	1:200	Proteintech Group, Inc. (Rosemont, IL) Ref# 12154-1-AP

Appendix 11 Secondary Antibody used for immunocytofluorescence

Type	Fluorophore	Dilution	Manufacturer and reference
Anti-rabbit IgG (H+L), $F(ab')_2$ fragment	Alexa Fluor 555	1:500	Cell Signaling Technology, Inc. Ref# 4413

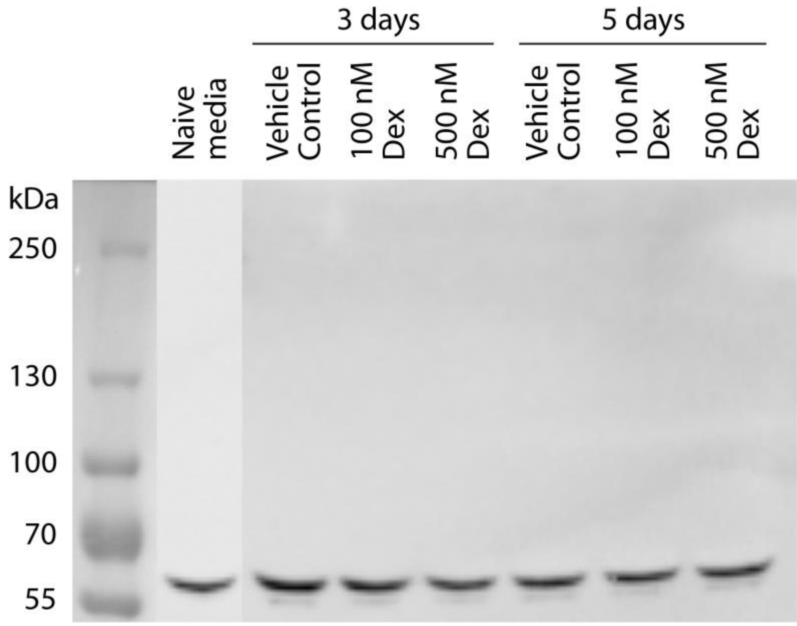

Appendix 12 Western blot of myocilin in pHTMC conditioned media with Dexamethasone (Dex) treatment. Conditioned media from pHTMCs *in vitro* was harvested after 3 or 5 days of exposure to vehicle control (0.1% ethanol), 100 nM, or 500 nM Dex. No media replacement occurred during the treatment period. The conditioned media was analysed using 4-15% Mini-PROTEAN TGX Precast SDS-PAGE gels followed by Western blotting. Naïve media was run as a control (on a separate gel). The samples show a single band at the expected size of approx. 57 kDa, corresponding to monomeric myocilin. Samples from three separate Dex treatments were tested (n=3).